THE REGULATION OF MITOCHONDRIAL FUNCTION DURING EARLY SEEDLING DEVELOPMENT IN CUCUMBER (*Cucumis sativus* L.).

BY

STEVEN ARTHUR HILL

DOCTOR OF PHILOSOPHY

UNIVERSITY OF EDINBURGH

1990

I hereby declare that this thesis was composed by myself, and that the work described herein is my own.

Steven A. Hill.

December 1990.

"In other studies you go as far as others have gone before you, and there is nothing more to know; but in a scientific pursuit there is continual food for discovery and wonder."

from *Frankenstein.*
Mary Shelley.

The endless cycle of idea and action,
Endless invention, endless experiment,
Brings knowledge of motion, but not of stillness;
Knowledge of speech, but not of silence;
Knowledge of words, and ignorance of the Word.
All our knowledge brings us nearer to our ignorance,
All our ignorance brings us nearer to death,
But nearness to death no nearer to God.
Where is the life we have lost in living?
Where is the wisdom we have lost in knowledge?
Where is the knowledge we have lost in information?

from *The Rock.*
T S Elliot.

TABLE OF CONTENTS.

ACKNOWLEDGEMENTS.

I thank my supervisor Professor Chris Leaver for providing the opportunity to carry out the work presented in this thesis, for his constant encouragement, and for his critical comments during the preparation of this thesis. My thanks also go to Dr James Bryce for practical advice and many stimulating discussions. I would also like to thank Dr Steve Smith for his sound advice, particularly at the end of my first year, and Dr Tony Trewavas for first suggesting the application of metabolic control theory in my experiments.

I acknowledge the generous financial support of Mr David Sainsbury, through the Gatsby Charitable Foundation.

I would like to thank all my friends and colleagues in Edinburgh, particularly Patrick and Claire, for making my time both in and out of the department so enjoyable.

I am forever indebted to my mother for her unquestioning and never-ending support.

Finally, but by no means least, I thank Susan, my very best of friends, for her patience, encouragement, and proof-reading, but most of all for just being there. It is to her that I dedicate this thesis.

ABSTRACT.

Plant mitochondria play an important role in a number of distinct metabolic pathways, including lipid mobilisation, photorespiration, and the generation of intermediates necessary for biosynthesis. In addition, in both photosynthetic and non-photosynthetic tissues, mitochondrial oxidative phosphorylation is a major source of ATP. These pathways have been well characterised, but little is known about their regulation, particularly in terms of the interactions between mitochondria and the rest of cellular metabolism. The general aim of the work presented in this thesis is to provide such information.

The cotyledons of a lipid storing seed, during early seedling development, provide a model system for the study of metabolic interactions. Light grown cotyledons pass through three metabolic phases during the first seven days after germination: lipid mobilisation, chloroplast development, and photosynthesis.

This thesis is concerned with the following areas: first, the nature of the developmental modulations in mitochondrial function, and the role of coarse control, at the level of protein synthesis, in bringing them about; and secondly, the importance of mitochondrial reactions in the regulation of cellular metabolism.

Changes in respiratory physiology in developing cotyledons have been characterised and correlated with changing metabolic phases. During lipid mobilisation carbon is diverted away from the decarboxylating reactions of the TCA cycle, whereas the capacity exists for full cycle operation in the photosynthetic phase. Mitochondrial glycine oxidation, necessary for the maintenance of the photorespiratory cycle, is induced during photosynthetic development. The non-phosphorylating pathway of electron transport, via the alternative oxidase, is present, and the access of substrates to this pathway appears to be regulated such that high rates of succinate and glycine oxidation can occur simultaneously. These changes are brought about, at least in part, by protein synthesis.

The steps regulating succinate oxidation by isolated cotyledon mitochondria have been determined using the quantitative techniques of metabolic control theory. During lipid mobilisation, succinate metabolism is regulated by the adenine nucleotide translocator and the processes of succinate uptake into the mitochondria. A mitochondrial role in the integration of biosynthesis and degradation is proposed in the light of these results. In the photosynthetic phase the regulation of succinate oxidation is by the steps of the respiratory chain. There is evidence to suggest that variation in succinate oxidation rates during development is a result of the synthesis of specific proteins.

Studies into the pathway of pyruvate metabolism in developing cotyledons indicate that carbon may be diverted into the TCA cycle during chloroplast biogenesis, through pyruvate production by the mitochondrially located NAD-malic enzyme. It is suggested that this mitochondrial route of carbon entry would enable TCA cycle flux to be regulated by the demand for intermediates required for biosynthetic pathways, rather than the rate of sucrose production from lipid. Evidence is presented for the more conventional route of carbon entry into the TCA cycle from cytosolic pyruvate during the photosynthetic phase. Results indicate that the developmental modulation of pyruvate metabolism is regulated at the level of protein synthesis.

Application of metabolic control theory to *in vitro* systems capable of hexose production from organic acids, provides further support for the proposed role of mitochondria during lipid mobilisation. The adenine nucleotide translocator and other mitochondrial steps have significant flux control coefficients for hexose production *in vitro*.

The results presented are used as the basis for the development of a hypothesis concerning the importance of mitochondria in the regulation of plant metabolism.

ABBREVIATIONS.

AcSCoA	acetyl coenzyme A
AdNT	adenine nucleotide translocator
ADP	adenosine diphosphate
AMP	adenosine monophosphate
ATP	adenosine triphosphate
BSA	bovine serum albumin
CATR	carboxyatractyloside
CCO	co-ordinate control operation
CoA	coenzyme A
DCPIP	2,6-dichlorophenol-indophenol
DPI	days post-imbibition
EDTA	ethylenediaminetetraacetic acid
EGTA	ethyleneglycol bis-(β-aminoethylether) N,N,N',N'-tetraacetic acid
ER	endoplasmic reticulum
FBP	fructose-1,6-bisphosphate
FBPase	fructose-1,6-bisphophate 1-phosphatase
FW	fresh weight
GAPDH	NADP glyceraldehyde-3-phosphate dehydrogenase
HEPES	4-(2-hydroxyethyl)-1-piperazine ethanesulphonic acid
HPR	hydroxypyruvate reductase
ICDH	isocitrate dehydrogenase
ICL	isocitrate lyase
ME	NAD-malic enzyme
MES	2-(N-morpholino)ethanesulphonic acid
mRNA	messenger ribonucleic acid
NAD	nicotinamide adenine dinucleotide (oxidised form)
NADH	nicotinamide adenine dinucleotide (reduced form)
NADP	nicotinamide adenine dinucleotide phosphate (oxidised form)
NADPH	nicotinamide adenine dinucleotide phosphate (reduced form)
OAA	oxaloacetate
2-OG	2-oxoglutarate
P_i	inorganic phosphate
PP_i	inorganic pyrophosphate
PDC	pyruvate dehydrogenase complex
PEP	phospho(enol)pyruvate
PEPCK	phospho(enol)pyruvate carboxykinase
PFK	ATP fructose-6-phosphate 1-phosphotransferase (phosphofructokinase)
PFP	PP_i fructose-6-phosphate 1-phosphotransferase
PK	pyruvate kinase
PMSF	phenylmethylsulphonyl fluoride
RUBISCO	ribulose bisphosphate carboxylase oxygenase
SDS	sodium dodecyl sulphate
SEM	standard error of the mean
TBST	Tris buffered saline/Tween-20
TCA	tricarboxylic acid
TEMED	N,N,N',N'-tetramethylethylenediamine
TES	N-tris(hydroxymethyl)methyl-2-aminoethanesulphonic acid
TMPD	N,N,N',N'-tetramethyl-1,4-benzenediamine
UDP	uridine diphosphate
v/v	volume per volume (given as a percentage)
w/v	weight per volume (given as a percentage)

CHAPTER 1.
INTRODUCTION

Germination and early seedling development is a process fundamental to plant growth and development. It is accompanied by a wide range of biochemical and morphological changes which are modified temporally and spatially, both by 'preprogrammed' developmental sequences and environmental influence. This regulation operates at a number of levels from the modulation of gene expression to the allosteric modification of specific enzyme activities, so that a study of germination should provide insight into many important regulatory events in plant development.

This thesis describes an investigation into the control of some aspects of mitochondrial respiratory metabolism during the immediate post-germinative development of the cotyledons of *Cucumis sativus* L. (cucumber), a lipid and protein storing seed. The following introduction will consider four areas: first, the biochemistry of germination and early seedling growth, with particular reference to lipid storing seeds; secondly, the function of mitochondria in plants and the aims of the work presented in this thesis; thirdly, the methodology of investigations into the control of metabolism; and fourthly, the experimental approach used in this thesis.

1.1 Biochemistry and Physiology of Germination and Early Seedling Development.

1.1.1 General Introduction.

The seed, a quiescent, almost completely metabolically inactive structure, occupies an important position in the ecology of most higher plant species as the primary means by which the results of sexual reproduction, and, in some cases, asexual reproduction (apomixis), are dispersed in time and space (see Bewley and Black, 1985 for a review of the physiology of germination and early development).

The angiosperm seed consists of four parts:

(i) The embryo: a diploid tissue produced by the fusion of the haploid egg cell and one of the haploid male pollen tube nuclei. The embryo comprises the embryonic axis (the radicle, hypocotyl and plumule) and one or more cotyledons.

(ii) The endosperm: a triploid nutritional tissue derived from the fusion of the diploid endosperm mother cell and the second haploid pollen tube nucleus.

(iii) The perisperm: a development of the maternal nucellus tissue.

(iv) The testa or seed coat: formed from the maternal integument tissue.

Seeds may be classified on the basis of the major storage compounds present and their location within the seed. These storage reserves support the growth and development of the seedling until it becomes photosynthetically competent. In the grasses the major food store is carbohydrate located in the endosperm. Among the dicotyledonous plants (dicots), protein

is the major storage product in the legumes, whilst in a second important group lipid is the major storage reserve, found either in the endosperm or cotyledons. The major storage compound and it's localisation within the seed of a number of species is listed in Table 1.1.

During germination the seed rehydrates, becomes metabolically active, and initiates the developmental programme which ultimately results in a mature plant. A definition of germination is offered by Bewley and Black (1985) as the period between water uptake by the seed and the start of elongation of the embryonic axis, usually the radicle. There then follows a period which I shall term 'early seedling development' which extends from the end of germination to the completion of expansion of the first true leaf. This is the point at which the leaf becomes a net exporter of photosynthate, primarily sucrose (Milthorpe and Moorby, 1979). Early seedling development in dicots can be divided into two types on the basis of the final position and fate of the cotyledons: epigeal, where the cotyledons are lifted above the soil by hypocotyl extension, and often expand and become photosynthetic; and hypogeal, where the cotyledons remain beneath the soil and the first true leaves are lifted clear of the soil by expansion of the epicotyl. In monocotyledonous plants the single cotyledon is modified to become an absorptive rather than storage organ, and the pattern of early seedling development is more complex. The pattern of early seedling development for a number of species is listed in Table 1.1.

Accompanying the morphological changes observed during germination and early seedling development there are a number of related ultrastructural and biochemical changes. Germination is accompanied by a major reorganisation of the cellular membrane structure associated with the rehydration phase. Within 20 minutes of imbibition in soybean cotyledons, modifications in the plasma membrane, the appearance of endoplasmic reticulum, and the development of intra-mitochondrial structures are observed (Webster and Leopold, 1977). This correlates with the rapid induction of respiration and the resumption of general metabolic processes during germination (Bewley and Black, 1985). Ultrastructurally, the major changes observed during early seedling development are related to the mobilisation of storage reserves. These include the disappearance of lipid and protein bodies and starch grains and the appearance of specialised organelles, such as glyoxysomes (Trelease *et al.*, 1971).

The mobilisation of storage reserves is the primary metabolic event of early seedling development. Within the storage tissues, high molecular weight reserves (carbohydrates, lipids and proteins) are converted into low molecular weight compounds (sugars and amino-acids), which are then translocated to the growing regions (both elongation zones and meristems) of the embryo or axis. In seeds exhibiting epigeal germination, with the major storage reserves located in the cotyledons (for example, cucumber) this process is further complicated because, in the light, some of the remobilised

carbon is utilised within the cotyledons themselves to support the differentiation of the photosynthetic apparatus.

A second important biochemical change which occurs during germination and early seedling development is an increase in the respiration rate of both the embryonic axis and the storage tissues (Bewley and Black, 1985). Kolloffel and Sluys (1970) identified a number of phases in the respiration of germinating pea cotyledons, which were found to be valid, in general, for a number of storage tissues (Tuquet and Dizengremel, 1984). This general pattern is illustrated in Figure 1.1. Phase I represents an initial induction of respiration due to the rehydration, and subsequent activation, of mitochondrial components already present (Bewley and Black, 1985). There then follows a lag phase (Phase II) before radicle emergence, at which point a second increase in respiration rate, during early seedling development, commences (Phase III). Senescence of the storage tissues is accompanied by a decrease in the respiration rate (Phase IV). A similar pattern, albeit with a different time scale, is observed in the cotyledons of bean and soybean (Opik and Simon, 1963; Dizengremel and Tuquet, 1984; Azcon-Bieto *et al.*, 1989).

1.1.2 The Metabolism of Stored Lipid.

Triglycerides, located in membrane bound organelles termed lipid bodies, are the major storage lipids in seeds and are converted in four stages into sucrose for export (see Beevers, 1980; and Kindl, 1987 for reviews):

1. Hydrolysis of the triglycerides to give free fatty acids (FFA) and glycerol.
2. β-oxidation of the FFA to give acetyl CoA.
3. Conversion of the acetyl-CoA to 4-carbon acids (succinate or malate).
4. Conversion of 4-carbon acids to sucrose via the enzyme phospho(enol)pyruvate carboxykinase (PEPCK) and reverse glycolysis.

Storage lipid is hydrolysed by lipases (see Huang, 1987 for a review of plant lipases). There is some uncertainty as to which subcellular compartment contains these enzymes. In castor bean endosperm there is an acid lipase associated with the lipid body (spherosome) membrane (Ory *et al.*, 1968), which has a high activity prior to germination, declining to a lower level as storage lipid is utilised. In addition the glyoxysomes contain an alkaline lipase (Muto and Beevers, 1974) which shows a much greater activity with monoglycerides as substrate than with either di- or tri-glycerides (Huang, 1987). The physiological significance of this activity is unclear (Huang *et al.*, 1983). The lipid body acid lipase activity found in castor bean endosperm prior to germination is absent from many other oilseeds (Huang, 1987), of which the majority fall into two classes as regards the pattern of lipolytic enzymes (Huang *et al.*, 1983). The first group, which includes rapeseed,

TABLE 1.1. *The seed storage reserves and pattern of early seedling development in a number of species.* Information taken from Bewley and Black (1985).

Species	Major Storage Compound	Localisation	Pattern of Early Seedling Development
Barley	carbohydrate	endosperm	hypogeal
Maize	carbohydrate	endosperm	hypogeal
Oats	carbohydrate	endosperm	hypogeal
Rye	carbohydrate	endosperm	hypogeal
Wheat	carbohydrate	endosperm	hypogeal
Broad bean	carbo./protein	cotyledons	hypogeal
Pea	carbo./protein	cotyledons	hypogeal
Peanut	lipid	cotyledons	epigeal
Soybean	protein	cotyledons	epigeal
Castor bean	lipid	endosperm	epigeal
Rape	lipid	cotyledons	epigeal
Cucumber	lipid	cotyledons	epigeal

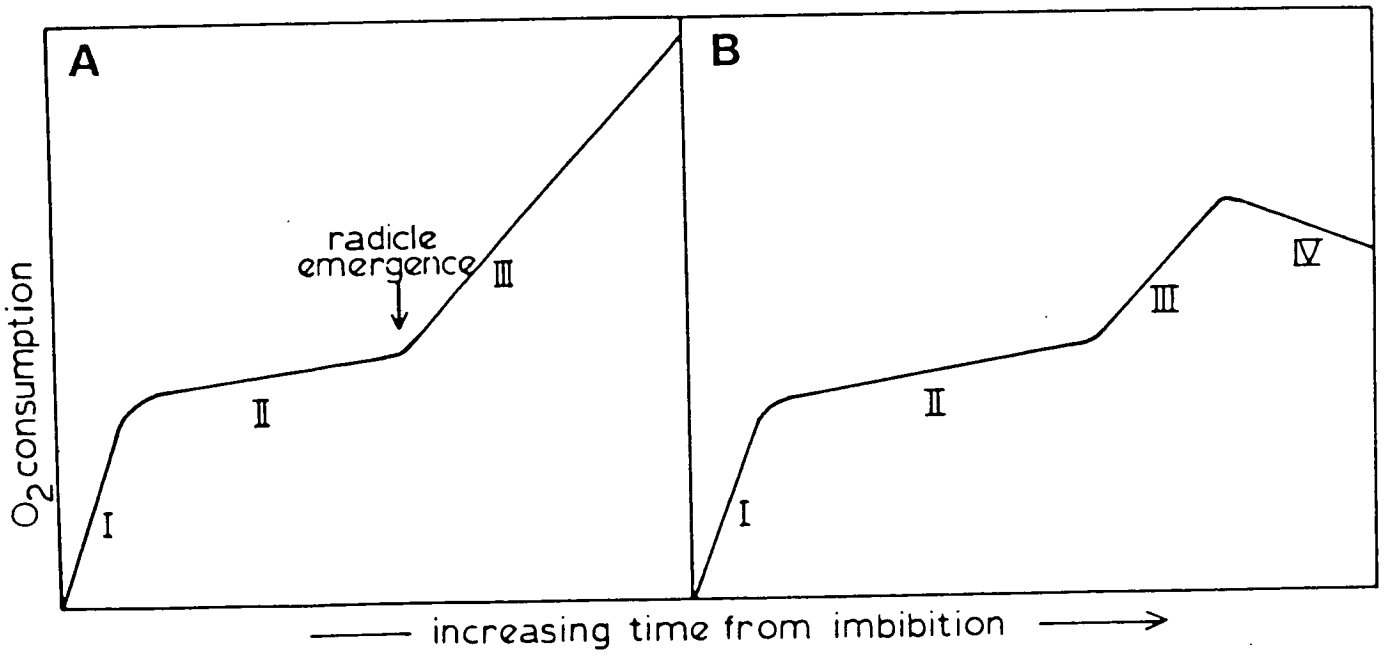

FIGURE 1.1: *Oxygen uptake during germination and early seedling development.* The pattern of oxygen uptake during germination and early seedling development in:

A. embryo tissue.

B. storage tissue.

Refer to text for details. (From Bewley and Black, 1985).

mustard and cotton, possesses an acid or neutral lipase in the lipid body which is induced during germination. The second group, which has soybean, peanut and cucumber among its members, does not have any lipase activity associated with the lipid body at any stage, but possesses a glyoxysomal alkaline lipase.

In germinating oilseeds, the enzymes of the β-oxidation cycle are located exclusively in the glyoxysomes (Cooper and Beevers, 1969b). There are four steps in the β-oxidation cycle (Figure 1.2; see Kindl (1987) for review). First the fatty acid is activated to its acyl-CoA derivative by fatty acyl-CoA synthetase. This is then oxidised by acyl-CoA oxidase, an FAD containing enzyme producing hydrogen peroxide, to the enoyl-CoA derivative, which is converted into the 3-ketoacyl-CoA by cleavage of water and dehydrogenation, both reactions being catalysed by the so-called multifunctional protein. Acetyl-CoA is split from the β-keto ester by reacting with CoA, resulting in an acyl-CoA having a carbon chain that is two carbon atoms shorter than the starting material (reaction catalysed by thiolase). In animal cells the enzymes of the β-oxidation cycle are located both in the mitochondria, where the oxidation of acyl-CoA is catalysed by an NAD dependent dehydrogenase linked to the respiratory chain, and in the peroxisome. There is now some evidence that β-oxidation may also be located in plant mitochondria, particularly in non-fatty tissues: both carnitine-dependent fatty acid uptake and β-oxidation have been reported in pea cotyledon mitochondria (Wood *et al.*, 1984, 1986; Burgess and Thomas, 1986; Thomas and Wood, 1986). The enzymes of β-oxidation have also been detected in mitochondria from the spadices of *Arum maculatum* and oilseed rape seeds (Masterson *et al.*, 1990). In contradiction to these observations there is evidence apparently confirming the sole peroxisomal location of β-oxidation in non-fatty tissues (Gerhardt, 1983; Macey, 1983; Macey and Stumpf, 1983). The resolution of this conflicting data awaits further investigation.

Acetyl-CoA is converted to 4-carbon acids via the glyoxylate cycle (see Figure 1.3; Beevers, 1980). This cycle was first described for microorganisms growing on acetate as the sole carbon source (Kornberg and Krebs, 1957). The cycle is dependent upon two enzymes which are unique to it: isocitrate lyase, which splits isocitrate into succinate and glyoxylate; and malate synthase, which produces malate from glyoxylate and acetyl-CoA. Combined with the TCA cycle enzymes citrate synthase, aconitase and malate dehydrogenase, these enzymes can convert two molecules of acetyl-CoA into a 4-carbon acid, such as succinate or malate. The characteristic enzymes of the glyoxylate cycle are present in castor bean endosperm (Kornberg and Beevers, 1957) and a wide range of other lipid storing tissues, including the cotyledons of cucumber, sunflower and marrow (Beevers, 1980). Confirmation that the pathway does indeed operate *in vivo* was obtained by studying the fate of

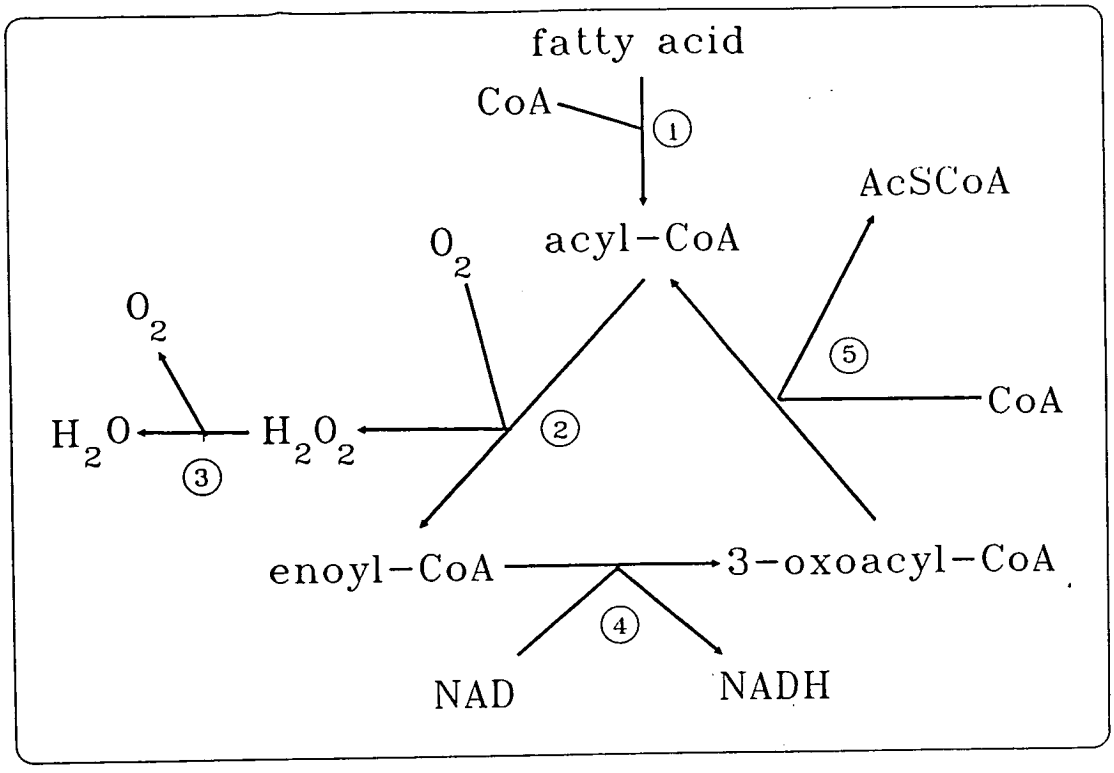

FIGURE 1.2: *The pathway of β-oxidation.* The enzymes are: 1. fatty acyl CoA synthetase, 2. acyl CoA oxidase, 3. catalase, 4. multifunctional protein, 5. thiolase.

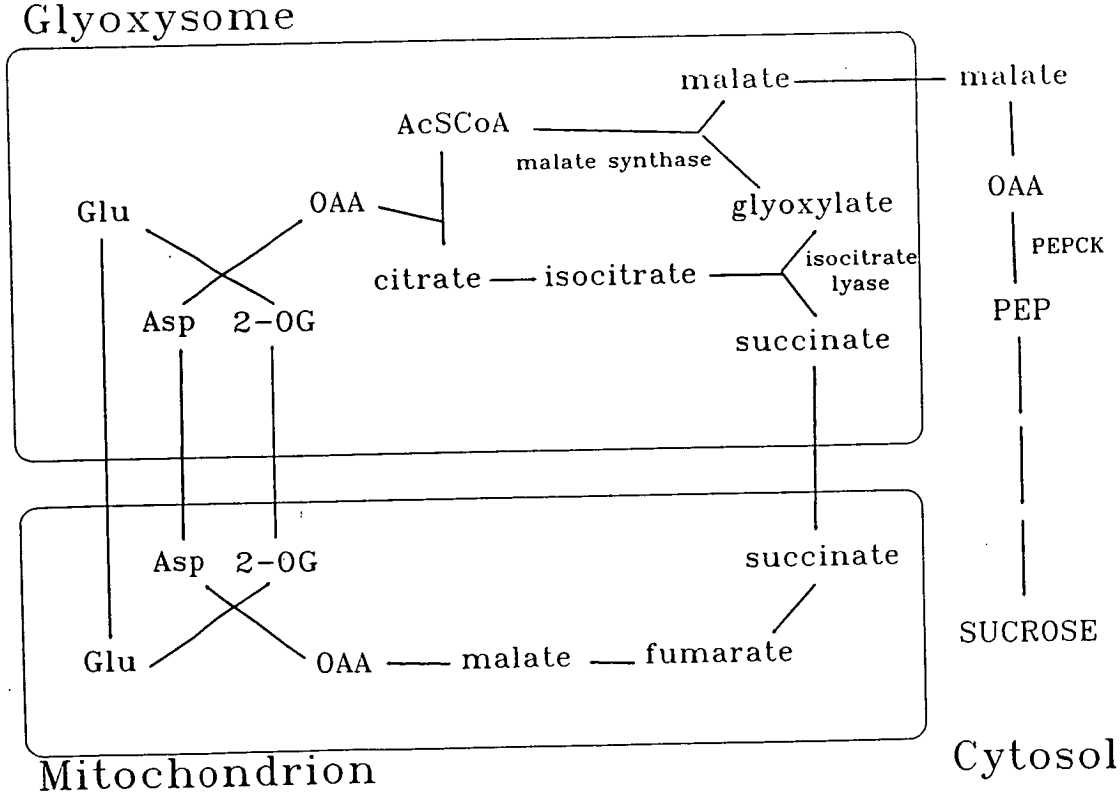

FIGURE 1.3: *The pathway of the glyoxylate cycle.*

^{14}C-labelled acetate when fed to isolated castor bean endosperm (Canvin and Beevers, 1961). These experiments also highlighted the efficiency of the process, with only 25 % of the supplied label being lost as carbon dioxide.

Both malate synthase and isocitrate lyase are located in the glyoxysome (Breidenbach and Beevers, 1967; Breidenbach *et al.*, 1968), but this organelle does not contain all the enzymes required for the operation of the glyoxylate cycle (Cooper and Beevers, 1969a). Succinate dehydrogenase and fumarase are both located exclusively in the mitochondria, so that it is necessary for there to be transport of metabolites between glyoxysomes and mitochondria. Additionally, there must be a mechanism for the reoxidation of glyoxysomal NADH produced during β-oxidation. The glyoxysome membrane contains an electron transfer chain, which can oxidise NADH *in vitro*, but the physiological significance of this is unclear as it apparently lacks a terminal electron acceptor (Fang *et al.*, 1987). There is considerable experimental support for the mitochondrial oxidation of glyoxysomal NADH (Cooper and Beevers, 1969b; Lord and Beevers, 1972; Beevers, 1978). Convincing evidence for the operation of a malate/aspartate shuttle for the transport of both carbon and reducing equivalents between glyoxysomes and mitochondria is provided by the work of Mettler and Beevers (1980) on glyoxysomes and Millhouse *et al.* (1983) on mitochondria. It is the reaction scheme based on this work that is illustrated in Figure 1.3.

The final stage in the conversion of lipid to sucrose is sucrose synthesis itself, which occurs in the cytosol (Nishimura and Beevers, 1979). The key enzyme, which is unique to germinating seedlings, is phospho(enol)pyruvate carboxykinase (PEPCK), converting oxaloacetate to phospho(enol)pyruvate. This is then metabolised to hexose phosphate, the irreversible step in glycolysis (phosphofructokinase, PFK) being by-passed by a fructose-1,6-bisphosphate 1-phosphatase (FBPase). Sucrose is then formed from fructose-6-phosphate and UDP-glucose by sucrose phosphate synthase.

Studies concerning the regulation of the conversion of fat to sucrose have focussed on two major areas, namely, the regulation of the glyoxylate cycle by the *de novo* synthesis of the key enzymes malate synthase and isocitrate lyase (Becker *et al.*, 1978), and fine control of the cytosolic reactions between oxaloacetate and sucrose. The former will be dealt with in some detail in section 1.1.3. Analysis of the regulation of sucrose synthesis in the cotyledons of post-germinative marrow (*Cucurbita pepo*) seedlings indicates that PEPCK and FBPase are the only steps in the pathway significantly displaced from equilibrium, and are therefore the likely sites of regulation (Leegood and ap Rees, 1978c). More recent work on germinating pea cotyledons suggests that sucrose-phosphate synthase and sucrose phosphatase are potential regulatory steps (Lunn and ap Rees, 1990).

The activity of PEPCK is unaffected by a range of intermediary metabolites (Leegood and ap Rees, 1978a), so this step does not appear to be a good candidate for fine

control *in vivo*. However, both castor bean endosperm and marrow cotyledons contain appreciable activity of phospho(enol)pyruvate carboxylase (PEPCase) (Benedict and Beevers, 1961; Leegood and ap Rees, 1978c), which catalyses what is essentially the reverse reaction and is affected by a number of metabolites (Wong and Davies, 1973). Thus the net flux between oxaloacetate and phospho(enol)pyruvate could be influenced by a change in the activity of PEPCase. The regulatory properties of PEPCase from a gluconeogenic tissue have not been determined, but the enzyme from maize leaves is activated by hexose phosphates, Pi and AMP, and inhibited by ATP and ADP (Wong and Davies, 1973). FBPase is also part of a complex 'futile cycle', consisting of three enzymes: FBPase itself, PFK and pyrophosphate fructose-6-phosphate 1-phosphotransferase (PFP). The latter, unlike the other two, is freely reversible and the direction in which it operates *in vivo* has yet to be established (ap Rees, 1985). The maximum activity of PFK is less than 3 % of that of FBPase in marrow cotyledons (Leegood and ap Rees, 1978b), so that its affects on regulation of the pathway may be ignored. FBPase from castor bean endosperm is inhibited by Pi and AMP (Youle and Huang, 1976) and PFP from the same source is inhibited by Pi and 3-phosphoglycerate, and activated by fructose-6-phosphate (Kruger *et al.*, 1983; Kombrink and Kruger, 1984; Kombrink *et al.* 1984). In addition both enzymes are affected by the regulatory metabolite fructose-2,6-bisphosphate (Kruger and Beevers, 1984, 1985), FBPase being inhibited and PFP being activated. The enzymes responsible for the synthesis and degradation of fructose-2,6-bisphosphate respond to metabolites such that an increase in Pi or fructose-6-phosphate, or a decrease in 3-phosphoglycerate results in an increase in fructose-2,6-bisphosphate levels (Kruger and Beevers, 1985).

These observations are consistent with the following hypothesis for the control of gluconeogenesis *in vivo*. β-oxidation produces more NADH than is required for gluconeogenesis and the mitochondrial oxidation of this NADH leads to ATP synthesis. Owing to the near equilibrium of the adenylate kinase reaction (Kobr and Beevers, 1971; Leegood and ap Rees, 1978c) this leads to a concomitant decrease in both AMP and Pi, resulting in a drop in the level of fructose-2,6-bisphosphate and consequent increase in the flux to sucrose synthesis pathway, if PFP is assumed to function in the glycolytic direction. The rate of sucrose synthesis is further modulated by the steady state levels of intermediates in the pathway - if 3-phosphoglycerate builds up the flux increases; if fructose-6-phosphate builds up the flux decreases. This hypothesis is supported by the following observations: (a) ATP levels rise at the onset of gluconeogenesis (Kobr and Beevers, 1971); and (b) anoxia or treatment with 3-mercaptopicilinic acid, which both reduce the flux to sucrose, leads to an increase in the fructose-2,6-bisphosphate level and a decrease in the 3-phosphoglycerate level (Kruger and Beevers, 1985). The regulation of

sucrose synthesis in gluconeogenic tissues thus appears to be similar to that described for photosynthetic tissues (Stitt *et al.*, 1987a).

1.1.3 Glyoxysome and Peroxisome Biogenesis.

This topic has attracted a considerable attention in recent years, and has been reviewed extensively (Beevers, 1979; Huang *et al.*, 1983; Trelease, 1984; Kindl, 1987). The following is not a complete review of the literature, but an overview of selected aspects of microbody biogenesis during early seedling development. Three aspects will be considered; the development of glyoxysomes immediately following germination; the conversion of glyoxysomes into leaf-type peroxisomes during greening of lipid storing cotyledons; and the control of gene expression underlying both these processes.

It is not clear whether glyoxysomes are present in ungerminated seeds, but there is considerable evidence to support a massive increase in either glyoxysome number or size during early seedling development (Gerhardt and Beevers, 1970; Trelease *et al.*, 1971; Becker *et al.*, 1978). Based largely on ultrastructural evidence and comparative biochemistry, a model has been proposed to account for glyoxysome biogenesis, termed the endoplasmic reticulum (ER) vesiculation model (Beevers, 1979). In its simplest form this model states that proteins destined for the glyoxysomal membrane or matrix are synthesised on the rough ER and are inserted into the ER membrane or cotranslationally transported to the lumen of the ER, according to the signal hypothesis of Blobel and Dobberstein (1975). The proteins are then post-translationally modified and translocated to regions of the smooth ER, where glyoxysomes are formed as ER vesicles. The ultrastructural evidence for this model is based mainly on the observation of close associations between glyoxysomes and the ER (Gruber *et al.*, 1970), though membrane continuity between these organelles is observed, if somewhat infrequently (Choinski and Trelease, 1978). Further support is provided by the observations that phospholipid profiles of the ER and glyoxysome membranes are similar (Donaldson and Beevers, 1977) and the apparent cosedimentation of glyoxysome specific enzymes with enzymatic markers for the ER (Gonzalez and Beevers, 1976; Kagawa and Gonzalez, 1981). There is some doubt as to the validity of the latter two pieces of evidence. Despite the similarity in the phospholipid profiles between the ER and glyoxysome membranes there are significant differences in the distribution of phosphatidylcholine between the inner and outer leaves of the membranes (Cheesebrough and Moore, 1980). Identification of very high molecular weight cytosolic aggregates of glyoxysome enzymes may account for the cosedimentation data (Kindl, 1982a). There is now an appreciable body of evidence to suggest that glyoxysomal proteins are synthesised on cytosolic ribosomes and exist as a cytosolic pool, prior to post-translational import into the glyoxysome (Kindl, 1982a; Kruse and Kindl, 1982; Fujiki *et al.*, 1984). The following revision of the ER vesiculation model seems consistent with the available data: the

glyoxysome membrane is derived from the ER, but by a mechanism more complex than simple membrane flow; glyoxysomal matrix and membrane associated proteins are synthesised in the cytosol and imported post-translationally. The route taken by proteins integral to the glyoxysome membrane is unclear.

During the greening of lipid mobilising tissues there is a switch in the major microbody type from glyoxysome to leaf-type peroxisome. These two organelles must coexist as there is synthesis of glyoxysome components during greening (Betsche and Gerhardt, 1978; Koller and Kindl, 1978). Two models have been used to describe this transition:

1. The interconversion model: peroxisomal proteins are inserted into the glyoxysomes, forming the so-called glyoxyperoxisome, and then glyoxysome specific proteins are removed (Trelease *et al.*, 1971).

2. The two population model: peroxisomes are synthesised entirely *de novo* and glyoxysomes are completely removed (Kagawa and Beevers, 1975).

The evidence in favour of the interconversion model is as follows. Ultrastructural studies show that the number of microbodies present does not change during greening (Trelease *et al.*, 1971), and single microbodies are observed appressed to both a lipid body and a chloroplast during the transition phase (Schopfer *et al.*, 1976; Bergfeld *et al.*, 1978). Transmission electron microscope studies on immunogold labelled cotyledon sections have demonstrated the simultaneous occurrence of glyoxysome and peroxisome proteins within a single microbody (Titus and Becker, 1985). Experiments with isolated microbodies demonstrate interactions between products of β-oxidation and the glyoxylate cycle with the peroxisome-specific glycolate to glycine pathway (Kindl, 1982b). There is a specific degradation of malate synthase in microbodies isolated from greening pumpkin cotyledons (Mori and Nishimura, 1989). Evidence in support of the two population model comes largely from the work of Kagawa and Beevers (1975), who describe a major loss of protein from the glyoxysomal fraction in dark grown water-melon seedlings, which is accelerated by light. There is also evidence for new membrane synthesis in microbodies during greening (Kagawa *et al.*, 1975). The validity of both these pieces of data is questionable because of contamination of the microbody fractions, by proteins bodies in the first instance (Becker *et al.*, 1978), and by plastid membrane fragments in the second case (Huang *et al.*, 1983). Thus there seems to be an overwhelming weight of evidence in favour of the interconversion model of Trelease *et al.* (1971).

The processes of glyoxysome biogenesis and glyoxysome/peroxisome interconversion are of necessity accompanied by changes in gene expression. In developing cotyledons, post-germinative increases in malate synthase and isocitrate lyase activities are accompanied by changes in the levels of their polypeptides and mRNA (Smith and Leaver, 1986; Allen *et al.*, 1988). Expression of genes controlled by the cucumber malate synthase

promoter in transgenic *Nicotiana plumbaginofolia* and *Petunia hybrida* plants suggests that expression of malate synthase may be induced by metabolites characteristic of lipid mobilisation and repressed during greening (Graham *et al.*, 1990). This hypothesis is further supported by the presence of a putitative cAMP-responsive cis-acting DNA sequence in the 5' flanking region of the gene, which may be involved in responses to metabolite status or plant growth regulators (Graham *et al.*, 1989). Recent work indicates that malate synthase is also present in senescing leaves (Gut and Matile, 1988) and that this is due to induction of the malate synthase gene (Graham, 1989). This may be in response to the products of chloroplast membrane or pigment degradation (I. A. Graham, pers. comm.). The expression of peroxisomal components in greening cucumber cotyledons is also regulated at the level of gene expression and is strictly light dependent (Hondred *et al.*, 1987). The importance of growth regulators and metabolite status in the regulation of storage reserve mobilisation will be considered in the following section.

1.1.4 The Control of Storage Reserve Mobilisation.

It has long been established that the presence of the axis (or embryo in seeds with major endosperm storage reserves) is required for storage reserve mobilisation (Davies and Slack, 1981). Two possible roles for the axis/embryo have been postulated; either as the source of a diffusible activator ("hormonal control") or as the consumer of the products of storage reserve mobilisation ("the sink effect"). In the grasses, particularly barley, there is considerable data to confirm a role for embryo produced plant growth regulators, namely gibberellic acids and abscisic acid, in the induction of carbohydrate mobilising enzymes at the level of gene expression (see, for example, Jacobsen and Beach, 1985). In dicots the situation is more complex (Davies and Slack, 1981). In castor bean, germination and lipid mobilisation are accelerated by the application of exogenous gibberellic acids, the effect being abolished by abscisic acid (Northcote, 1986). This is correlated with an increase in the transcripts for glyoxylate cycle enzymes (Martin *et al.*, 1984; Rodriguez *et al.*, 1987). In germinating lettuce seeds, both cytokinins and gibberellic acids can replace the effect of the axis on mannase production in the endosperm, whilst abscisic acid has an inhibitory effect (Halmer and Bewley, 1979). In cucumber seedlings there is no evidence for a role for plant growth regulators in the control of lipid mobilisation. Although axis removal results in a reduction in lipid mobilisation in the cotyledons, there is no effect on the activity of lipase, isocitrate lyase, malate synthase or FBPase (Slack *et al.*, 1977; Davies and Chapman, 1979a). There is an inverse relationship between the inhibition of lipid hydrolysis and the accumulation of sucrose in the cotyledons, providing evidence that lipid mobilisation is controlled by the sink effect of the axis (Slack *et al.*, 1977; Davies and Chapman, 1979b). Testa removal to allow free oxygen exchange to the cotyledons may also have a regulatory role during germination of squash seeds (Cerana *et al.*, 1974).

1.2 Mitochondria in Plants.

1.2.1 Fundamental mitochondrial functions.

The primary role of mitochondria in all organisms is the generation of ATP by oxidative phosphorylation. The mechanism by which this is achieved was first described by Mitchell (1966) and has become known as the chemiosmotic hypothesis. Oxidation of carbohydrates by the TCA cycle leads to the production of NADH, which is oxidised by Complex I of the electron transfer chain. Electrons resulting from this reaction are transferred to oxygen by the components of the electron transfer chain, which, in the process, transfer protons across the inner mitochondrial membrane to the inter-membrane space. The proton gradient generated drives protons back across the inner membrane through the F_1-F_0 ATP synthase, which couples proton flow to the synthesis of ATP from ADP and phosphate.

1.2.2 Functions unique to plant mitochondria.

In addition to the basic mitochondrial components described above, the TCA cycle and electron transfer chain, mitochondria from higher plants possess a number of additional features.

(i) *Modified TCA cycle.* The pathway of the TCA cycle in plant mitochondria is shown in Figure 1.4. In addition to the usual enzymes, plants possess NAD-malic enzyme (Macrae, 1971). This enzyme catalyses the reductive decarboxylation of malate to pyruvate. The function of this enzyme is unknown, but it has been suggested (Wiskich and Dry, 1985) that the presence of this enzyme would allow either operation of the TCA cycle without a 3-carbon substrate, or the removal of intermediates from the cycle. The only tissue examined to date where only low activities of this enzyme are found is the nitrogen fixing nodules of soybean (Bryce and Day, 1990). This is thought to facilitate the production of oxaloacetate required for nitrogen fixation.

(ii) *Modified electron transfer chain.* In addition to the usual electron transfer chain components, mitochondria from plants also possess a number of complexes not coupled to proton translocation. A schematic representation of the plant electron transfer chain is shown in Figure 1.5. The following additional complexes are present:

a. Rotenone-insensitive NADH dehydrogenase (Brunton and Palmer, 1973).

b. External NADH dehydrogenase (Douce *et al.*, 1972).

c. Cyanide-insensitive alternative oxidase (Bendall and Bonner, 1971).

The rotenone insensitive by-pass of complex I is able to oxidise matrix NADH without translocating protons across the inner mitochondrial membrane. The function of this by-pass is not clear, but recent work has shown that high rates of state 4 (ADP limited) respiration by soybean cotyledon and nodule

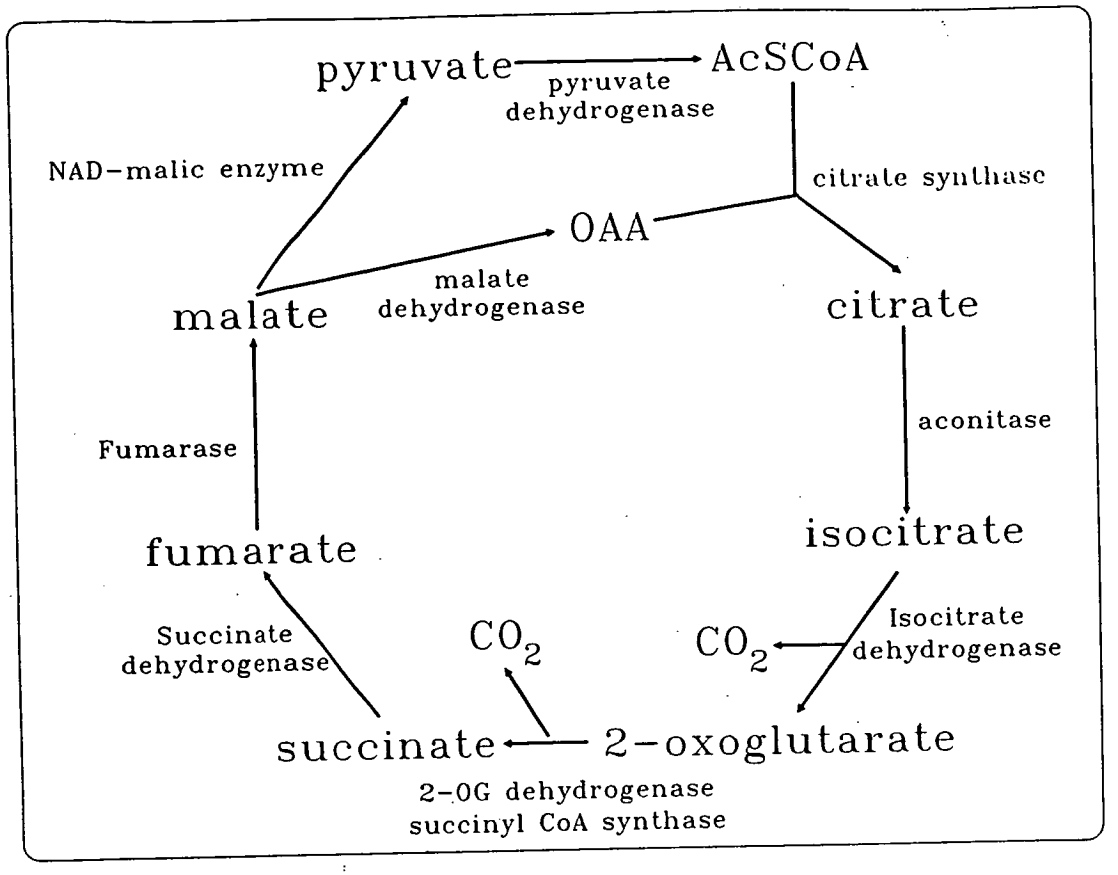

FIGURE 1.4: *The TCA cycle in plant mitochondria.*

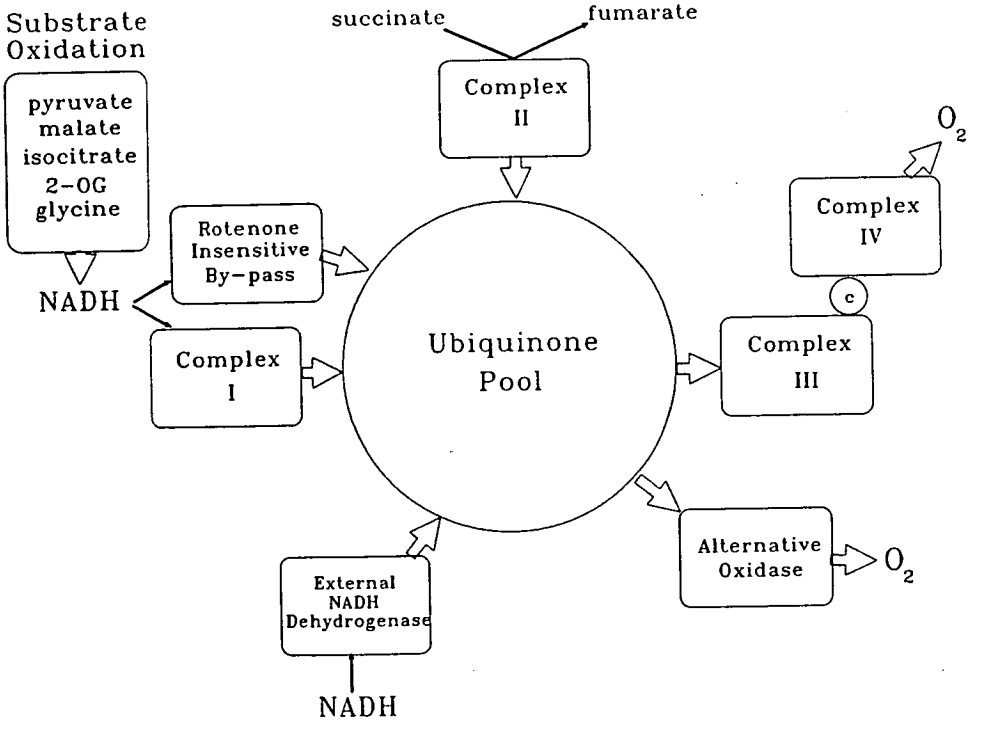

FIGURE 1.5: *The electron transfer chain in plant mitochondria.*

mitochondria are correlated with high capacities of the by-pass (Bryce *et al.*, 1990). This suggests that this step may be important in maintaining respiration when ATP/ADP ratios are high. Increased engagement of the by-pass is only likely to occur during state 4 respiration as, under these conditions, the mitochondrial NADH/NAD ratio is high (Day *et al.*, 1987) and the affinity of the by-pass for NADH is lower than that of complex I (Moller and Palmer, 1982).

There are at least two externally facing complexes capable of oxidising cytosolic NADH (Palmer and Ward, 1985). The first is located in the outer mitochondrial membrane and is not linked to the inner membrane electron transfer chain (Douce *et al.*, 1973). The second is located in the inner mitochondrial membrane and passes electrons directly to the ubiquinone pool (Douce *et al.*, 1973). There is evidence to suggest that internal NADH is oxidised preferentially when mitochondria are confronted with a mixture of NADH and a TCA cycle substrate (Cowley and Palmer, 1980; Dry *et al.*, 1983), though the mechanism of this interaction is unclear. The external NADH dehydrogenase has an absolute requirement for calcium, as NADH oxidation is completely inhibited by EGTA, this inhibition being reversed by adding calcium (Moller *et al.*, 1981; Moore and Akerman, 1982).

Cytochrome oxidase is inhibited by cyanide. However, plant tissues differ from those of animals in that they show marked cyanide resistant respiration (see Lance *et al.*, 1985 for review). This respiration is due to the presence of a second route for the transfer of electrons from ubiquinone to oxygen, termed the alternative pathway (Lance *et al.*, 1985). This pathway is inhibited by salicyl hydroxamic acid (SHAM) and its derivatives (Lance *et al.*, 1985). The alternative oxidase has been characterised in some detail - it catalyses the transfer of electrons from ubiquinone to oxygen, by-passing both complexes III and IV of the respiratory chain. Despite some initial controversy, the function of the alternative oxidase has been localised to a protein in the inner mitochondrial membrane which has been partially purified (Hiser and McIntosh, 1990). Two major hypotheses have been offered to explain the function of the alternative pathway. Bahr and Bonner (1973) suggested that the alternative oxidase may allow mitochondrial substrate oxidations, required to supply carbon skeletons for biosynthesis, to take place while cellular ATP levels are high. An alternative hypothesis was put forward by Lambers and Steingrover (1978), who argue that the alternative pathway represents a mechanism of disposing of 'excess' photosynthate. The work of Azcon-Bieto *et al.* (1983) is taken as support for this hypothesis, as these workers demonstrate increased engagement of the alternative pathway in wheat leaves at the end of the light period, as compared with the end of the night. Moreover, feeding of sugars to leaves after a period of darkness stimulated the alternative pathway. This data does not, however, exclude the possibility that increased carbohydrate levels stimulate the biosynthetic processes in which the hypothesis of Bahr and Bonner (1973) involves the

alternative pathway. In addition, pruning of barley seedlings leads to wide variations in both the carbohydrate status and respiratory rate in the roots, but no change in the engagement of the alternative pathway (Bingham and Farrar, 1987). The role of the alternative pathway remains an open question, but, considering its widespread nature, and the range of biochemical adaptations found in plants which maximise carbon fixation, the hypothesis of Bahr and Bonner (1973) seems the more likely.

(iii) *Glycine oxidation.* The phenomenon of photorespiration observed in C3 plants is due to the lack of specificity of ribulose bisphosphate carboxylase. Oxygen, rather than carbon dioxide, is fixed, resulting in the synthesis of the C2 acid glycolate which is converted to 3-phosphoglycerate via the cycle shown in Figure 1.6. (Douce, 1985). A crucial reaction in this cycle is the conversion of two molecules of glycine to serine, which is catalysed within the mitochondria by two enzymes, glycine decarboxylase and serine hydroxymethyl transferase (Neuburger *et al.*, 1986). The fate of the NADH produced in this reaction is a matter of debate. In isolated mitochondria NADH is undoubtedly reoxidised by the respiratory chain with the concomitant synthesis of ATP (Douce *et al.*, 1977). However, it is argued that *in vivo*, NADH is required for the reduction of hydroxypyruvate to glycerate and so is transferred to the peroxisome by means of a malate aspartate shuttle (Dry *et al.*, 1987). The use of rapid fractionation techniques has demonstrated that inhibition of photorespiration in barley leaf protoplasts results in a drop in both the cytosolic and mitochondrial ATP/ADP ratios (Gardestrom and Wigge, 1989). The fate of NADH generated by glycine oxidation has been further complicated by recent studies into the simultaneous oxidation of glycine and malate by isolated pea leaf mitochondria (Wiskich *et al.*, 1990). The observation that addition of malate stimulates the state 4 glycine oxidation rate leads these authors to suggest that NADH synthesised during glycine oxidation can be reoxidised by malate dehydrogenase operating in the oxaloacetate to malate direction, and, moreover, to hypothesise that there are two distinct pools of malate dehydrogenase within the mitochondrial matrix (Wiskich *et al.*, 1990).

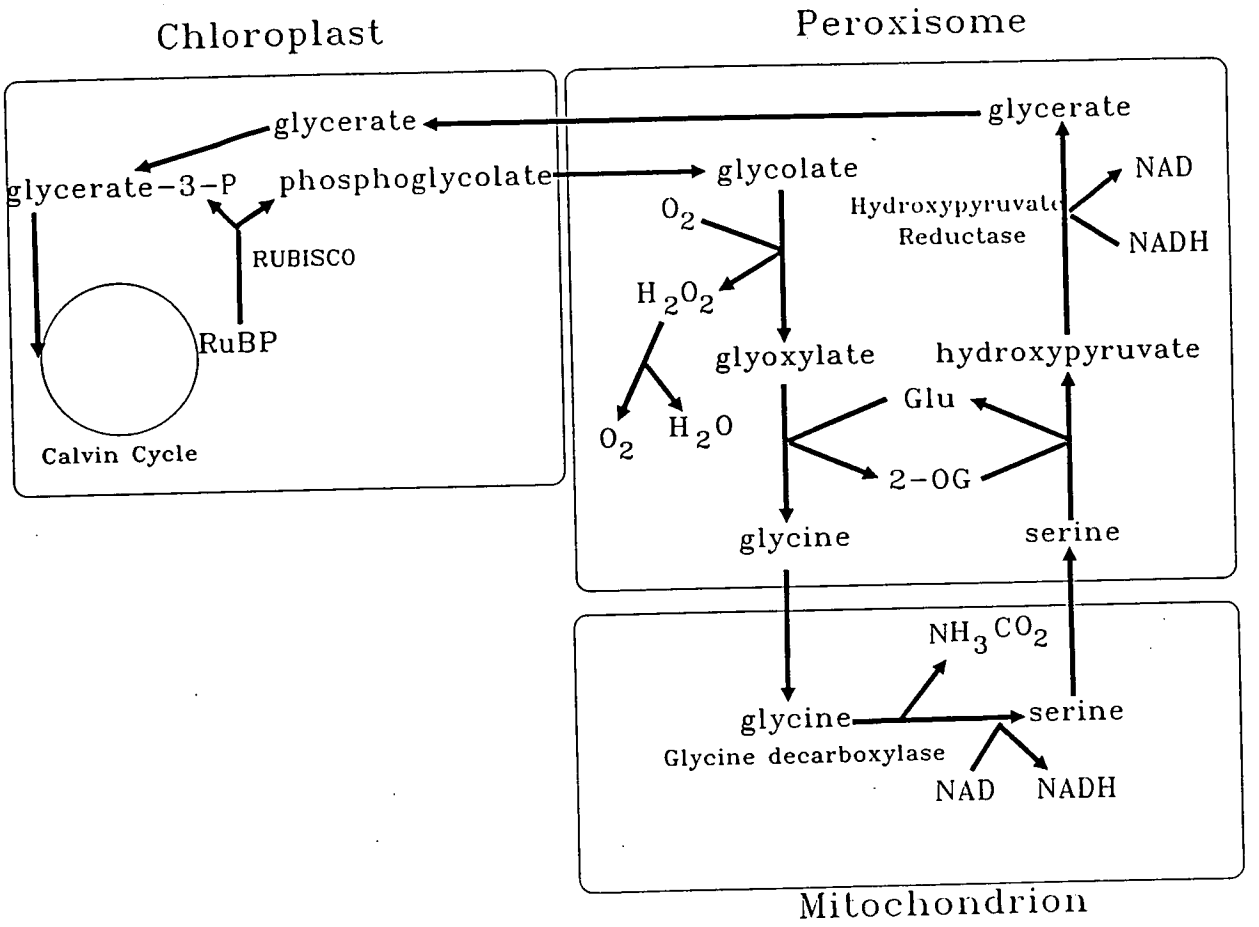

FIGURE 1.6: *The pathway of photorespiration.*

1.2.3 The integration of mitochondrial function with metabolism.

In addition to the generation of ATP, mitochondria in plant tissues play a significant role in a number of other aspects of plant metabolism. The following have already been mentioned: gluconeogenesis from lipid (1.1.2); the generation of intermediates for biosynthesis (1.2.2); and photorespiration (1.2.2). The composition of plant mitochondria differs from that of animals in a number of aspects, as described above, presumably to enable these functions to be carried out as efficiently as possible. It is not unreasonable to suppose that control mechanisms must exist such that the mitochondrial components of specific pathways operate at the optimum rate. Despite the detailed attention which the nature of the pathways operating in mitochondria and their regulation have attracted (see Douce, 1985; and Dry *et al.*, 1987 for reviews), little work has been carried out concerning the integration of mitochondrial respiration with cellular metabolism. It is the aim of the work presented in this thesis to attempt to fill this gap in our knowledge of the control of plant metabolism. This will involve the investigation of three major hypotheses, using cucumber cotyledons during early seedling development: first, that mitochondrial metabolism is controlled such that respiration and the diverse functions which mitochondria perform are integrated with cellular biochemical demands; secondly, that this control varies during early seedling development due to the changing metabolism of cotyledon tissue; and thirdly, that these changes are brought about by changes in mitochondrial composition due to the *de novo* synthesis of proteins (mitochondrial biogenesis).

1.3 The Study of Metabolic Control.

In order to study the integration of mitochondrial respiration with metabolism it is necessary to gain a detailed understanding of the control of respiration and associated processes. The following describes in detail the methodology with which I have chosen to approach this problem - metabolic control theory.

1.3.1 General Introduction.

The elucidation of how living systems are controlled has occupied biologists since the earliest developments of the subject. This has been particularly true of the study of metabolism, where the problem of how the rates of metabolic pathways are regulated in order to optimise an organisms growth and reproduction is central to the field.

A theoretical approach to this problem was first provided by Blackman (1905) in his 'Optima and Limiting Factors'. The essential thesis of this work became known as the Law of Limiting Factors and dominated thinking on metabolic regulation for over half a century. The Law, based on the observations of Blackman and others on photosynthesis, states that 'when a process is conditioned as to its rapidity by a number of separate factors, the rate of this process is limited by the pace of the slowest factor'. The

fundamental flaw in this law, as applied to metabolic pathways, is that it totally ignores the principle of mass action, which states that the rate of a chemical reaction is proportional to the concentration of the starting material. Metabolic pathways tend to reach a steady state where the concentrations of all associated metabolites are constant and the rate of all the steps is the same - Blackman's 'slowest factor' does not exist. The idea of a single factor controlling a metabolic process was taken a stage further with the introduction of the concept of the pacemaker reaction by Krebs (1957). This dictates that a single step 'limits' flux through a metabolic pathway, and that this is the step catalysed by the enzyme with the lowest catalytic activity. The invalidity of this approach is revealed by a comparison of the maximum activities of enzymes and the flux through pathways *in vivo*: most enzymes operate *in vivo* well below their maximum activities. Despite this, methodologies were developed to determine 'pacemaker' reactions by Chance (1958) and Newsholme and Start (1973). Both of these methods are essentially qualitative and assume that one, or a small proportion , of the reactions in a pathway exert control. The theoretical consideration of metabolism was revolutionised by the seminal ideas of Kacser and Burns (1973) and Heinrich and Rapoport (1974), which have come to be termed metabolic control theory. These authors abandoned the concept of the 'pacemaker' reaction, and considered metabolism as an integrated system rather than a collection of unrelated steps. This allowed them to develop a quantitative framework for the description of metabolic control, which forms the basis for the remainder of this discussion.

The 'systems approach' to biology owes its development to the pioneering work of Weiner and colleagues in the late 1940s. This led to the publication of 'Cybernetics - control and communication in the animal and the machine' by Weiner (1948). The essence of the systems approach is that the interaction between the components of a system results in systemic properties which are dependent on both the properties of the components and the interrelationship between them. Using the arguments of group theory Beer (1965) demonstrated that a complete understanding of the control of a system requires a complete knowledge of the system itself. However, large complex systems can be divided into subsystems and the regulatory interactions between these subsystems determined (Beer, 1965). Successive applications of this process should lead ultimately to the complete understanding of the control of the large system. Metabolic control theory provides an analytical means whereby this approach can be applied to metabolic pathways.

1.3.2 General principles.

Metabolic control theory, as described by Kacser and Burns (1973) and Heinrich and Rapoport (1974), is dependent upon assignment of numerical coefficients to the responses of the steady state system variables (for example, flux) to small changes in the

system parameters (for example, enzyme concentration). These are termed the control coefficients (${}^{V}C_{P}$), the effect of a parameter, P, on a variable, V, is given as:

$$ {}^{V}C_{P} = \frac{dV/dP}{V/P} \tag{1.1} $$

The coefficients of most interest are those describing the effect of changes in enzyme concentration on system parameters including flux, metabolite concentrations and transition time, known as the flux, concentration and transition time control coefficients, respectively.

The control coefficients are properties of the whole system. Such systemic effects arise because each component of the system, an enzyme, is linked to all the others via shared metabolite pools. The nature of these is also quantified in terms of local properties, termed the elasticity coefficients (ε). These are defined as the response in the rate of a reaction to a change in a metabolite concentration, under systemic conditions. This is expressed mathematically as:

$$ {}^{v}\varepsilon_{S} = \frac{dv/dS}{v/S} \tag{1.2} $$

where v is the velocity of the reaction and S is the metabolite concentration. The elasticity coefficient of an enzyme can be related directly to its kinetic properties. For example, Kacser (1987) has demonstrated that for a reversible step, where the enzyme catalysing the reaction obeys Michaelis-Menton kinetics, the elasticity to the substrate of the reaction, S, is given by:

$$ {}^{v}\varepsilon_{S} = \frac{S}{S - P/K_{eq}} - \frac{S/K_{S}}{1 + S/K_{S} + P/K_{P}} \tag{1.3} $$

where P is the product concentration, K_{eq} is the equilibrium constant, K_{S} is the Michaelis-Menton constant in the forward direction (with respect to S), and K_{P} is the Michaelis-Menton constant in the reverse direction (with respect to P).

1.3.3 The fundamental theorems: summation and connectivity.

Having defined the coefficients described above, Kacser and Burns (1973) were able to prove two important relationships between them.

The summation theorem states that for any pathway, under steady state conditions, with the starting material and end product held at fixed concentrations, the sum of all the flux control coefficients is unity.

$$ \sum_{\text{all } i} {}^{J}C_{i} = 1 \tag{1.4} $$

The connectivity theorem relates the flux control coefficients and the elasticity coefficients. It states that if two enzymes E_1 and E_2 have a shared metabolite X the following relationship holds:

$$^{J}C_1\,^{v1}\varepsilon_X + {}^{J}C_2\,^{v2}\varepsilon_X = 0 \qquad (1.5)$$

where V_i is the velocity of enzyme E_i. One of the implications of these theorems is that for a simple, linear, pathway, knowledge of the elasticities enables the flux control coefficients to be calculated, and *vice versa* (Kacser and Burns, 1973).

1.3.4 Theoretical refinements.

Based on the general principles described in sections 1.3.2 and 1.3.3 metabolic control theory has been extended to cover a wide variety of types of pathway. Central to much of this development has been the use of matrix notation to relate control coefficients to elasticities (Fell and Sauro, 1985; Sauro *et al.*, 1987; Westerhoff and Kell, 1987). This approach has been formalised in mathematical terms by Griesch (1988) and Reder (1988). In general terms the connectivity relationship can be expressed as:

$$E.C = M \qquad (1.6)$$

Where E is the elasticity matrix, C the control matrix, and M the stoichiometry matrix. The elasticity matrix has elements e_{ij} which are the elasticity of metabolite i on step j. The control matrix has elements corresponding to all the flux, concentration, and branch point control coefficients of the system. The stoichiometry matrix has elements m_{ij} which are the stoichiometry of metabolite i with respect to reaction j. The use of matrices has the advantage that the control of a pathway can be described in a simple form irrespective of its structural complexity. The matrix method has been used to extend control analysis to branched pathways (Fell and Sauro, 1985; Sauro *et al.*, 1987), substrate cycles (Fell and Sauro, 1985) and moiety conserved cycles (Hofmeyr *et al.*, 1986).

The matrix method is also important for the determination of flux control coefficients, since elasticities are relatively easy to measure and the stoichiometry matrix can be deduced from the pathway structure. The control coefficients can be calculated from:

$$C = E^{-1}.M \qquad (1.7)$$

The impact of inaccuracies in elasticity measurements on the calculated flux control coefficients has been quantified (Small and Fell, 1990b).

Control analysis has also been applied to covalently modifiable enzymes (Small and Fell, 1990a) and the effects of enzyme cooperativity on systemic properties described (Acerenza and Kacser, 1990). The theory has also been extended to cover transitions between steady states with the definition of the transition time control coefficient (Torres *et al.*, 1989; Melendez-Hevia *et al.*, 1990). The methodology of Beer (1965) to simplify complex systems has recently been explicitly stated in terms of metabolic control as the 'top-down' approach (Brown, Hafner, and Brand, 1990).

1.3.5 Experimental applications of metabolic control theory.

No attempt will be made in the following section to describe all the experimental applications of metabolic control theory to date. However, examples of the use of a number of fundamental methods will be considered, with particular reference to plant systems wherever possible.

The use of elasticities measured *in vivo* to calculate flux control coefficients was first used by Groen *et al.* (1986) in their study of gluconeogenesis from lactate in isolated rat liver cells. Elasticities were calculated either by the measurement of kinetic parameters and disequilibrium constants, or by variation of the flux through the pathway using the inhibitor mercaptopicilinic acid. A complete description of the flux control coefficients of the pathway under a range of externally controlled conditions was achieved by the application of the summation and connectivity theorems.

Inhibitor titrations have been used to directly determine flux control coefficients in isolated mitochondria from animals (Groen *et al.*, 1982), yeast (Mazat *et al.*, 1986) and plants (Padovan *et al.*, 1989). The 'top-down' approach has also been applied to mitochondrial respiration *in vitro* (Hafner *et al.*, 1990) and *in vivo* (Brown, Lakin-Thomas, and Brand, 1990). The latter method involved the use of inhibitors to measure the elasticity of components of the mitochondrial respiratory chain and phosphorylation system to the proton gradient.

Metabolic mutants have been used for the determination of flux control coefficients in a number of systems, including the control of photosynthate partitioning in leaves. Measurement of metabolite levels in a number of mutants in enzymes of the sucrose and starch synthesis pathways has revealed that the control of sucrose synthesis is shared between fructose-1,6-bisphosphatase and sucrose phosphate synthase, whilst control of starch is shared between a number of steps, with most of the control residing at ADP-glucose pyrophosphorylase (Kruckeberg *et al.*, 1989; Neuhaus *et al.*, 1989; Stitt, 1989; Neuhaus *et al.*, 1990; Neuhaus and Stitt, 1990; Smith *et al.*, 1990). This work also shows that changing light intensities have a profound impact on the distribution of control (see, for example, Neuhaus and Stitt, 1990).

Genetic transformation has been used to produce a range of citrate synthase levels in *E. coli*, allowing direct determination of flux control coefficient (Walsh and Koshland, 1985).

The addition of purified enzymes to extracts of rat liver cells *in vitro* has allowed the estimation of flux and transition time control coefficients for a number of the steps of glycolysis (Torres *et al.*, 1986, 1989).

1.4 Experimental Approach.

1.4.1 Developmental system.

The system chosen for studying the integration of mitochondrial function with metabolism is the differentiating cotyledon of cucumber (*Cucumis sativus* L.) during the first seven days following imbibition. This system was selected for the following reasons:

1. The developmental regulation of glyoxysomal metabolism has been studied in some detail in this system in our laboratory (see, for example, Becker *et al.*, 1978).

2. The system is experimentally convenient. Plants are easy to grow free of fungal and bacterial contamination and material is available for experiment no more than seven days after planting.

3. The cotyledon tissue passes through a number of metabolic phases during the period examined, all of which potentially involve mitochondrial function.

4. Cell division does not occur in the cotyledons (Becker *et al.*, 1978), so that any changes observed represent cellular differentiation. In addition, biochemical parameters can easily be expressed on a per cell basis.

1.4.2 Experimental rationale.

Mitochondrial function in the system described was analysed by investigating the developmental variation in the metabolic properties of the mitochondria and their composition, and relating these to the biochemistry of the tissue. This was achieved by first measuring a number of heterotrophic and autotrophic indicators to define cotyledon metabolism. Mitochondrial function was determined by measuring mitochondrial enzyme activities, and rates of substrate oxidation by isolated mitochondria. The control of mitochondrial respiration was then further investigated on the basis of these results, using the methods of metabolic control analysis wherever possible. Attempts were made to relate changes in mitochondrial function to changes in mitochondrial biogenesis.

It was hoped that this approach would yield information concerning the integration of mitochondrial respiration with metabolism and how this is controlled in the cotyledons of cucumber during early seedling development.

The application of metabolic control theory, which involves the analysis of a steady state, to a developmental system, which is not a steady state, can be justified in two ways:

1. Experimental measurements of flux control coefficients were carried out under steady state or near steady state conditions.

2. Although development is a dynamic process when considered over the timescale of days, particular points in development, when examined over the time scale of minutes, approximate to a steady state.

CHAPTER 2.
MATERIALS AND METHODS.

2.1 Materials.

2.1.1 Seed.

Seed of *Cucumis sativus* L. var 'Masterpiece' was supplied by Wm K McNair, 67 Hamilton Drive, Portobello, Edinburgh.

2.1.2 Chemicals and Enzymes.

Chemicals were supplied by British Drug Houses (BDH), Bethesda Research Laboratories (BRL), The Sigma Chemical Company or Boehringer Mannheim, unless otherwise indicated. Chemicals were of the highest available grade. All enzymes were supplied by the Sigma Chemical Company.

2.1.3 Centrifuge Equipment.

Sorvall RC-5B centrifuges were used, in conjunction with Sorvall GSA (6x250 ml capacity) and Sorvall SS-34 (6x50 ml capacity) fixed angle rotors and a Sorvall HB-4 (4x50 ml capacity) swing out rotor. Centrifugations were carried out in 250 ml polycarbonate bottles (Nalgene), 50 ml polycarbonate tubes (Nalgene), 15 or 30 ml glass Corex tubes (Coring). Eppendorf or MSE Micro-Centaur fixed angle microfuges (12000 g) were used to centrifuge 1.5 ml polypropylene tubes (Treff) during small scale manipulations.

2.1.4 Spectrophotometer.

Absorbence was measured using a Beckman DU-64 spectrophotometer equipped with an auto 6-sampler. For enzyme assays data was gathered and analysed using a Beckman Kinetics Soft-Pac module and output on an Epson LX-800 dot matrix printer.

2.1.5 Statistical Analysis.

Descriptive statistics were calculated and Student's t-tests carried out using StatWorks1.2 (Cricket Software Inc.) running on an Apple MacIntosh. Linear regression analysis and curve fitting was performed using Fig-P (Biosoft) running on an IBM PC compatible.

2.2 Growth Conditions and Harvesting.

Seeds of Cucumber, *Cucumis sativus* L. var 'Masterpiece' were imbibed in tap water in the dark at 4°C for 16 hours. The seeds were sown onto wadding (Robinson and Sons Ltd.) thoroughly soaked in distilled water and germinated at 28°C on a 12 hour light/dark cycle with a 5°C night temperature depression in a Fisons model 600G3/THTL growth chamber. The relative humidity around the seedlings was maintained at a high level using a transparent plastic propagator. The light intensity was 200 µmol quanta m^{-2} s^{-1}. For dark grown material the seed trays were wrapped in tinfoil and placed in a black plastic bag within the same growth chamber as the light grown material. Seeds were

planted and harvested within 1 hour of the start of the light period. Cotyledons were harvested onto ice for mitochondrial isolation and preparation of cell free extracts for enzyme assay and SDS-polyacrylamide gel electrophoresis and into liquid nitrogen for substrate level determinations and used immediately.

2.3 Isolation of Mitochondria from Cucumber Cotyledons.

2.3.1 Solutions.

Grinding Buffer:
0.3 M sucrose
25 mM sodium pyrophosphate buffer
10 mM potassium dihydrogen orthophosphate
2 mM EDTA
2 mM magnesium chloride
2 mM glycine
1 %(w/v) polyvinylpyrrolidone-40
1 %(w/v) bovine serum albumin
30 mM iso-ascorbic acid (just before use)
pH 7.6 with potassium hydroxide

Wash Buffer:
0.3 M sucrose
10 mM TES buffer
1 mM glycine
0.1 %(w/v) bovine serum albumin
pH 7.2 with potassium hydroxide

Gradient A:
0.3 M sucrose
10 mM potassium dihydrogen orthophosphate
1 mM glycine
0.1 %(w/v) bovine serum albumin
38 %(v/v) Percoll (Pharmacia)
pH 7.5 with potassium hydroxide

Gradient B:
0.3 M sucrose
10 mM potassium dihydrogen orthophosphate
1 mM glycine
0.1 %(w/v) bovine serum albumin
38 %(v/v) Percoll (Pharmacia)
10 %(w/v) polyvinylpyrrolidone-40
pH 7.5 with potassium hydroxide

2.3.2 Preparation of Washed Mitochondria.

Cotyledons (10-50g) were harvested onto ice, washed with cold distiled water and chilled for 30 minutes at 0°C. All subsequent operations were carried out at 4°C or below. The cotyledons were homogenised in 3 volumes of grinding buffer with four 1-2 second bursts of a Polytron homogeniser at setting 7. The homogenate was filtered through 4 layers of muslin and the filtrate centrifuged at 1000 g_{av} for 5 minutes. The supernatant was

collected and centrifuged at 12000 g_{av} for 20 minutes. The resulting pellet was resuspended in 20 ml Wash buffer using a teflon-in-glass homogeniser and this suspension centrifuged at 1000 g_{av} for 5 minutes. The supernatant was collected and centrifuged at 12000 g_{av} for 20 minutes. The pellet was resusupended in 2 ml Wash buffer and this designated the crude mitochondrial fraction.

2.3.3 Purification of Mitochondria on Percoll Gradients.

The crude mitochondrial fraction obtained form 2.3.2 was contaminated with thylakoid membranes, glyoxysomes, peroxisomes and protein and lipid storage bodies, so that it was necessary to further purify this fraction by density gradient centrifugation. Gradients containing 38 %(v/v) Percoll (Pharmacia) and a linear gradient of 0-10 %(w/v) polyvinylpyrrolidone-40 were produced my mixing 16 ml each of gradient solutions A and B in a centrifuge tube using a linear gradient maker. The crude mitochondrial fraction was carefully layered onto this mixture and the tube centrifuged at 40000 g_{av} for 45 minutes. The mitochondrial band (see 2.3.4) was removed using a pasteur pipette, diluted with 5-10 volumes of Wash buffer and centrifuged at 12000 g_{av} for 15 minutes. The pellet was resuspended in 30 ml Wash buffer (without glycine) and centrifuged at 12000 g_{av} for 15 minutes. The pellet was resuspended in a small volume (0.4-2.0 ml) Wash buffer (without glycine) and designated the pure mitochondrial fraction. For oxygen electrode experiments and enzyme assays mitochondria were used immediately. In all other cases mitochondria were pelleted for 5 minutes in a microfuge and the pellet 'snap' frozen in liquid nitrogen and stored at -80°C until required.

2.3.4 Distribution of Marker Enzymes on Percoll Gradients.

The distribution of organelles on the Percoll gradients was investigated by fractionating the gradient after centrifugation and assaying for the presence of the following marker enzymes: fumarase (mitochondria), NADP glyceraldehyde-3-phosphate dehydrogenase (chloroplast), isocitrate lyase (glyoxysomes) and hydroxypyruvate reductase (peroxisomes). The gradient was fractionated after centrifugation by carefully inserting a tube connected to a peristaltic pump to the bottom of the tube. The contents were removed at a constant flow rate of 2 ml min^{-1} and 17 X 2 ml fractions were collected, split into 4 0.5 ml aliquots and frozen at -80°C for subsequent enzyme assay. The results of this analysis carried out on material isolated from 5 day-old light-grown cotyledons is shown in Figure 2.1. Similar results were obtained with both light and dark grown material of other ages. The gradient procedure used effected adequate separation of mitochondria from chloroplasts, glyoxysomes and peroxisomes.

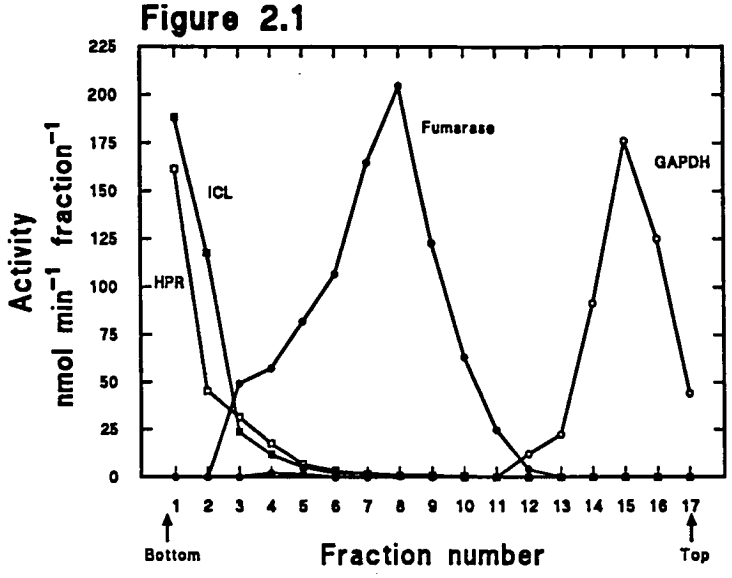

FIGURE 2.1: *The distribution of marker enzymes on Percoll gradients.* An extract of 5 day old light grown cotyledons was made as described in the text, separated on a Percoll density gradient, which was split into 17 X 2 ml fractions as described. Each fraction was assayed for fumarase, NADP glyceraldehyde-3-phosphate dehydrogenase, isocitrate lyase, and hydroxypyruvate reductase. More than 95 % of the activity of each enzyme added to the gradient was recovered.

2.3.5 Recovery and Purity of Mitochondrial Fraction.

The purification of cucumber cotyledon mitochondria described above was further analysed by following the recovery of fumarase activity. Small samples were taken at each stage in the extraction and assayed for fumarase activity and total protein content. The effect of the extract on the measurement of fumarase activity was checked by carrying out duplicate assays on extract to which known amounts of commercially obtained enzyme were added. The difference in activity between the samples containing the added enzyme and those without was taken as a measure of the effect of the extract on fumarase activity. In addition the pure mitochondrial fraction was also assayed for contaminating marker enzyme activities in order to assess the degree of contamination by other organelles. The results of these analyses carried out on material isolated from 5 day old light grown cotyledons is shown in Tables 2.1 and 2.2

TABLE 2.1. *Recovery of Fumarase Activity During Isolation of Mitochondria.* Mitochondria were isolated from 5 day old light grown cotyledons as described. At each stage in the purification procedure samples were taken and assayed for protein content and fumarase activity.

Fraction	Protein mg	Activity* µmol min^{-1}	Sp. Activity nmol min^{-1} mg^{-1}	Yield %	Purification fold
Crude Homogenate	1780	7.13 (95)	4	100	1
Filtrate	1340	5.37 (94)	4	75	1
First 1000g Supernatant	318	4.14 (89)	13	58	3
First 12000g Pellet	207	3.04 (91)	15	43	4
Second 1000g Supernatant	60	1.75 (95)	29	24	7
Second 12000g Pellet	40	1.24 (98)	31	17	8
Percoll Gradient Band	7.0	0.75 (96)	107	10	27
Pure Mitochondrial Fraction	6.4	0.70 (98)	110	10	28

Similar results were obtained with both light and dark grown material of other ages. These results indicate both that there is a consistent yield of mitochondria from all developmental stages examined and that the mitochondrial preparations used in this work were substantially free of contamination from other organelles.

* Recovery of fumarase activity added to extract is shown in parentheses.

TABLE 2.2. *Contaminating Activities in the Pure Mitochondrial Fraction.* Mitochondria were isolated from 5 day old light grown cotyledons as described and assayed for glyceraldehyde-3-phosphate dehydrogenase, isocitrate lyase, and hydroxypyruvate reductase.

Enzyme	Activity $\mu mol\ min^{-1}$	Specific Activity $nmol\ min^{-1}\ mg^{-1}$	Recovery %
GAPDH	0.03	4.7	94
Isocitrate Lyase	0.01	1.6	97
Hydroxypyruvate Reductase	0.01	1.6	101

2.4 Measurement of Mitochondrial Respiration *in vitro*.

Mitochondrial respiration was assayed by making polarographic measurements of oxygen concentration (Walker, 1987).

2.4.1 Equipment.

Reactions were carried out in two chambers containing oxygen electrodes (Hansatech, UK) linked to two CB1 control boxes (Hansatech, UK). These control boxes provide the necessary polarising voltage to allow the operation of the electrodes and amplify the signal produced by it. The output signal from the control boxes was displayed on a dual pen chart recorder (Rikadenki, Japan) without further modification. The temperature of the reaction chambers was kept at 25°C by circulating water through surrounding jackets from a water bath at this temperature.

2.4.2 Calibration.

Two points were used for calibration:

1. Oxygen saturated distilled water, which was taken to correspond to 253 µM oxygen at 25°C.

2. Oxygen free distilled water, produced by adding a few crystals of sodium dithionite to water in the reaction chamber.

$$Na_2S_2O_4 + O_2 + H_2O \rightarrow NaHSO_4 + NaHSO_3$$

The calibration procedure was begun with distilled water in the reaction chamber. The gain control on the control box was adjusted so that a full scale deflection (1 volt) was obtained on the chart recorder. A few crystals of sodium dithionite were added to the reaction chamber. The oxygen concentration declines rapidly at first, then more slowly until it reaches a steady level. This point corresponds to an oxygen concentration of zero and should be at or near zero on the chart recorder. If the latter did not apply or the initial

rate of signal reduction was low, then the electrode was cleaned and the membrane separating the electrode from the reaction chamber was replaced. The oxygen free distilled water was removed from the reaction chamber, which was then washed thoroughly with distilled water until a full scale deflection was again obtained on the chart recorder.

2.4.3 Oxidation of Respiratory Substrates.

Reactions were carried out in 1-2 ml standard reaction medium (0.3 M sucrose, 10 mM TES buffer, 10 mM potassium dihydrogen orthophosphate, 5 mM magnesium chloride, 0.1 %(w/v) bovine serum albumin, pH 6.8-7.5 depending on experiment) containing mitochondria (0.2-1.0 mg protein). Respiration was initiated by the addition of 10 mM substrate and varying amounts of ADP. For the measurement of ADP:O ratios 100 nmol ADP was added per ml of reaction, while to produce prolonged state 3 respiration for inhibitor titration experiments 1 µmol ADP was added per ml of reaction. The following substrate dependent additions were also made:

1. Malate: 10 mM glutamate, to prevent build up of oxaloacetate (Wiskich and Dry, 1985),

2. Succinate: 0.25 mM ATP, to activate succinate dehydrogenase,

3. Pyruvate: 0.1 mM thiamine pyrophosphate, a co-factor of pyruvate dehydrogenase.

4. 2-Oxoglutarate: 0.1 mM thiamine pyrophosphate, a co-factor of 2-oxoglutarate dehydrogenase.

2.4.4 Estimation of Mitochondrial Outer Membrane Intactness.

Outer membrane intactness was estimated by measuring cyanide-sensitive cytochrome c dependent ascorbate oxidation according to Neuburger (1985). The rate obtained with the 'intact' pure mitochondrial fraction was compared to that obtained by lysis of the pure mitochondrial fraction in distilled water for 10 seconds. The reaction was carried out in standard reaction medium (see 2.4.3) at pH 7.2 in the presence of 8 mM iso-ascorbate and 30 µM cytochrome c. The cyanide-sensitive component was measured by subtraction after the addition of 0.25 mM potassium cyanide.

2.4.5 Measurement of Cytochrome c Oxidase (EC1.9.3.1) Activity.

Cytochrome c oxidase activity was measured by following TMPD dependent ascorbate oxidation in the oxygen electrode according to Padovan *et al.* (1989). The reaction was carried out in 2 ml standard reaction medium (see 2.4.3) at pH 7.2 containing 0.2-0.4 mg mitochondrial protein in the presence of 2.5 mM TMPD and 10 mM iso-ascorbate, the reaction being initiated by the addition of the latter.

2.4.6 Measurement of NAD Malic Enzyme (EC1.1.1.39) Activity.

The contribution of NAD Malic enzyme to the oxidation of malate was measured by following the production of pyruvate during oxidation at pH 6.8, to ensure maximum activity of the enzyme, and in the absence of glutamate or any other system for the removal of oxaloacetate. The reaction was set up, in the oxygen electrode, in 2 ml standard reaction medium (see 2.4.3) containing 0.4-1.0 mg mitochondrial protein, 10 mM malate and 2 µmol ADP. At suitable points 300 µl samples were removed from the electrode and immediately added to 100 µl ice cold 20 %(v/v) perchloric acid. These samples were frozen at -20°C before estimating the pyruvate content. Before estimation of pyruvate (see 2.7.1) 700 µl distilled water and sufficient 5 M potassium carbonate to increase the pH to approximately 7.5 were added. The resulting precipitate was pelleted by centrifuging for 5 minutes in a microfuge, 900 µl of the supernatant being used in the pyruvate assay (see 2.7.1).

2.5 Preparation of Cell-free Extracts of Cucumber Cotyledons.

All steps in the preparation of cell-free extracts were carried out at 4°C or below unless otherwise indicated.

2.5.1 Extracts for Enzyme Assay.

(i) Organelle located enzymes: Twenty cotyledons were ground, first in a pestle and mortar then in a teflon-in-glass homogeniser, in 8 ml of the following buffer:

50 mM triethanolamine-HCl buffer, pH 7.0
2 mM magnesium chloride
1 mM EDTA
2 %(w/v) polyvinylpyrrolidone-40

The homogenate was transferred to a preweighed centrifuge tube and the volume made up to 10 ml by weight. The extract was used immediately for enzyme assay.

(ii) Cytosolic enzymes: A homogenate was produced as described in (i) above. The homogenate was centrifuged at 30000 g for 20 minutes and the supernatant used immediately for enzyme assay.

In both cases recovery experiments were performed as follows. For each extract a duplicate was prepared which had a known amount of the enzyme to be assayed added with the grinding buffer. An activity equivalent to the expected activity in the extract was added. Comparison of the activity measured in the two extracts gives an indication of the losses during extraction.

2.5.2 Extracts for Substrate Measurement.

Extracts were prepared according to Leegood and ap Rees (1978c) with modifications. Twenty cotyledons were harvested directly into liquid nitrogen contained in a mortar and ground immediately to a fine powder. The powder was transferred with some remaining liquid nitrogen to a centrifuge tube and 3 ml 20 %(v/v) perchloric acid added. The resulting mixture was left on ice for 60 minutes. The extract was neutralised with 5 M potassium carbonate and centrifuged at 30000 g for 5 minutes. The pellet was washed twice with distilled water and the supernatant and washings combined and used immediately for the measurement of substrate levels.

Recovery experiments were performed as follows. For each extract a duplicate was prepared which had a known amount of the substrate to be measured added with the perchloric acid. An amount equivalent to the expected amount in the extract was added. Comparison of the amounts measured in the two extracts gives an indication of the losses during extraction.

2.5.3 Extracts for SDS Polyacrylamide Gel Electrophoresis.

Twenty cotyledons were ground, first in a pestle and mortar and then in a teflon-in-glass homogeniser in 8 ml of the following buffer:

50 mM Tris-HCl buffer, pH 7.0
50 mM potassium acetate
5 mM magnesium acetate
2 mM dithiothreitol
1 %(w/v) sodium dodecyl sulphate (SDS)

The homogenate was transferred to a preweighed centrifuge tube and boiled for 5 minutes. The extract was allowed to cool, made up to 10 ml by weight with grinding buffer, and centrifuged at 10000 g for 10 minutes at 20°C. The supernatant was aliquoted into 10 1.5 ml centrifuge tubes and stored at -20°C until required.

2.6 Enzyme Assays.

2.6.1 Fumarase (EC4.2.1.2).

Fumarase was assayed according to Hill and Bradshaw (1969) in the reverse direction by following the production of fumarate which absorbs at 250 nm. The assay was carried out in 1 ml of the following solution:

80 mM potassium phosphate buffer, pH 7.4
0.1 %(v/v) Triton X-100

The reaction was initiated by the addition of 50 mM potassium malate. The change in absorbence at 250 nm was converted into nmol fumarate produced by multiplying by the conversion factor 204.9 (see 2.6.12 for sample calculation).

2.6.2 NAD-Isocitrate Dehydrogenase (EC1.1.1.41).

NAD-specific isocitrate dehydrogenase was assayed according to Plaut (1969) by following the production of NADH at 340 nm. The reaction was carried out in 1 ml of the following solution:

100 mM Tris-acetate buffer, pH 7.2
1 mM manganese chloride
0.5 mM ADP
0.5 mM NAD

The reaction was initiated by the addition of 1 mM sodium *threo*-DL-isocitrate. The change in absorbence at 340 nm was converted into nmol NADH produced by multiplying by the conversion factor 160.5 (see 2.6.12 for sample calculation).

2.6.3 Pyruvate Dehydrogenase Complex (EC1.2.4.1).

Pyruvate dehydrogenase complex was assayed according to Budde *et al.* (1988) by following the production of NADH at 340 nm. The reaction was carried out in 1 ml of the following solution:

65 mM TES-KOH buffer, pH 7.6
0.1 %(v/v) triton X-100
0.5 mM magnesium chloride
2 mM NAD
0.2 mM thiamine pyrophosphate
0.2 mM lithium coenzyme A
1 mM cysteine

The reaction was initiated by the addition of 1 mM sodium pyruvate. The change in absorbence at 340 nm was converted into nmol NADH produced by multiplying by the conversion factor 160.5 (see 2.6.12 for sample calculation).

2.6.4 Succinate Dehydrogenase (Complex II)(EC1.3.99.1).

Succinate dehydrogenase was assayed as 2,6-dichlorophenol-indophenol (DCPIP) reductase activity according to Burke *et al.* (1982), except ATP was included in the reaction to ensure full activation of the enzyme. Reduction of DCPIP leads to the production of a blue colour which absorbs at 580 nm. The reaction was carried out in 1 ml of the following solution:

30 mM tricine-NaOH buffer, pH 7.5
50 µM DCPIP
0.25 mM ATP

The reaction was initiated by the addition of 10 mM sodium succinate. The change in absorbence at 580 nm was converted into nmol DCPIP reduced by multiplying by the conversion factor 47.6 (see 2.6.12 for sample calculation).

2.6.5 Hydroxypyruvate reductase (EC1.1.1.26).

Hydoxypyruvate reductase was assayed with glyoxylate as substrate according to Tolbert (1971) by following the removal of NADH at 340 nm. The reaction was carried out in 1 ml of the following solution:

80 mM potassium phosphate buffer, pH 6.2
0.18 mM NADH
0.16 %(v/v) Triton X-100

The reaction was initiated by the addition of 75 mM sodium glyoxylate. The change in absorbence at 340 nm was converted into nmol NADH consumed by multiplying by the conversion factor of 160.5 (see 2.6.12 for sample calculation).

2.6.6 Isocitrate lyase (EC4.1.3.1).

Isocitrate lyase was assayed according to Cooper and Beevers (1969a) by reacting the glyoxylate produced by the enzyme with phenylhydrazine. The glyoxylate/phenylhydrazine complex absorbs strongly at 324 nm. The reaction was carried out in 1 ml of the following solution:

80 mM potassium phosphate buffer, pH 6.9
5.8 mM dithiothreitol
11.2 mM magnesium chloride
12.8 mM phenylhydrazine hydrochloride

The reaction was initiated by the addition of 13 mM sodium *threo*-DL-isocitrate. The change in absorbence at 324 nm was converted into nmol glyoxylate produced by multiplying by the conversion factor 58.8 (see 2.6.12 for sample calculation).

2.6.7 NADP-Glyceraldehyde-3-phosphate dehydrogenase (EC1.2.1.9).

NADP-Glyceraldehyde-3-phosphate dehydrogenase was assayed in the reverse direction according to Winter *et al* (1982) by producing 1,3-diphosphoglycerate from 3-phosphoglycerate using phosphoglycerate kinase and following the change in absorbence at 340 nm. The reaction was carried out in 1 ml of the following solution:

50 mM HEPES-KOH buffer, pH 8.0
10 mM magnesium chloride
5 mM cysteine
5 mM ATP
0.2 mM NADPH
0.03 %(v/v) Triton X-100
0.6 units phosphoglycerate kinase

The reaction was initiated by the addition of 2 mM 3-phosphoglyceric acid. The change in absorbence at 340 nm was converted into nmol NADPH consumed by multiplying by the conversion factor 160.5 (see 2.6.12 for sample calculation).

2.6.8 Pyruvate kinase (EC2.7.1.40).

Pyruvate kinase was assayed according to Thomas and ap Rees (1972b) by coupling the reaction to the oxidation of NADH by lactate dehydrogenase and following the change in absorbence at 340 nm. The reaction was carried out in 1 ml of the following solution:

50 mM triethanolamine-HCl buffer, pH 7.5
0.15 mM NADH
0.23 mM ADP
8 mM magnesium chloride
150 mM potassium chloride
10 units lactate dehydrogenase

The reaction was initiated by the addition of 3.9 mM phospho(enol)pyruvate (tri(cyclohexylammonium) salt). The change in absorbence at 340 nm was converted into nmol pyruvate produced by multiplying by the conversion factor 160.5 (see 2.6.12 for sample calculation).

2.6.9 ATP-Dependant Phosphofructokinase (EC2.7.1.11).

ATP-Dependant phosphofructokinase was assayed according to Smyth *et al.* (1984) by coupling the reaction to the oxidation of NADH by glycerol phosphate dehydrogenase and following the change in absorbence at 340 nm. The reaction was carried out in 1 ml of the following solution:

100 mM HEPES-NaOH buffer, pH 8.0
0.16 mM NADH
2.5 mM magnesium chloride
10 mM fructose-6-phosphate
1 unit aldolase
1 unit α-glycerol phosphate dehydrogenase
5 units triose phosphate isomerase

The reaction was initiated by the addition of 1 mM ATP (sodium salt). The absorbence at 340 nm was divided by two to correct for the 2-fold amplification of the coupling system and converted into nmol fructose-1,6-bisphosphate produced by multiplying by the conversion factor 160.5 (see 2.6.12 for sample calculation).

2.6.10 Fructose-1,6-bisphosphate 1-phosphatase (EC3.1.3.11).

Fructose-1,6-bisphosphate 1-phosphatase was assayed according to Smyth *et al.* (1984) by coupling the reaction to the reduction of NADP by glucose-6-phosphate dehydrogenase and following the change in absorbence at 340 nm. The reaction was carried out in 1 ml of the following solution:

100 mM HEPES-NaOH buffer, pH 7.0
0.5 mM NADP
2.5 mM magnesium chloride

10 units phosphoglucose isomerase
2 units glucose-6-phosphate dehydrogenase

The reaction was initiated by the addition of 1 mM fructose-1,6-bisphosphate. The change in absorbence at 340 nm was converted into nmol fructose-6-phosphate by multiplying by the conversion factor 160.5 (see 2.6.12 for sample calculation).

2.6.11 Hexokinase (EC2.1.7.4).

Hexokinase was assayed according to Dry, Nash and Wiskich (1983) by coupling the reaction to the reduction of NADP by glucose-6-phosphate dehydrogenase and following the change in absorbence at 340 nm. The reaction was carried out in 1 ml of the following solution:

25 mM tris-HCl buffer, pH 8.2
5.5 mM magnesium chloride
5 mM ATP
0.35 mM NADP
50 mM KCl
0.6 mg ml^{-1} glucose-6-phosphate dehydrogenase.

The reaction was initiated by the addition of 5 mM glucose. The change in absorbence at 340 nm was converted into nmol glucose-6-phosphate produced by multiplying by the conversion factor 160.5 (see 2.6.12 for sample calculation).

2.6.12 Sample Calculation.

Assays involving the measurement of NADH at 340 nm.

Extinction coefficient of NADH = 6.23 $mM^{-1}cm^{-1}$

Rate of change in A_{340} = y min^{-1}

Rate of change in concentration of NADH = y/6.23 mM min^{-1}

For 1 ml reaction volume,

Rate of change in amount of NADH = y/6.23 X 0.001 mmol min^{-1}

= y/6.23 X 0.001 X 10^6 nmol min^{-1}

= 160.5 X y nmol min^{-1}.

2.7 Measurement of Substrate Levels

2.7.1 Pyruvate.

Pyruvate was measured by coupling it to NADH consumption by lactate dehydrogenase. Measurements were carried out in 3 ml total volume containing the following:

100 mM potassium phosphate buffer, pH 7.5
0.08 mM NADH

Absorbence was read at 340 nm, prior to the addition of 50 units lactate dehydrogenase to initiate the reaction. The reaction was allowed to proceed until the absorbence fell to a steady value. The change in absorbence at 340 nm was converted into nmol pyruvate present by multiplying by the conversion factor 481.5 (see 2.7.3 for calculation).

2.7.2 Phospho(enol)pyruvate.

Phospho(enol)pyruvate was measured by first converting it to pyruvate using pyruvate kinase and then measuring the amount of pyruvate produced as in 2.7.1. Measurements were carried out in 3 ml total volume containing the following:

100 mM potassium phosphate buffer, pH7.5
0.20 mM NADH
0.23 mM ADP
8 mM magnesium chloride

Before the measurement of phospho(enol)pyruvate 50 units lactate dehydrogenase was first added to remove the pyruvate present in the extract. The absorbence was then read and 20 units pyruvate kinase added to initiate the reaction. The reaction was allowed to proceed until the absorbence fell to a steady value. The change in absorbence at 340 nm was converted to nmol phospho(enol)pyruvate present by multiplying by the conversion factor 481.5 (see 2.7.3 for calculation).

2.7.3 Sample Calculation.

Extinction coefficient of NADH = 6.23 $mM^{-1}cm^{-1}$

Change in A_{340} = y

Change in concentration of NADH = y/6.23 mM

Concentration of pyruvate = y/6.23 mM

For 3 ml reaction volume,

Amount of pyruvate = y/6.23 X 0.003 mmol

y/6.23 X 0.003 X 10^6 nmol

481.5 X y nmol

2.8 Reconstitution of Gluconeogenesis *in vitro*.

The method was based on the auxiliary enzyme approach of Torres *et al.*(1986) (see Chapter 6 for theoretical details). Fluxes were measured by recording NADH decay at 340 nm and by taking samples for pyruvate measurement (see 2.7.1). Where mitochondria were present oxygen consumption was also recorded.

Reactions were carried out in 2 ml reaction volume in a spectrophotometer cuvette containing cytosolic extract corresponding to 4/10 of a cotyledon. ATP was generated *in situ* either by a phosphocreatine/creatine kinase system or by mitochondrial oxidative phosphorylation. Phosphoglucose isomerase and phosphoglucomutase were added as auxiliary enzymes. In addition during the reconstitution of mitochondrial and cytosolic reactions 2-oxoglutarate/aspartate aminotransferase was also included.

2.8.1 Reconstitution of cytosolic steps only.

Reactions were carried out in the following solution:

50 mM triethanolamine-HCl buffer, pH 7.0
1 mM ATP
0.3 mM NADH
5 mM magnesium chloride
2.5 mM phosphocreatine
10 units creatine kinase
10 units phosphoglucose isomerase
10 units phosphoglucomutase

The reaction was initiated by the addition of 10 mM sodium oxaloacetate. Fluxes were measured between 2 and 5 minutes after the addition of oxaloacetate, when both NADH consumption and pyruvate production rates were linear. For pyruvate measurement 300 µl samples were taken as in 2.4.6.

2.8.2 Reconstitution of both mitochondrial and cytosolic steps.

Reactions were carried out in the following solution:

50 mM triethanolamine-HCl buffer, pH 7.0
0.3 M sucrose
5 mM magnesium chloride
0.5 mM ATP
0.5 mM ADP
10 mM potassium dihydrogen orthophosphate
0.3 mM NADH
1 mM EGTA
10 mM potassium glutamate
10 units phosphoglucose isomerase
10 units phosphogucomutase
10 units 2-oxoglutarate/aspartate aminotransferase
0.2-0.5 mg mitochondrial protein

The amount of mitochondrial protein required was calculated from the amount of fumarase activity present in the cotyledon extract before centrifugation. Duplicate reactions were carried out in an oxygen electrode chamber (see 2.4) and spectrophotometer cuvette to allow continuous recording of both oxygen and NADH consumption. The reactions were initiated by the addition of 10 mM sodium succinate. Fluxes were measured between 2 and 5 minutes after the addition of succinate, when NADH consumption, oxygen consumption and pyruvate production rates were all linear. Samples of 300 µl were taken from both reactions for pyruvate measurement as in 2.4.6.

2.9 Control Analysis.

2.9.1 Inhibitor Titrations.

Inhibitor titrations curves were obtained by adding an inhibitor to an oxygen electrode chamber containing mitochondria (0.2-1.0 mg protein) oxidising succinate under state 3 conditions (see 2.4.3). Following the establishment of a constant rate, another addition of inhibitor was made and the new rate measured. Inhibitor titrations were compared to a control carried out under identical conditions, but in the absence of inhibitor. The inhibitor titration curves were constructed by plotting the relative rate of respiration (normalised with respect to the basal flux in the absence of inhibitor) against inhibitor concentration.

2.9.2 Enzyme Titrations.

Enzyme titration curves were obtained by adding the required enzyme concentration to the reconstituted system before assay (see 2.8). The rates were compared to a control without added enzyme. Enzyme titration curves were constructed by plotting the relative flux (normalised with respect to the basal flux, without added enzymes) against enzyme concentration (given by enzyme activity divided by K_m).

2.10 Assay of Mitochondrial Membrane Transporters.

Transport of mono- and dicarboxylate acid anions into isolated mitochondria was measured using the ammonium salt swelling method of Zoglowek *et al* (1988). Mitochondrial swelling as an indicator of solute uptake was measured by the addition of 0.5-1.2 mg mitochondrial protein (see 2.3) to 1 ml of a solution containing the following:

5 mM TES-KOH buffer, pH 7.4
0.1 mM EGTA
3 µM antimycin A
100 mM ammonium salt

Immediately after the addition of the mitochondrial suspension the decrease in absorbence at 546 nm was measured. Ammonium salts not commercially available were produced by mixing ammonia solution and the free acid in the required proportion.

2.11 SDS-Polyacrylamide Gel Electrophoresis.

2.11.1 Preparation of Polyacrylamide Gels.

Proteins were separated by SDS-polyacrylamide gel electrophoresis on 15 %(w/v) polyacrylamide gels using the discontinuous buffer system of Laemmli (1970). Gels 1.5 mm or 0.8 mm thick were made from the following:

20 ml	30 %(w/v) acrylamide (Kodak) 0.2 %(w/v) N,N'-methylenebisacrlyamide
8 ml	1.875 M Tris-HCl buffer, pH 8.85
20 µl	TEMED
200 µl	10 %(w/v) ammonium persulphate
made to 40 ml with distilled water.	

This mixture was poured into a previously assembled gel cassette and allowed to polymerise for several hours under a layer of gel overlay solution (0.375 M Tris-HCl buffer pH 8.85, 0.1 %(w/v) SDS, 80 %(v/v) isopropanol). The gel overlay solution was removed before pouring a stacking gel made from the following:

2 ml	30 %(w/v) acrylamide (Kodak) 0.2 %(w/v) N,N'-methylenebisacrylamide
1.2 ml	0.6 M Tris-HCl buffer, pH 6.8
12 µl	TEMED
60 µl	10 %(w/v) ammonium persulphate
made up to 12 ml with distilled water.	

A well forming comb was inserted and the stacking gel allowed to polymerise for 30 minutes before use.

2.11.2 Preparation of Samples and Electrophoresis.

Samples of total cotyledon protein (see 2.5.3) were mixed with 1/3 volume of 4X sample loading buffer (0.24 M Tris-HCl buffer pH 6.8, 30 %(v/v) glycerol, 0.4 %(w/v) SDS, 0.02 %(w/v) bromophenol blue) to give a final protein concentration of 5-10 $mgml^{-1}$. The samples were boiled for 90 s, cooled on ice, then allowed to warm to room temperature. Mitochondrial pellets (see 2.3) were resuspended in 2X sample loading buffer (0.12 M Tris-HCl buffer pH 6.8, 15 %(v/v) glycerol, 0.2 %(w/v) SDS, 0.01 %(w/v) bromophenol blue) to give a final protein concentration of 5-10 $mgml^{-1}$. The samples were boiled for 3 minutes, cooled on ice, then allowed to warm to room temperature.

Samples were loaded onto gels using a syringe. A maximum of 250 µg protein per track was loaded on 1.5 mm gels for staining with Coomassie blue or immunoblotting and a maximum of 25 µg protein per track was loaded onto 0.8 mm gels for silver staining.

Gels were run in Laemmli electrode buffer (50 mM Tris-192 mM glycine, pH 8.2) with the upper buffer tank containing 0.1 %(w/v) SDS in addition. Gels were run overnight at 7 mA for 1.5 mm gels and 3 mA for 0.8 mm gels until the bromophenol blue reached the bottom. Gels were either stained for protein (see 2.11.3) or electroblotted onto nitrocellulose for the immunodetection of specific polypeptides (see 2.12).

2.11.3 Staining of Gels for Protein.

(i) Coomassie blue: Following electrophoresis gels were stained for 4 hours in 45 %(v/v) methanol, 8 %(v/v) acetic acid, 0.2 %(w/v) Coomassie brilliant blue R250. Gels were destained over a period of 16 hours with several changes of 45 %(v/v) methanol, 8 %(v/v) acetic acid. Gels were rinsed in distilled water before being dried under vacuum onto Whatman 3MM paper.

(ii) Silver staining: A procedure modified from Merril *et al* (1981) was used. Gels were fixed for 60 minutes in a solution containing 50 %(v/v) methanol, 12 %(w/v) trichloroacetic acid, and 2 %(w/v) copper (II) chloride. The gel was then washed in 10 %(v/v) ethanol/5 %(v/v) acetic acid for 30 minutes prior to a 3 minute oxidation step in 0.01 %(w/v) potassium permanganate. This was followed by three 10 minute washes in 10 %(v/v) ethanol/5 %(v/v) acetic acid, 10 %(v/v) ethanol, and finally distilled water. The gel was then incubated with 0.2 %(w/v) silver nitrate for 20 minutes, followed by brief rinses in distilled water and 10 %(w/v) potassium carbonate. The colour was developed with 0.02 %(v/v) formaldehyde in 2 %(w/v) sodium carbonate and stopped with a 10 %(v/v) ethanol/5 %(v/v) acetic acid wash. The gel was shrunk in 50 %(v/v) methanol for 60 minutes, rinsed in distilled water, and dried under vacuum onto Whatman 3MM paper.

2.12 Immunoblotting.

Proteins were transferred electrophoretically (Hoeffer) from 1.5 mm thick polyacrylamide gels onto 0.4 µm nitrocellulose membranes (Schleicher and Schull) in a buffer containing 25 mM Tris-192mM glycine pH 8.2, 20 %(v/v) methanol and 0.1 %(w/v) SDS (Towbin *et al.*, 1979) for 4 hours at 500 mA and 4°C. The membranes were then washed for 1 hour in 4 %(w/v) milk protein (Marvel) in TBST buffer (0.9 %(w/v) sodium chloride, 10 mM Tris-HCl buffer pH 8.0, 0.05 %(v/v) Tween-20). The filters were incubated overnight at room temperature in 1 %(w/v) milk protein (Marvel) in TBST buffer containing the appropriate dilution of antisera (100- to 1000-fold) and then washed in three changes of TBST buffer (20 minute washes) to remove excess antisera. The filters were incubated for 2 hours at room temperature in 1 %(w/v) milk protein (Marvel) in TBST buffer containing a 1000-fold dilution of alkaline phosphatase conjugated anti-rabbit immunoglobulin antisera (Sigma Chemical Company) and then washed once more in three changes of TBST buffer (20 minute washes). Antibody binding was detected by an alkaline

phosphatase specific stain. The filter was incubated in 100 mM Tris-HCl buffer pH 9.5 containing 4 mM magnesium chloride, 0.1 mg ml^{-1} nitro-blue tetrazolium and 0.06 mg ml^{-1} 5-bromo-4-chloro-3-indolyl phosphate (toluidine salt) until intense purple bands appeared.

2.13 Other Methods.

2.13.1 Protein Assay.

Protein was measured according to Bradford (1976) following precipitation of the protein with trichloroacetic acid. A 5 µl sample was taken and made up to 100 µl with distilled water before the addition of 100 µl 20 %(w/v) trichloroacetic acid. The resulting mixture was left at 4°C for at least 15 minutes and the protein precipitate collected by centrifugation. The precipitate was washed in 10 %(w/v) trichloroacetic acid and resuspended in 150 µl 100 mM sodium hydroxide. The amount of protein in 100 µl of this solution was estimated according to Bradford (1976). Bovine serum albumin was used as a standard.

2.13.2 Chlorophyll Assay.

Chlorophyll was measured according to Arnon (1949).

2.13.3 Lipid Assay.

Total lipid was determined according to Radin (1969) with modifications. Cotyledons (3 g) were ground in 10 ml of methanol-chloroform (2:1 v/v). Following low speed centrifugation, the supernatant was decanted and the pellet re-extracted by grinding again with methanol-chloroform. Supernatants from both extractions were shaken with an equal volume of 2 M potassium chloride. After phase separation, the organic phase was drained into a preweighed beaker, and the aqueous phase was then washed repeatedly with methanol-chloroform. The pooled organic phases were evaporated to dryness and the amount of extracted lipid determined by weight difference.

CHAPTER 3.

METABOLIC CHANGES AND MITOCHONDRIAL RESPIRATION DURING EARLY SEEDLING DEVELOPMENT.

3.1 Introduction and aims.

To form a basis for this study into the regulation of mitochondrial respiration during development it is necessary to quantify any changes in respiratory physiology during early seedling development. In addition, it is vital to establish the primary metabolic function of the cotyledons during the temporal progression of development so that respiration can be related to overall seedling physiology. Finally, it is also important to ensure that this study is comparable with previous investigations into the physiology of germination and early seedling growth in cucumber (for example, Becker *et al.*, 1978).

During early seedling development in the light, two major metabolic phases can be detected; the initial heterotrophic phase (lipid mobilisation) and the photo-autotrophic phase (photosynthesis). In addition it seems justified, based on biochemical rather than nutritional grounds, to define a third phase, during which the organelle and membrane system which supports photo-autotrophy is synthesised. This will be termed the chloroplast biogenesis phase. Although these divisions are artificial, and the phases will inevitably overlap, it is possible that there are points in development when each phase is predominant, which can be identified by the measurement of a variety of heterotrophic and photo-autotrophic indicators.

The respiratory physiology of the cotyledons can be described in three ways:

1. measurement of the activity of mitochondrial enzymes,
2. characterisation of the properties of isolated mitochondria *in vitro* (using an oxygen electrode),
3. examination of mitochondrial protein composition.

3.2 Heterotrophic and autotrophic phases.

In order to establish the precise timing of the phases described in 3.1 a number of heterotrophic and photo-autotrophic indicators were examined during the first 7 days following imbibition, and expressed on a per cotyledon basis. These were:

1. Lipid content.
2. Chlorophyll content.
3. Isocitrate lyase activity.
4. Hydroxypyruvate reductase activity.

The total protein profile of the cotyledons was also examined by SDS-polyacrylamide gel electrophoresis.

3.2.1 Heterotrophic indicators.

The variation in lipid content during germination and early seedling development is shown in Figure 3.1. The lipid content of the seed is 6 mg lipid cotyledon^{-1} and this falls, in light grown seedlings, to 0.5 mg lipid cotyledon^{-1} at 7 days post imbibition. The

rate of lipid breakdown reaches a maximum at 4 days post-imbibition (Figure 3.1). In dark grown material a similar pattern is observed, except that the rate of lipid breakdown is lower and the lipid mobilisation phase lasts longer (data not shown). The glyoxylate cycle enzyme isocitrate lyase (ICL) is a heterotrophic indicator specific to lipid mobilisation (Kornberg and Krebs, 1957). The activity of ICL during development is shown in Figure 3.2 and Table 3.1. In light grown material ICL activity appears soon after imbibition, peaks at 4 days post-imbibition and is virtually absent by 7 days post-imbibition. A similar pattern is observed in dark grown cotyledons, except that there is still appreciable ICL activity at 7 days post-imbibition. On the basis of this data, the lipid mobilisation phase is taken to extend from the onset of germination to 6 days post-imbibition in light grown cotyledons, and beyond 7 days post-imbibition in dark grown cotyledons. This data is comparable to that already published (Becker *et al.*, 1978), and is summarised in Figure 3.5.

TABLE 3.1: *Isocitrate lyase (ICL) activity in extracts of cucumber cotyledons.* Cotyledon extracts were prepared at each stage and assayed for isocitrate lyase as described in Chapter 2. Recoveries were measured as described in Chapter 2. Values are the mean ($\pm$ SEM) of 3 independent extracts. nd. = none detected.

Days post-imbibition	ICL activity nmol min^{-1} $cotyledon^{-1}$	Recovery %
0	nd.	94 $\pm$ 1
1	3.6 $\pm$ 0.4	95 $\pm$ 2
2	42.7 $\pm$ 2.3	96 $\pm$ 2
Light grown		
3	59.0 $\pm$ 1.2	97 $\pm$ 1
4	82.4 $\pm$ 1.3	92 $\pm$ 4
5	41.0 $\pm$ 4.4	96 $\pm$ 3
6	22.3 $\pm$ 2.3	93 $\pm$ 2
7	5.1 $\pm$ 0.4	98 $\pm$ 1
Dark grown		
3	52.7 $\pm$ 0.8	95 $\pm$ 2
4	76.0 $\pm$ 2.4	94 $\pm$ 2
5	55.8 $\pm$ 2.0	99 $\pm$ 3
6	36.2 $\pm$ 2.0	95 $\pm$ 1
7	23.9 $\pm$ 3.0	95 $\pm$ 3

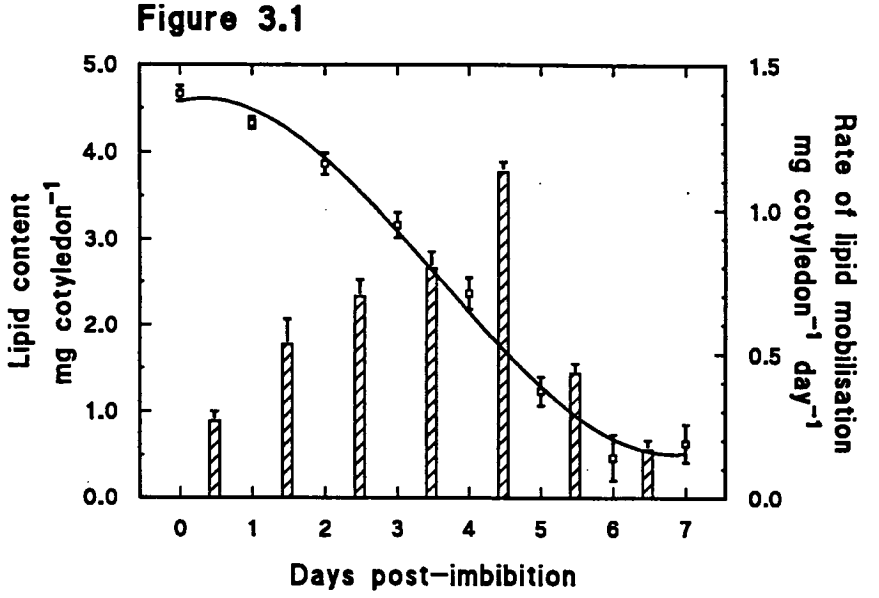

FIGURE 3.1. *Lipid mobilisation during germination and early seedling development.* The lipid content of methanol/chloroform extracts of whole seeds (0-2 days post imbibition) or light grown cotyledons (3-7 days post imbibition) was measured as described in Chapter 2. (□), lipid content; hatched bars, rate of lipid breakdown. Points are the mean (± SEM) of 3 independent extracts.

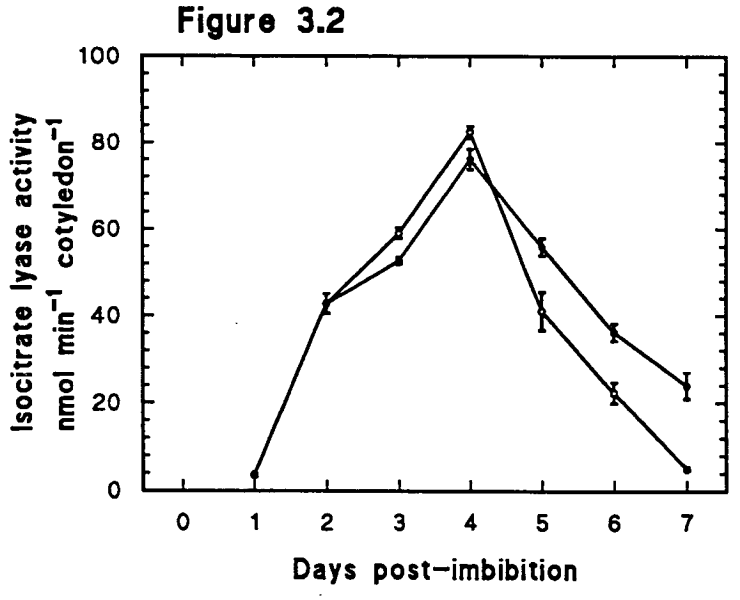

FIGURE 3.2. *Developmental variation in isocitrate lyase (ICL) activity.* Cotyledon extracts were prepared at each stage and assayed for isocitrate lyase as described in Chapter 2. (○), light grown; (●), dark grown. Points are the mean (± SEM) of 3 independent extracts.

3.2.2 Photo-autotrophic indicators.

The variation in chlorophyll content during germination and early seedling development is shown in Figure 3.3. Chlorophyll cannot be detected in the seed or in dark grown cotyledons. In light grown cotyledons chlorophyll first appears at 3 days post-imbibition and reaches a level of approximately 200 µg cotyledon^{-1} by day 7. This represents the maximum chlorophyll content of the cotyledons (data not shown). The rate of chlorophyll synthesis reaches a maximum at 5 days post-imbibition (Figure 3.3). The peroxisomal enzyme hydroxypyruvate reductase is specific to photosynthetic tissues. The changes in activity of this enzyme during development is shown in Figure 3.4 and Table 3.2. Hydroxypyruvate reductase is absent from dark grown material, and appears first in light grown cotyledons at 3 days post-imbibition, increasing linearly to 7 days post-imbibition. On the basis of this data the photosynthetic phase is taken to begin at 7 days post-imbibition, and the chloroplast biogenesis phase extends from 3 to 7 days post-imbibition. Photosynthetic development is absent from dark grown cotyledons. This data is similar to that already published (Becker *et al.*, 1978; Walden and Leaver, 1981), and is summarised in Figure 3.5.

TABLE 3.2: *Hydroxypyruvate reductase (HPR) activity in extracts of cucumber cotyledons. Cotyledon* extracts were prepared at each stage and assayed for hydroxypyruvate reductase as described in Chapter 2. Recoveries were measured as described in Chapter 2. Values are the means (± SEM) of 3 independent extracts. nd. = none detected.

Days post-imbibition	HPR activity nmol min^{-1} cotyledon^{-1}	Recovery %
0	nd.	93 ± 2
1	nd.	95 ± 3
2	nd.	93 ± 2
Light grown		
3	12.1 ± 2.1	95 ± 4
4	35.9 ± 3.6	94 ± 2
5	78.8 ± 4.2	94 ± 1
6	92.4 ± 2.7	94 ± 1
7	137 ± 6	93 ± 1
Dark grown		
3	nd.	94 ± 3
4	5.9 ± 1.2	95 ± 2
5	6.6 ± 1.6	95 ± 2
6	6.0 ± 2.0	95 ± 2
7	1.7 ± 0.9	97 ± 2

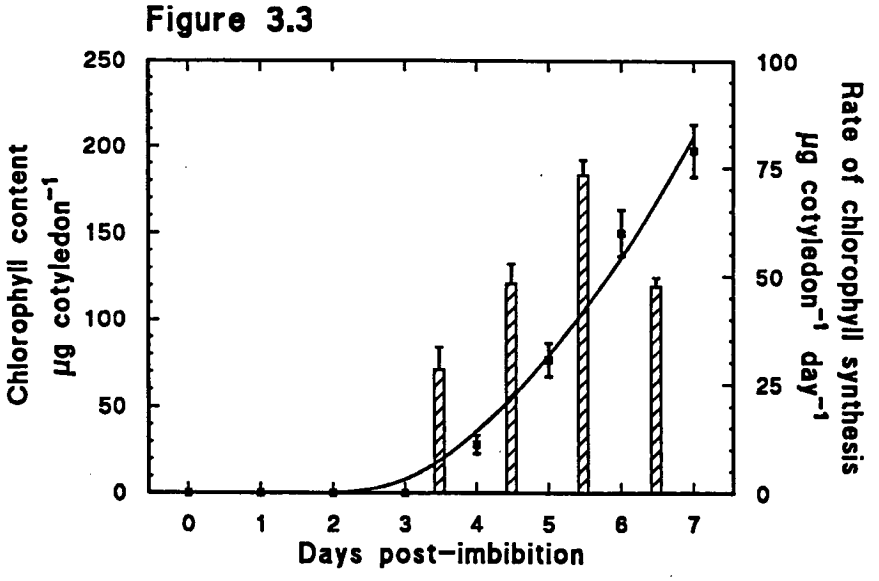

FIGURE 3.3. *Chlorophyll synthesis during germination and early seedling development.* The chlorophyll content of acetone extracts of whole seeds (0-2 days post imbibition) or light grown cotyledons (3-7 days post imbibition) was measured as described in Chapter 2. (■), chlorophyll content; hatched bars, rate of chlorophyll synthesis. Points are the mean (± SEM) of 3 independent extracts.

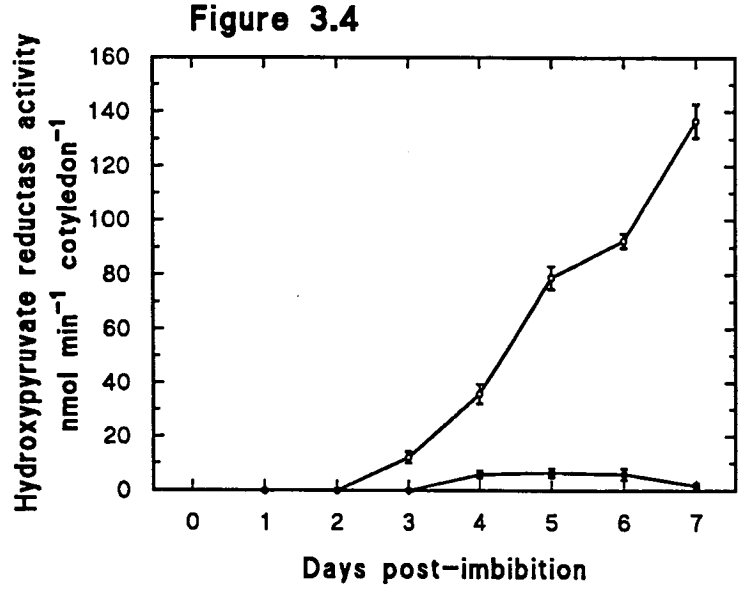

FIGURE 3.4. *Developmental variation in hydroxypyruvate reductase (HPR) activity.* Cotyledon extracts were prepared at each stage and assayed for hydroxypyruvate reductase as described in Chapter 2. (○), light grown; (●), dark grown. Points are the mean (± SEM) of 3 independent extracts.

3.2.3 Protein profile.

Proteins were isolated from light grown cotyledons at intervals from 0 to 7 days post-imbibition, fractionated according to size by SDS-polyacrylamide gel electrophoresis, and stained with either Coomassie blue or silver. A typical protein profile is shown in Figure 3.6. The following points are emphasised. First, a number of stained polypeptides corresponding to storage proteins can be identified (●). These are hydrolysed early in the heterotrophic phase. Secondly, polypeptides can be observed which appear transiently, reaching a maximum at around 4 days post-imbibition (▲). The high molecular weight members of this group are likely to correspond to polypeptides involved in lipid mobilisation, while the low molecular weight polypeptides are intermediates formed during the hydrolysis of storage protein. Thirdly, there are stained bands which increase in abundance from 4 to 7 days post-imbibition (△), which are probably involved in photosynthesis. This latter class is absent from the protein profile obtained with dark grown material (data not shown). These results are in accord with those already in the literature (Becker *et al.*, 1978).

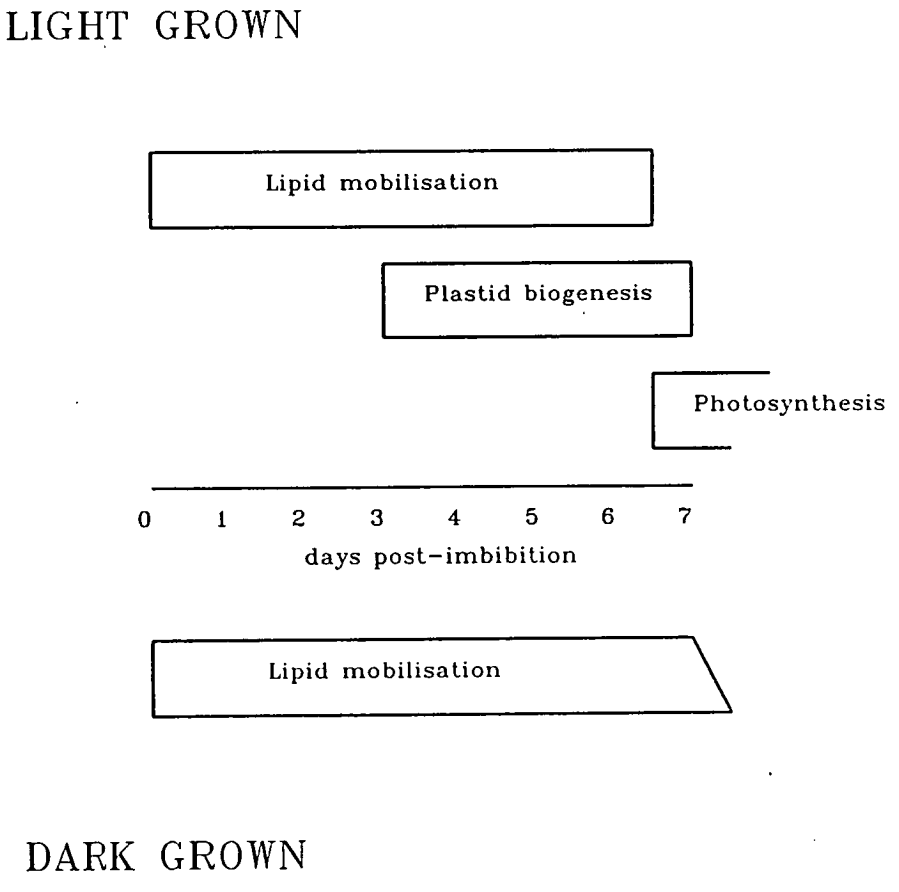

FIGURE 3.5: *Metabolic phases during germination and early seedling development in cucumber.*

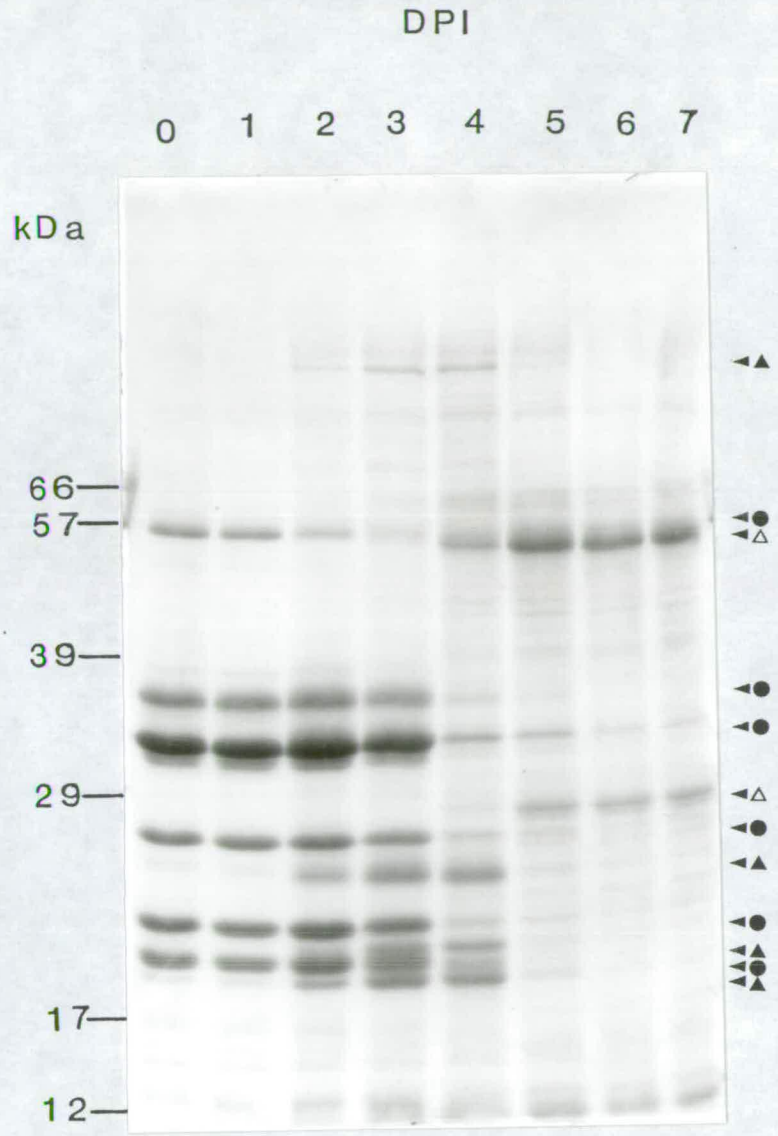

FIGURE 3.6: *Protein composition of developing cucumber cotyledons.* Proteins were isolated from cotyledons between 0 and 7 days post-imbibition, fractionated by SDS-polyacrylamide gel electrophoresis, and stained with Coomassie blue, as described in Chapter 2. Polypeptides have been divided into groups on the basis of their developmental expression, as described in the text. Each track contains the protein isolated from 1/20 cotyledon. The position of molecular weight markers is shown on the left.

3.3 Mitochondrial enzyme activities.

Fumarase and NAD-dependant isocitrate dehydrogenase (ICDH) activities were measured in cotyledon extracts , as both these enzymes are located exclusively in the mitochondria (Cooper and Beevers, 1969a). Fumarase was taken to be representative of the non-decarboxylating side of the TCA cycle, whereas ICDH is characteristic of the decarboxylating side. In order to confirm that the activity measured was near the maximum catalytic activity, the recovery of each enzyme during extraction was measured (see section 2.5.1).

The variation in activity of these enzymes during development is shown in Figure 3.7 and Table 3.3. In both light and dark grown cotyledons the activity of fumarase is significantly greater than that of ICDH, in contrast to the situation in the fully expanded first leaf where the activities of these enzymes are similar, being 68 $\pm$ 9 and 69 $\pm$ 4 nmol min^{-1} gFW^{-1}, respectively. Between 3 and 7 days post-imbibition there is a 5-fold increase in fumarase activity in light grown cotyledons and a 4-fold increase in dark grown cotyledons. ICDH activity only displays a significant increase in light grown cotyledons after day 5, concomitant with photosynthetic development; otherwise it does not change during the period investigated.

The following may be inferred from this data:

1. There is a much greater capacity for operation of the non-decarboxylating side of the TCA cycle (succinate to oxaloacetate) than the decarboxylating side (oxaloacetate to succinate), similar to the situation in germinating castor bean endosperm (Cooper and Beevers, 1969a; Millhouse *et al.*, 1983).

2. Fumarase increases in activity in response to cotyledon age, but is only slightly affected by light, implying a role for this increase in activity in lipid mobilisation.

3. ICDH increases in activity only in response to light, suggesting a role for full TCA cycle operation in the chloroplast biogenesis and photosynthetic phases.

TABLE 3.3: *Fumarase and isocitrate dehydrogenase (ICDH) activity in extracts of cucumber cotyledons.* Cotyledon extracts were prepared at each stage and assayed for fumarase and isocitrate dehydrogenase as described in Chapter 2. Recoveries were measured as described in Chapter 2. Values are the means (± SEM) of 3 independent extracts.

	Fumarase		ICDH	
Days post imbibition	Activity $nmolmin^{-1}$ cot^{-1}	Recovery %	Activity $nmolmin^{-1}$ cot^{-1}	Recovery %
1	13.9 ± 1.9	94 ± 2	2.8 ± 0.3	90 ± 1
2	14.3 ± 0.6	93 ± 2	3.0 ± 0.3	91 ± 2
Light grown				
3	16.9 ± 0.8	96 ± 3	3.8 ± 0.2	92 ± 2
4	34.0 ± 3.1	95 ± 2	5.2 ± 0.2	90 ± 1
5	38.7 ± 2.4	95 ± 2	6.6 ± 0.2	92 ± 2
6	47.3 ± 1.0	93 ± 1	10.4 ± 0.3	96 ± 1
7	51.4 ± 2.4	98 ± 2	16.5 ± 1.4	95 ± 2
Dark grown				
3	18.4 ± 0.5	95 ± 2	3.8 ± 0.3	91 ± 2
4	26.9 ± 1.7	94 ± 1	5.2 ± 0.1	91 ± 3
5	33.6 ± 1.2	93 ± 1	5.4 ± 0.2	94 ± 1
6	39.9 ± 0.9	96 ± 4	5.0 ± 0.6	96 ± 1
7	39.2 ± 1.5	94 ± 3	4.9 ± 0.1	93 ± 2

FIGURE 3.7

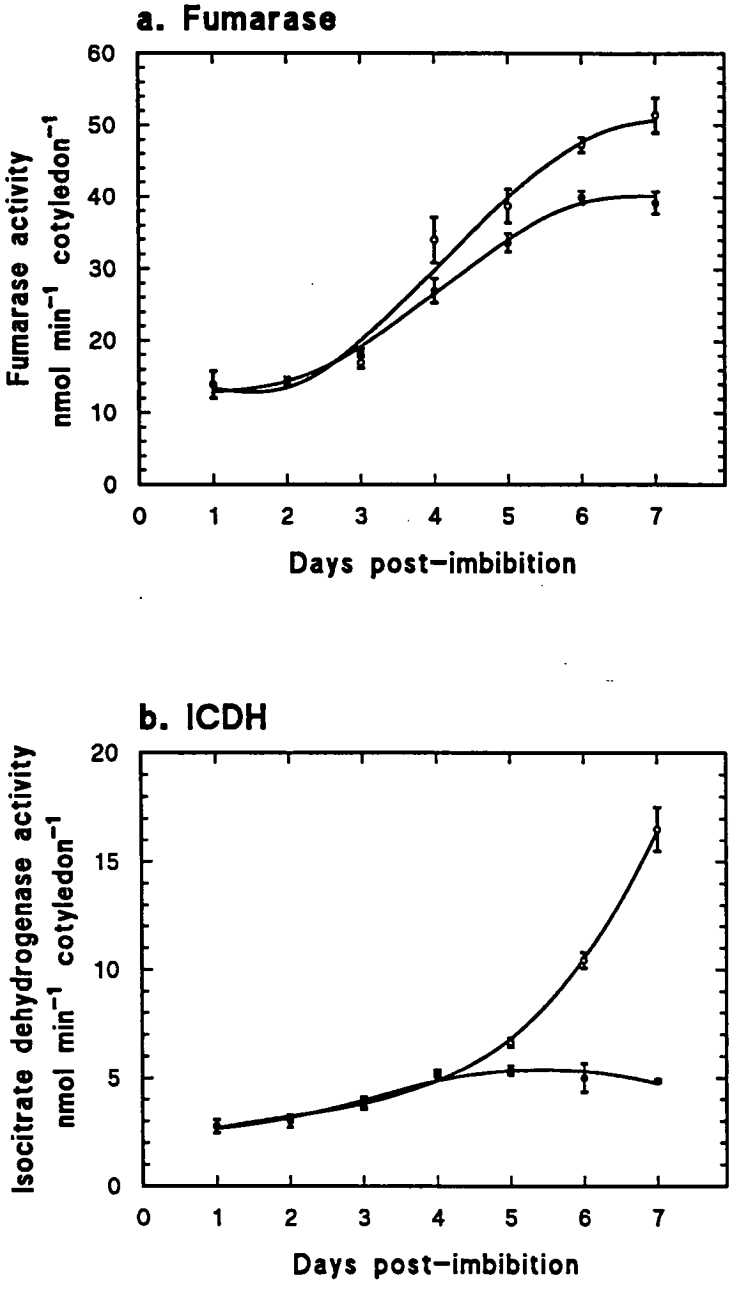

FIGURE 3.7. *Developmental variation in TCA cycle enzyme activities.* Cotyledon extracts were prepared at each stage and assayed for fumarase and isocitrate dehydrogenase (ICDH) as described in Chapter 2. (○), light grown; (●), dark grown. Points are the mean (± SEM) of 3 independent extracts.

a. Fumarase.

b. Isocitrate dehydrogenase (ICDH).

3.4 Mitochondrial Respiration.

The measured activities of mitochondrial enzymes suggested that there were developmentally and environmentally regulated changes in mitochondrial function. This was further investigated by characterisation of mitochondria isolated from light and dark grown cotyledons at various stages during development. Mitochondria were initially isolated from all stages (0-7 days post-imbibition), but it was found that only cotyledons at day 3 or later yielded mitochondria suitable for analysis. Mitochondrial preparations from 0, 1 and 2 day old cotyledons were characterised by low yield (<2 % fumarase activity recovered), low outer membrane intactness (<55 %), and low ADP:O ratios (<0.7 with succinate as substrate; <1.1 with malate as substrate). The mitochondrial preparations used in the following analysis had an outer membrane intactness greater than 95 % and an ADP:O ratio of at least 1.4 with succinate as substrate.

3.4.1 Oxidation of TCA cycle substrates.

The rate of oxygen comsumption by mitochondria isolated at various stages during development, in the presence of a variety of substrates and excess ADP (state 3 conditions) is shown in Figure 3.8. In light grown cotyledons there is a 4-fold increase, and in etiolated cotyledons a 3-fold increase in the rate of succinate oxidation between 3 and 7 days post imbibition. In the light this is accompanied by an increase in the rate of malate oxidation, contrasting with dark grown material where this rate does not change significantly during the period examined. Malate oxidation was carried out in the presence of glutamate, in order to prevent restriction of malate dehydrogenase by accumulated oxaloacetate. Glutamate was not oxidised by mitochondria isolated from cucumber cotyledons, even in the presence of the cofactor thiamine pyrophosphate. An increase was observed in the rate of oxidation of externally added NADH during development (Table 3.4). The rate of oxidation of 2-oxoglutarate is lower than that of succinate in mitochondria from both light and dark grown cotyledons at all stages after day 4. There is a slight increase in the rate of 2-oxoglutarate oxidation between 5 and 7 days post-imbibition in the light. Pyruvate oxidation is low or undetectable except after day 6 in light grown cotyledons. The capacity for glycine oxidation is confined to the mitochondria of light grown cotyledons and appears between 3 and 5 days post-imbibition.

The rates of oxygen uptake with the range of substrates, expressed in terms of amount of mitochondrial protein, are shown in Table 3.5. The following points are emphasised. There is no change in the rate of oxidation of any substrate during development, except glycine. The only effects of a light environment on oxidation rates are the induction of glycine oxidation, and the lower malate oxidation rate in dark grown material. Mitochondria from cucumber cotyledons rapidly oxidise external NADH.

TABLE 3.4: *The rate of NADH oxidation by cucumber cotyledon mitochondria.* Mitochondria were isolated from each stage and oxygen uptake in the presence of 10 mM NADH and 100 nmol ADP was measured as described in Chapter 2. Values are the mean (± SEM) of 3 independent experiments.

Days post imbibition	Oxygen uptake nmol min^{-1} $cotyledon^{-1}$
Light grown	
3	1.02 ± 0.13
4	2.85 ± 0.14
7	4.24 ± 0.32
Dark grown	
4	1.33 ± 0.10
7	2.27 ± 0.25

TABLE 3.5. *The rate of oxygen uptake by mitochondria isolated from cucumber cotyledons at 3 and 7 days post imbibition.* Mitochondria were isolated and oxygen uptake measured in the presence of the substrate indicated (at 10 mM) and 100 nmol ADP as described in Chapter 2. The following were also present in addition: 0.25 mM ATP during succinate oxidation; 10 mM glutamate during malate oxidation; 0.1 mM thiamine pyrophosphate during pyruvate and 2-oxoglutarate oxidation; and 0.1 mM malate during pyruvate oxidation. The oxygen uptake rates for malate and pyruvate are corrected for glutamate and malate oxidation respectively. Values are the mean (± SEM) of 3 independent experiments. nd. = none detected.

	Oxygen uptake, nmol min^{-1} mg $protein^{-1}$			
	Light grown		Dark grown	
Substrate	3 DPI	7 DPI	3 DPI	7 DPI
Succinate	275 ± 67	250 ± 43	186 ± 46	127 ± 33
Malate	210 ± 53	185 ± 48	153 ± 27	86 ± 20
2-Oxoglutarate	75 ± 31	63 ± 25	86 ± 23	79 ± 35
Pyruvate	16 ± 2	9.2 ± 0.4	10 ± 1	7.7 ± 0.2
Glycine	nd.	86 ± 27	nd	nd
NADH	212 ± 41	187 ± 32	164 ± 25	150 ± 36

The measurement of mitochondrial oxidation rates provides further support for the assertion that there is a greater capacity on the non-decarboxylating side of the TCA cycle (Millhouse *et al.*, 1983). In addition the following points also emerge:

1. There is a light dependant increase in the rate of malate oxidation, but a developmentally regulated increase in the succinate oxidation rate, suggesting a role for the former in photosynthetic development and the latter in lipid mobilisation.

FIGURE 3.8

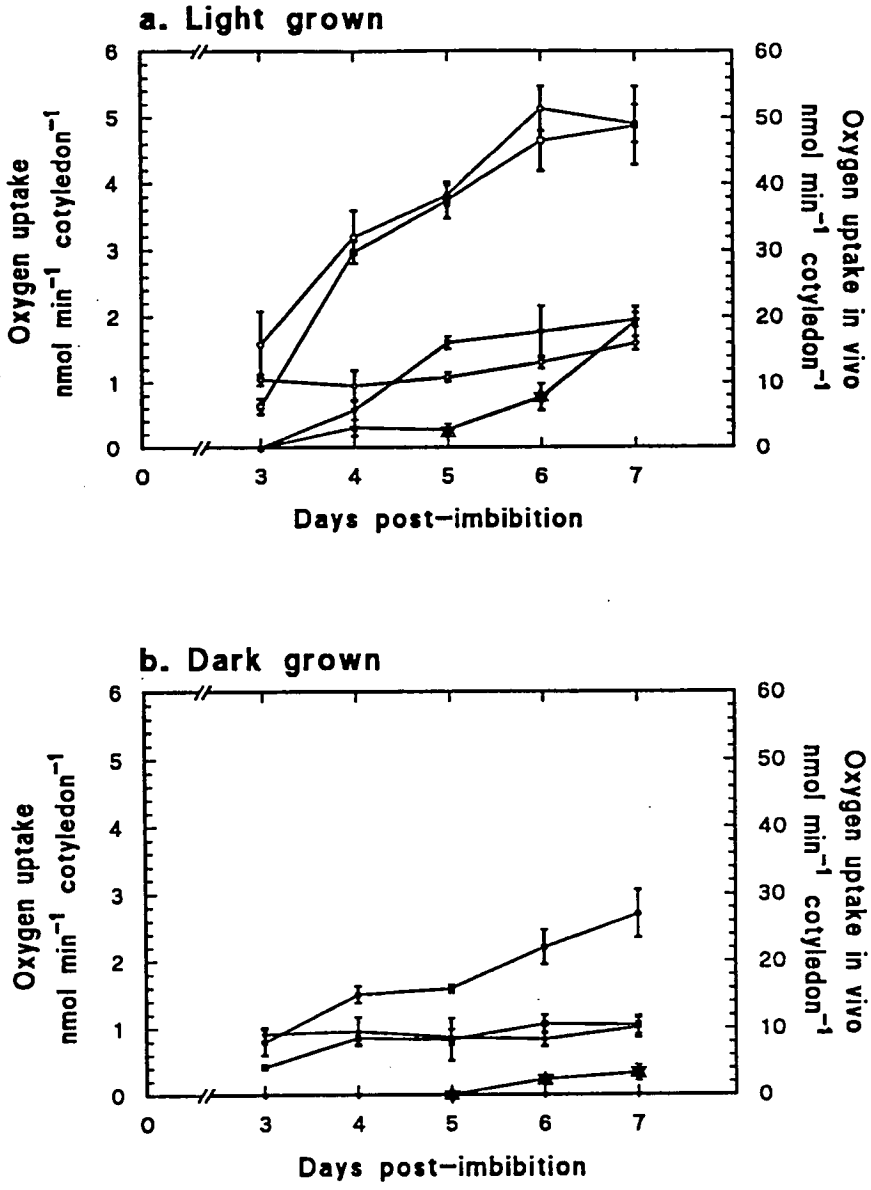

FIGURE 3.8 *Developmental variation in mitochondrial respiration.* Mitochondria were isolated at each stage and oxygen uptake measured in the presence of the substrate indicated (at a concentration of 10 mM) and 100 nmol ADP as described in Chapter 2. (○,●), succinate; (□,■), malate; (◇,◆), 2-oxoglutarate; (☆,★), pyruvate; (▽,▼), glycine. The following were also present in addition: 0.25 mM ATP during succinate oxidation; 10 mM glutamate during malate oxidation; 0.1 mM thiamine pyrophosphate during pyruvate and 2-oxoglutarate oxidation; and 0.1 mM malate during pyruvate oxidation. The oxygen uptake rates for malate and pyruvate are corrected for glutamate and malate oxidation, respectively. The left-hand axes refer to the rate in isolated mitochondria, the right hand axes to the *in vivo* rate, corrected for mitochondrial yield (assumed to be 10 %, see 2.3.5). Points are the mean (± SEM) of 3 independent experiments.

a. Light grown cotyledons.
b. Dark grown cotyledons.

2. There are increases in 2-oxoglutarate and pyruvate oxidation rates coincident with the photosynthetic phase, suggesting an increase in TCA cycle operation associated with this stage.

3.4.2 Non-phosphorylating electron transport.

The capacity for non-phosphorylating electron transport was assessed in mitochondria isolated from 4 and 7 day old cotyledons. Two parameters were measured: first, the capacity of the alternative pathway, as indicated by the proportion of state 3 respiration insensitive to antimycin A, an inhibitor of coupled electron transport at complex III; and secondly, the engagement of the alternative pathway during state 3 oxidation, measured by comparing the ADP:O ratio in the presence and absence of salicylhydroxamic acid (SHAM), an inhibitor of the alternative oxidase (Lambowitz *et al.*, 1972). The results obtained are shown in Table 3.6. The percentage of state three respiration insensitive to antimycin A is between 30 and 40 %, and there is no significant difference between mitochondria from 4 or 7 day old light or dark grown cotyledons. During single substrate oxidations under state 3 conditions the alternative pathway is engaged at a level of approximately 10 % of the oxidation rate. When succinate is oxidised together with an NAD-linked substrate (malate or glycine) there is an increased engagement of the alternative oxidase to 20-25 %. However, when glycine and malate are oxidised together, the alternative pathway remains engaged at the 10 % level. In mitochondria isolated from light grown cotyledons at 7 days post-imbibition, oxidation of succinate with malate or glycine is additive -that is, the rate is close to that predicted from the individual oxidation rates -whereas the rate of oxidation of malate plus glycine is lower than expected (Table 3.7). This data is consistent with the hypothesis that succinate oxidation has preferential access to the alternative pathway, and this allows succinate oxidation to proceed at high rates, simultaneously with oxidation of NAD-linked substrates. Under these conditions it is also possible that the rotenone-insensitive by-pass of complex I (NADH dehydrogenase) may be activated, but this was not investigated.

TABLE 3.6: *Antimycin A insensitive respiration and alternative pathway flux in cucumber cotyledons mitochondria.* Mitochondria were isolated as described in Chapter 2. Antimycin A insensitive oxygen uptake was measured in the presence of the substrate indicated (each at 10 mM), 100 nmol ADP, and 5 µM antimycin A. The flux through the alternative pathway was determined by measuring the ADP:O ratio for each substrate in the presence and absence of 1 mM salicilylhydroxamic acid. Results are expressed as a percentage of the state 3 rate of oxygen uptake. Values are the mean (± SEM) of 3 independent experiments.

	4 DPI		7 DPI	
Substrate	Antimycin A Insensitive %	Alternative Pathway %	Antimycin A Insensitive %	Alternative Pathway %
Light grown				
Succinate	32 ± 4	9 ± 1	39 ± 3	10 ± 2
Malate	40 ± 5	11 ± 2	33 ± 4	9 ± 2
Glycine			37 ± 5	11 ± 1
Succinate + malate	35 ± 5	22 ± 3	33 ± 2	24 ± 2
Succinate + glycine			36 ± 4	18 ± 3
Glycine + malate			37 ± 4	11 ± 1
Dark grown				
Succinate	33 ± 3	11 ± 2	32 ± 4	9 ± 3
Malate	34 ± 3	11 ± 2	32 ± 3	9 ± 1
Succinate + malate	32 ± 3	24 ± 4	31 ± 3	27 ± 5

TABLE 3.7: *Oxidation rates of single and combined substrates by mitochondria isolated from light grown cucumber cotyledons at 7 days post imbibition.* Mitochondria were isolated and the rate of oxygen uptake measured in the presence of the substrate indicated (each at 10 mM) and 100 nmol ADP as described in Chapter 2. When malate was present 10 mM glutamate was also present.

	Oxygen uptake, nmol min^{-1} mg $protein^{-1}$	
Substrate	Expt. 1	Expt. 2
Succinate	176	159
Malate	132	112
Glycine	62	71
Succinate + Malate	296	281
Succinate + Glycine	227	237
Malate + Glycine	142	135

3.4.3 Mitochondrial protein composition.

There are three hypotheses which could explain the changes in mitochondrial function described in 3.3.2 and 3.4.1. These are that the changes in enzyme activity are due to either allosteric modifications, covalent modifications or *de novo* protein synthesis. The following evidence supports the latter hypothesis. There is an increase in the amount of mitochondrial protein isolated from cotyledons during development (Figure 3.9). There is no signifieant change during development in the fumarase activity in isolated mitochondria when expressed per unit weight of mitochondrial protein content (Table 3.8), so that the increase in total fumarase activity, expressed in terms of cotyledon number, is likely to be due to synthesis of mitochondrial proteins. Finally, immunoblotting experiments show that the steady state level of glycine decarboxylase immunoreactive species increase during development. This is direct evidence that the increase in the capacity for glycine oxidation is accompanied by synthesis of glycine decarboxylase subunits (Figure 3.10).

TABLE 3.8: *Fumarase activity in cucumber cotyledon mitochondria.* Mitochondria were isolated and assayed for fumarase activity as described in Chapter 2. Values are the mean ($\pm$ SEM) of 3 independent experiments.

Days post imbibition	Fumarase activity nmol min^{-1} mg $protein^{-1}$
Light grown	
3	331 $\pm$ 11
4	412 $\pm$ 36
5	315 $\pm$ 16
6	298 $\pm$ 13
7	280 $\pm$ 16
Dark grown	
3	371 $\pm$ 15
4	379 $\pm$ 23
5	321 $\pm$ 15
6	303 $\pm$ 18
7	252 $\pm$ 9

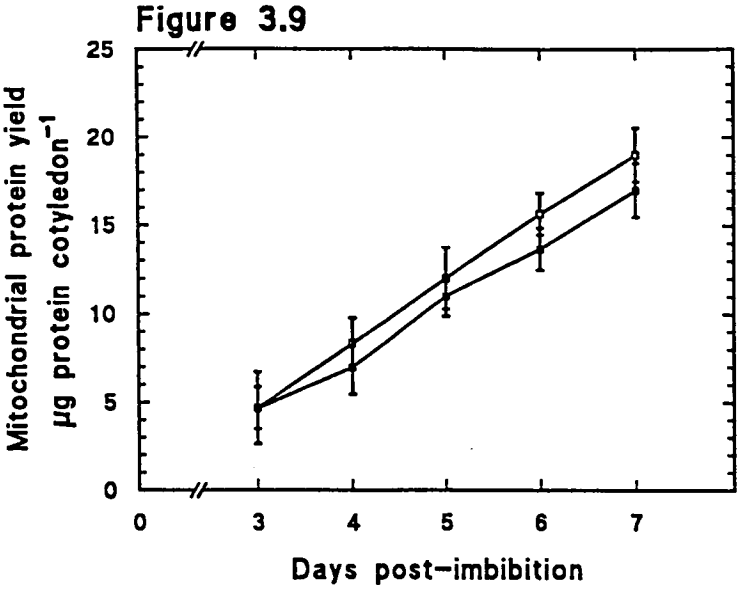

FIGURE 3.9. *Developmental variation in mitochondrial yield.* Mitochondria were isolated at each stage, and the protein precipitated with trichloroacetic acid and assayed as described in Chapter 2. (□), light grown cotyledons; (■), dark grown cotyledons. Points are the mean (± SEM) of 3 independent extracts.

FIGURE 3.10. *Developmental variation in the level of the P-protein of glycine decarboxylase.* Proteins were isolated from cotyledons at 3 to 7 days post-imbibition, fractionated by SDS-polyacrylamide gel electrophoresis, transferred to nitrocellulose and probed with an antibody specific for the P-protein of glycine decarboxylase, as described in Chapter 2. Each track contains the protein isolated from 1/20 cotyledon. The position of molecular weight markers is indicated on the left.

3.5 Discussion.

3.5.1 Nutritional phases and respiration during early seedling development.

Figure 3.5 shows the extent of the three defined phases during early seedling development. As expected, there is considerable overlap between the phases, but it is possible to identify points at which one or other predominates. Four days post-imbibition in light grown material is taken as the point in development characteristic of lipid mobilisation, as this is when both the rate of lipid mobilisation itself and the activity of the key enzymes responsible are at a maximum. Only the very early stages of photosynthetic development are apparent at this stage. Chlorophyll synthesis is at a maximum at 5 days post-imbibition, so this is taken as the point characteristic of chloroplast biogenesis. Since all the photosynthetic parameters measured had reached their maximum value by 7 days post-imbibition, photosynthesis is taken to predominate at this stage. In dark grown material photosynthetic development and function are absent, while lipid mobilisation proceeds in a similar fashion to light grown cotyledons. Therefore any changes in respiratory physiology present in light grown material not found in dark grown cotyledons are likely to be associated with photosynthesis. It should be emphasised that the changes observed represent cellular differentiation, as there is no cell division in the cotyledons during the period examined (Becker *et al.*, 1978).

Changes in mitochondrial respiration can be correlated with changes in nutritional status. The general conclusions from the data presented in this chapter are that during lipid mobilisation the flow of carbon through the decarboxylating side of the TCA cycle is restricted, but during chloroplast biogenesis and the associated development of photosynthetic function the capacity exists for operation of the complete TCA cycle. The restriction of TCA cycle decarboxylation is consistent with evidence from tissue slices of castor bean endosperm (Canvin and Beevers, 1961). In this tissue, the activity of enzymes and oxidation rate of substrates on the non-decarboxylating side of the TCA cycle are higher than those on the decarboxylating side (Cooper and Beevers, 1969a; Millhouse *et al.*, 1983). An exception to this is the oxidation rate of malate, which is low due to the restriction of malate dehydrogenase by oxaloacetate, which is exported at very low rates from castor bean endosperm mitochondria (Millhouse *et al.*, 1983). The rates of malate oxidation described in this chapter were measured in the presence of glutamate, in order to remove oxaloacetate by transamination. Pyruvate is not metabolised via the TCA cycle in castor bean endosperm (Neal and Beevers, 1960) and this appears, at least in part to be due to a low capacity for mitochondrial pyruvate oxidation (Millhouse *et al.*, 1983). These results are in conflict with those of Brailsford *et al.* (1986) who describe relatively rapid rates of pyruvate oxidation in isolated castor bean endosperm mitochondria. Cucumber

cotyledon mitochondria show higher activities of the external NADH dehydrogenase than those from castor bean endosperm (Table 3.4; Millhouse *et al.*, 1983; Brailsford *et al.*, 1986).

In soybean cotyledons, which also mobilise both protein and lipid during early seedling development, similar increases in the capacity for oxidation of succinate, malate, external NADH, and glycine by isolated mitochondria are observed (Azcon-Bieto *et al.*, 1989). Mitochondria isolated from greening cucumber cotyledons do not oxidise glutamate, in contrast to soybean mitochondria, which oxidise this substrate rapidly (Day *et al.*, 1988b). This may reflect a differing role for storage protein in these species: as a source of amino acids in cucumber, but, additionally, as a source of energy in soybean. The difference between the capacity for oxidation of TCA cycle substrates from the non-decarboxylating and decarboxylating sides of the TCA cycle is less marked in soybean (Bryce and Day, 1990) than cucumber. This may again be due to the reduced importance of lipid, as compared to protein as a source of stored reserves, in the former species.

Mitochondria from soybean cotyledons exhibit their maximum rates of TCA cycle substrate oxidation when the chlorophyll content of the cotyledons is highest (Azcon-Bieto *et al.*, 1989). These results, together with those presented in this chapter, confirm the importance of TCA cycle operation during chloroplast biogenesis and photosynthesis. This data complements the growing body of evidence which suggests that operation of the TCA cycle and oxidative phosphorylation is important in illuminated photosynthetic tissues (Chapman and Graham, 1974; Hampp *et al.*, 1982; Stitt *et al.*, 1982; Azcon-Bieto and Osmond, 1983; Gardestrom and Wigge, 1988).

3.5.2 Respiration and lipid mobilisation.

The aim of this section is to compare the rate of lipid breakdown at 4 days post-imbibition in light grown cotyledons with the available respiratory activities at this stage. The rate of lipid breakdown at 4 days post-imbibition is 1.3 mg lipid day^{-1} $cotyledon^{-1}$ (Figure 3.1). If the lipid is assumed, for reasons of simplicity, to consist exclusively of tripalmitoyl glycerol, the rate of palmitate breakdown is 1.2 mg day^{-1} $cotyledon^{-1}$, since palmitate accounts for 94 % of the mass of tripalmitoyl glycerol. The rate of breakdown is equivalent to 3.5 nmol min^{-1} $cotyledon^{-1}$.

Each mole of palmitate gives rise to 4 moles of succinate, so that the rate of succinate synthesis is 14 nmol min^{-1} $cotyledon^{-1}$. The maximum rate of succinate oxidation at 4 days post-imbibition is 32 $\pm$ 4 nmol min^{-1} $cotyledon^{-1}$ (Figure 3.8a), and the maximum fumarase activity is 34 $\pm$ 3 nmol min^{-1} $cotyledon^{-1}$ (Table 3.3), so that mitochondrial succinate oxidation is sufficient to account for the observed rate of lipid breakdown.

Each mole of palmitate gives rise to 11 moles of NADH external to the mitochondria, so that the rate of NADH synthesis is 38.5 nmol min^{-1} $cotyledon^{-1}$.

Assuming maximal conversion of succinate to hexose phosphate, the rate of NADH utilisation during sucrose synthesis is 14 nmol min^{-1} $cotyledon^{-1}$, giving a net rate of NADH synthesis of 24.5 nmol min^{-1} $cotyledon^{-1}$. The maximum rate of external NADH oxidation by mitochondria isolated at 4 days post imbibition is 28.5 ± 1.4 nmol min^{-1} $cotyledon^{-1}$, which is sufficient to account for the observed rate of NADH synthesis.

3.5.3 The role of non-phosphorylating electron transport.

The data described in section 3.4.2 provides evidence that the non-phosphorylating pathway of electron transport in mitochondria from cucumber cotyledons is of importance in succinate oxidation under conditions when NAD-linked substrates are also being oxidised. There is no apparent developmental change in the capacity of the alternative pathway when expressed as a percentage of the state 3 respiratory rate, but, as these rates increase during development, the actual flux through the alternative pathway must also increase. Similar data is also available for mitochondria from soybean cotyledons, with the exception that malate is not oxidised via the alternative pathway in mitochondria isolated from etiolated cotyledons (Azcon-Bieto *et al.*, 1989).

In soybean cotyledons the flux through the alternative pathway shows a non-linear dependence on the level of ubiquinone reduction (Dry *et al.*, 1989), suggesting that the increased engagement of the alternative pathway, when succinate is oxidised together with an NAD-linked substrate, is due to saturation of the cytochrome pathway. The absence of any increase in the flux through the alternative pathway when glycine and malate are oxidised together may either be because the combined rate is not sufficiently high to lead to enough ubiquinone reduction to activate the alternative pathway, or as a consequence of differential access of NADH produced from the two substrates to Complex I. The latter explanation is supported by the non-additive nature of malate plus glycine oxidation, which is also observed in pea leaf mitochondria (Dry, Day and Wiskich, 1983). In this tissue, this is, at least in part, explained by differential access to pyridine nucleotides and the respiratory chain by glycine decarboxylase and malate dehydrogenase (Dry and Wiskich, 1985). Recent findings provide support for the existence of metabolic domains within the matrix of pea leaf mitochondria, which allow NADH produced during glycine oxidation to be reoxidised by malate dehydrogenase, operating in the oxaloacetate to malate direction, at the same time as malate oxidation by malate dehydrogenase linked to the respiratory chain (Wiskich *et al.*, 1990). The data presented in this chapter are consistent with a similar system operating within the matrix of cucumber cotyledon mitochondria, thus preventing saturation of the cytochrome pathway when malate and glycine are oxidised simultaneously, reserving the available alternative pathway capacity for succinate oxidation. Similar preferential access of substrates to the alternative pathway is found for succinate in

soybean cotyledon mitochondria (Day *et al.*, 1988a), and pyruvate in castor bean endosperm mitochondria (Brailsford *et al.*, 1986).

In conclusion, mitochondria from cucumber cotyledons have properties such that rapid succinate oxidation, an integral part of lipid mobilisation, can take place under conditions when TCA cycle operation, photorespiratory flux and cytosolic ATP/ADP ratios are high, as would be predicted to occur during lipid mobilisation and photosynthesis.

3.5.4 Modulation of mitochondrial biogenesis and function.

The results contained in this chapter provide evidence for changing mitochondrial function during early seedling development and give some indication that the *de novo* synthesis of both nuclear and mitochondrially encoded mitochondrial proteins may be involved. There are a number of reports of the synthesis of mitochondrial proteins during germination and early seedling development in peanut cotyledons (Breidenbach *et al.*, 1966, 1967), soybean cotyledons (Azcon-Bieto *et al.*, 1989), and maize embryos (Ehrenshaft and Brambl, 1990). However, it has been claimed that the increase in respiration observed in pea cotyledons during germination is primarily due to the import and assembly of previously synthesised polypeptides, held in cytoplasmic pools (Matsuoka and Asahi, 1983). It is well established that the increase in glycine decarboxylase activity in green leaves is caused by light, due to an effect on gene expression (Douce, 1985).

3.6 Conclusions.

The data presented in this chapter suggests that mitochondrial function in cucumber cotyledons is modulated during early seedling development in parallel with the changing metabolic requirements of the tissue. The remainder of this thesis is concerned with the regulation of mitochondrial function, the integration of respiration with cellular metabolism, and the importance of *de novo* protein synthesis in bringing about the changes described. Three aspects will be considered in detail:

1. The regulation of succinate oxidation.
2. The control of entry of pyruvate into respiratory metabolism.
3. The role of mitochondria in the regulation of sucrose synthesis from lipid.

CHAPTER 4.
THE CONTROL OF SUCCINATE OXIDATION.

4.1 Introduction and Aims

The experiments with isolated mitochondria described in Chapter 3 demonstrate that the rate of succinate oxidation increases between 3 and 7 days post imbibition in both light and dark grown cucumber cotyledons. Since there is an increase in oxidation rate irrespective of the light environment, this change is likely to be associated with lipid mobilisation. However, the oxidation rate in mitochondria isolated from 7 day old light grown cotyledons is greater than that of dark grown cotyledons of the same age, suggesting that succinate oxidation may also be important for photosynthetic function.

The work described in this chapter is an investigation into the regulation of succinate oxidation by isolated mitochondria in order to establish: first, the means by which this process is regulated both during lipid mobilisation and photosynthesis; and secondly, the role of *de novo* protein synthesis in the observed increases in succinate oxidation rate. These objectives were achieved by measuring the distribution of flux control coefficients in mitochondria isolated from 3 and 7 day old cotyledons and examining the variation in the level of the enzymes responsible for the major controlling steps during development. For the purposes of this study, succinate oxidation is taken to include not only the conversion of succinate into fumarate, but also the uptake of succinate into the mitochondria, the transfer of electrons to oxygen by the respiratory chain and the synthesis of ATP, as shown in Figure 4.1.

4.2 Theory and Experimental Approach.

Flux control coefficients were determined in isolated mitochondria oxidising succinate in the presence of excess ADP (state 3) using the inhibitor titration approach of Groen *et al.* (1982). This method uses specific inhibitors to reduce the activity of individual steps in the pathway without affecting the other reactions. The pathway of succinate oxidation in isolated mitochondria (Figure 4.1.) consists of seven steps, four of which were investigated using the following inhibitors:

(1) Complex II - malonate,

(2) Complex III - antimycin A,

(3) Complex IV - azide,

(4) Adenine nucleotide translocator (AdNT) - carboxyatractyloside (CATR).

According to Kacser and Burns (1973) the effect of an inhibitor on the steady state flux through a pathway is dependent on two parameters, the effect of the inhibitor on the isolated enzyme, and the flux control coefficient of the enzyme on the pathway flux. This relationship is shown in equation 4.1:

$$\frac{dJ/J}{dI/I} = C_j \cdot \frac{dv_j/v_j}{dI/I} \qquad (4.1)$$

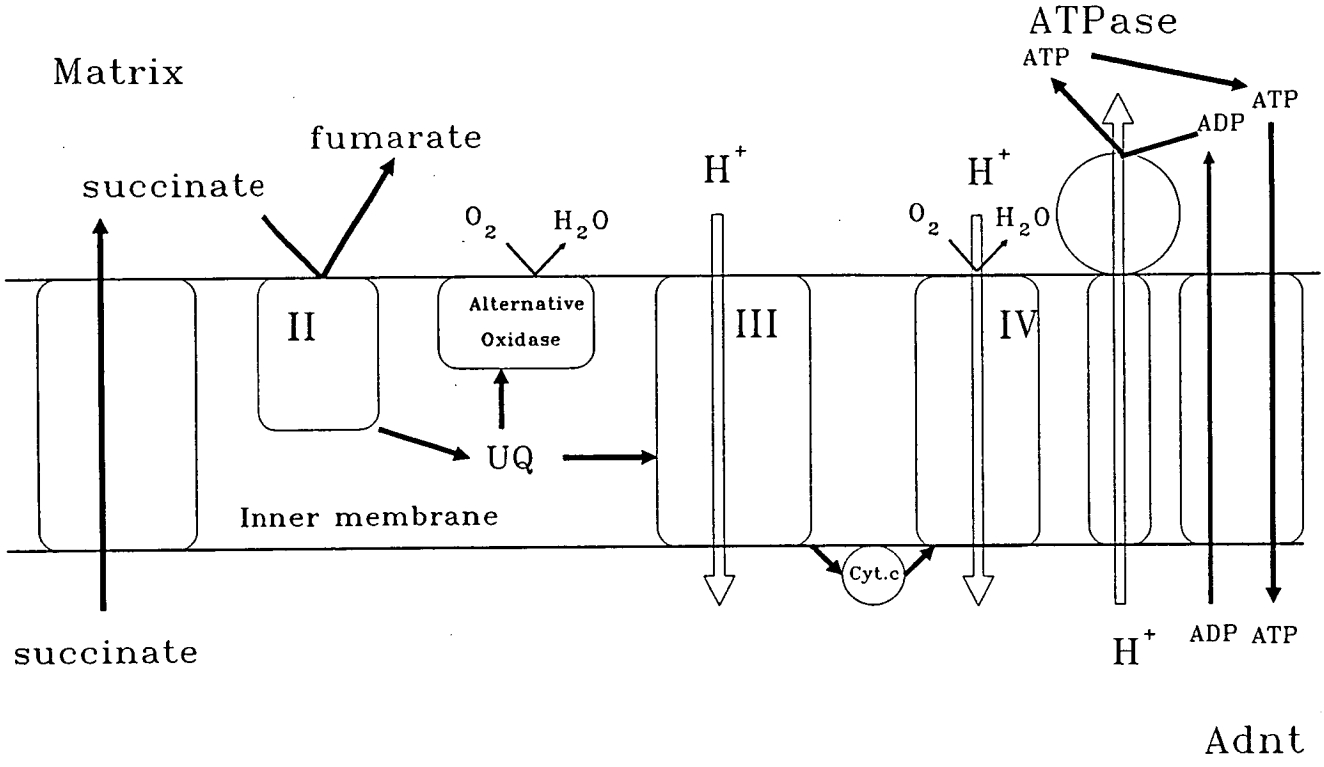

FIGURE 4.1: *The pathway of succinate oxidation by isolated mitochondria.*

where J is the pathway flux, I the inhibitor concentration, v_j the velocity of step j, and C_j the flux control coefficient of step j on the flux J. Thus,

$$C_j = \frac{(dJ/J)/dI}{(dv_j/v_j)/dI} \qquad (4.2)$$

The parameter $(dJ/J)/dI$ can be determined by measuring the initial slope of an inhibitor titration curve of J against I (dJ/dI), and the pathway flux in the absence of inhibitor (J). Similarly, $(dv_j/v_j)/dI$ can be obtained by titrating the individual enzyme with inhibitor, under pathway conditions. When irreversible inhibitors are used, a linear relationship exists between inhibitor concentration and enzyme velocity, so that equation 4.2 simplifies to equation 4.3:

$$C_j = \frac{dJ/J}{dI/I_{max}} \qquad (4.3)$$

where I_{max} is the minimum amount of inhibitor required to give maximum inhibition. The flux control coefficients of Complexes II and IV were calculated using equation 4.2, while those of Complex III and the adenine nucleotide translocator were calculated using equation 4.3, since both antimycin A and CATR are irreversible inhibitors.

The flux control coefficients of the remaining three steps (that is, the dicarboxylate uptake system, the alternative oxidase, and the ATPase) were calculated as follows. The flux control coefficient of the mitochondrial ATPase was assumed to be negligible since the value of this coefficient is low in both turnip (Padovan *et al.*, 1989) and rat liver (Groen *et al.*, 1982) mitochondria. The flux control coefficient of the alternative oxidase was calculated from the branch point relationship (Fell and Sauro, 1985):

$$C_{AO} = \frac{a}{1-a} \cdot (C_{III} + C_{IV}) \qquad (4.4)$$

where a is the proportion of the total flux through the alternative pathway, assumed to be 0.1 (see 3.4.2). Finally, the flux control coefficient of the dicarboxylate transporter was calculated from the summation theorem (Kacser and Burns, 1973):

$$C_{DT} = 1 - (C_{II}+C_{III}+C_{IV}+C_{AdNT}+C_{AO}) \qquad (4.5)$$

4.3 Flux Control Coefficients.

4.3.1 Titration curves.

Typical inhibitor titration curves are shown in figures 4.2, 4.3, 4.4 , and 4.5. The examples shown illustrate curves obtained when the flux control coefficient is low (<0.05) or high. The following points are emphasised. High values for the flux control coefficient of the adenine nucleotide translocator are associated with low values of I_{max} for CATR (Figure 4.2), suggesting that these differences may be due to variation in the level of the adenine nucleotide translocator polypeptides. This contrasts with Complex III, where similar values of I_{max} (antimycin A) are found in preparations with differing flux control coefficients (Figure 4.3). The residual oxygen uptake after maximum inhibition with CATR (Figure 4.2) corresponds to the rate of ADP-limited respiration (state 4). There is also residual respiration after maximum inhibition with antimycin A (Figure 4.3) and azide (data not shown), due to the alternative pathway. Almost complete inhibition of oxygen uptake is achieved with malonate (data not shown).

CATR binds to the ATP/ADP binding site of the adenine nucleotide translocator (Riccio *et al.*, 1975), so that it is possible that this inhibitor may also bind to other enzymes which have adenine nucleotides as substrates or effectors. A prime candidate is hexokinase, which has been shown to be associated with the outer surface of isolated mitochondria (Dry, Nash, and Wiskich, 1983). If this were the case CATR concentrations within the mitochondria during titrations would depend upon the level of extra-mitochondrial hexokinase, introducing inaccuracies in flux control coefficient measurements. CATR inhibits hexokinase associated with cucumber cotyledon mitochondria (Figure 4.6), but much higher levels are required than for the inhibition of respiration (I_{50} for respiration 20-70 pmol CATR mg protein^{-1}, for hexokinase >100 nmol CATR mg protein^{-1}). The effect of hexokinase on the measurement of flux control coefficients was tested by removing it from the outer mitochondrial membrane by protease digestion. Incubation at 25°C for 6 minutes with Pronase removes most of the mitochondrial hexokinase, without significantly reducing fumarase or cytochrome oxidase activities (Figure 4.7). Protease treated mitochondria, and control samples incubated at 25°C in the absence of protease, showed no significant difference in flux control coefficient of the adenine nucleotide translocator (Table 4.1). It is therefore assumed that the flux control coefficients presented in the following section are accurate estimates.

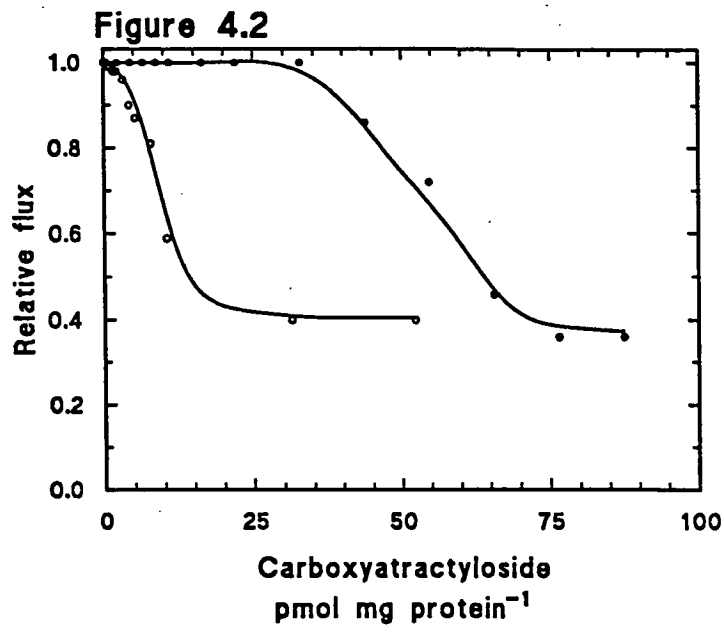

FIGURE 4.2. *Effect of carboxyatractyloside on the state 3 rate of succinate oxidation by isolated cucumber cotyledon mitochondria.* Mitochondria were isolated from 3 day old light grown (○) and dark grown (●) cotyledons as described in Chapter 2. Oxygen uptake was measured in the presence of 10 mM succinate, 0.25 mM ATP, 1 µmol ADP, and increasing amounts of carboxyatractyloside. The uninhibited rates of succinate oxidation were 124 and 165 nmol min^{-1}(mg protein)$^{-1}$ for mitochondria from light and dark grown cotyledons respectively.

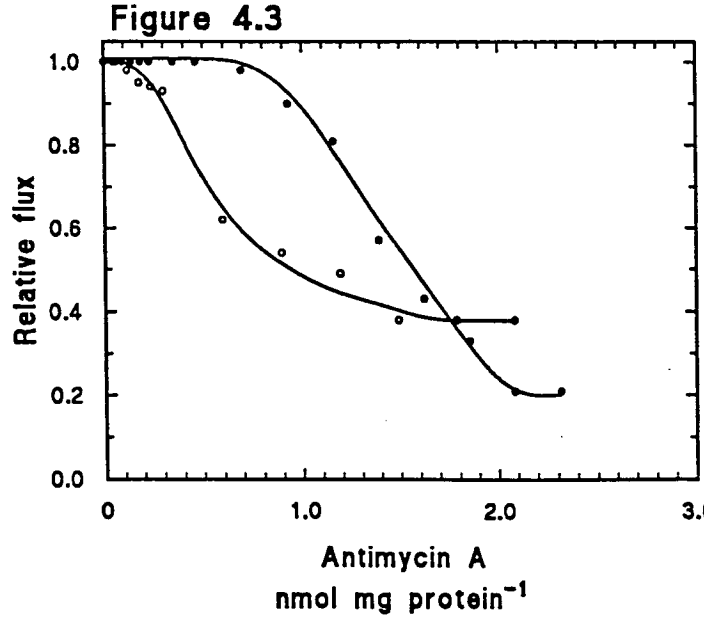

FIGURE 4.3. *Effect of antimycin A on the state 3 rate of succinate oxidation by isolated cucumber cotyledon mitochondria.* Mitochondria were isolated from 3 day old dark grown (●) and 7 day old light grown (○) cotyledons as described in Chapter 2. Oxygen uptake was measured in the presence of 10 mM succinate, 0.25 mM ATP, 1 µmol ADP, and increasing amounts of antimycin A. The uninhibited rates of succinate oxidation were 173 and 179 nmol min^{-1}(mg protein)$^{-1}$ for mitochondria from 3 day old dark grown and 7 day old light grown cotyledons respectively.

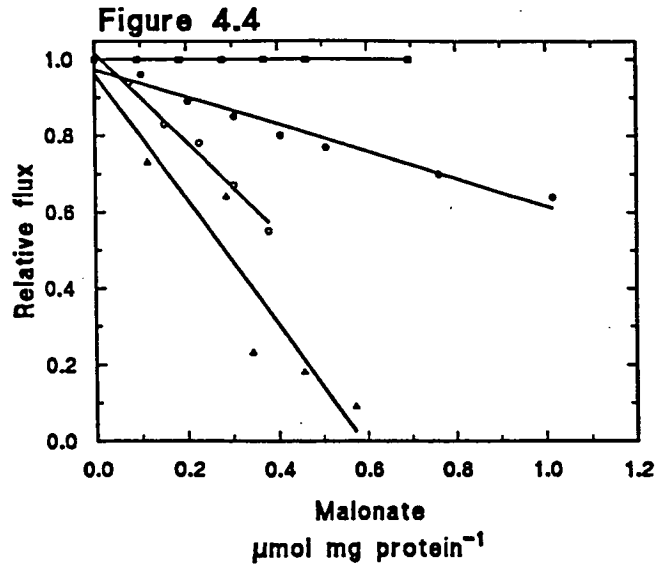

FIGURE 4.4. *Effect of malonate on succinate dehydrogenase activity and the state 3 rate of succinate oxidation by isolated cucumber cotyledon mitochondria.* Mitochondria were isolated from 3 day old dark grown (■) and 7 day old light grown (○) and dark grown (●) cotyledons as described in Chapter 2. Oxygen uptake was measured in the presence of 10 mM succinate, 0.25 mM ATP, 1 µmol ADP, and increasing amounts of malonate. Succinate dehydrogenase activity (▲) was measured in mitochondria from 7 day old light grown cotyledons The uninhibited rates were 301, 138, 162, and 185 nmol min^{-1} (mg protein)$^{-1}$for succinate dehydrogenase, 3 day old dark grown cotyledons, 7 day old light grown cotyledons, and 7 day old dark grown cotyledons, respectively.

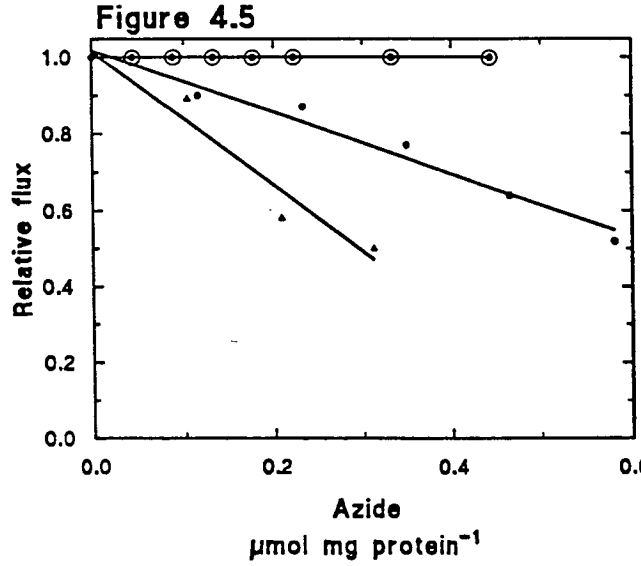

FIGURE 4.5. *Effect of azide on cytochrome oxidase activity and the state 3 rate of succinate oxidation by isolated cucumber cotyledon mitochondria.* Mitochondria were isolated from 3 day old light grown (◎) and dark grown (●) cotyledons as described in Chapter 2. Oxygen uptake was measured in the presence of 10 mM succinate, 0.25 mM ATP, 1 µmol ADP, and increasing amounts of azide. Cytochrome oxidase activity (▲) was measured in mitochondria from 7 day old light grown cotyledons The uninhibited rates were 208, 178, and 124 nmol min^{-1}(mg protein)$^{-1}$ for cytochrome oxidase, and 3 day old light and dark grown cotyledons, respectively.

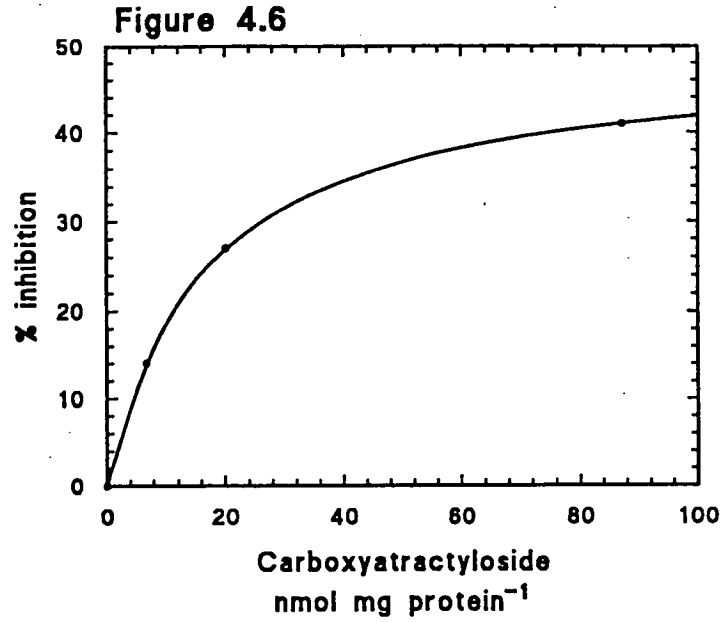

FIGURE 4.6. *Effect of carboxyatractyloside on the activity of hexokinase bound to the outer mitochondrial membrane.* Mitochondria were isolated from 7 day old light grown cotyledons and assayed for hexokinase as described in Chapter 2. The uninhibited hexokinase activity was 101 nmol min^{-1} (mg protein)$^{-1}$.

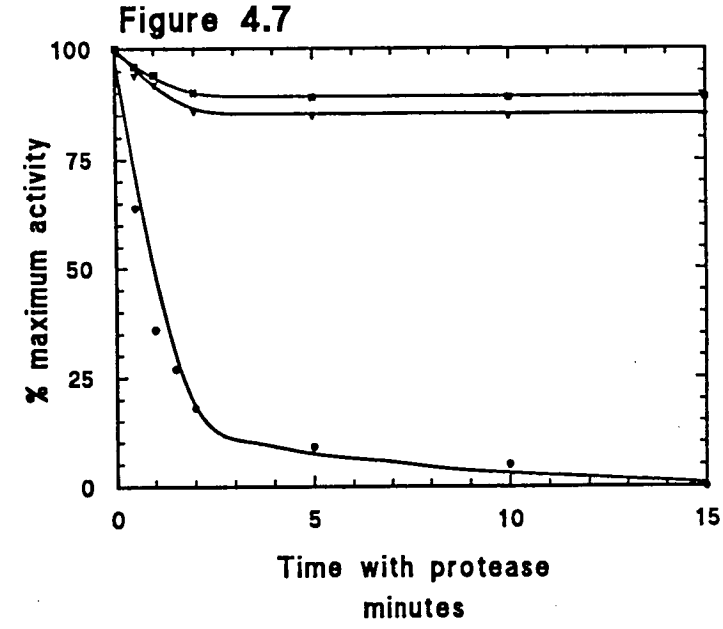

FIGURE 4.7. *Protease treatment of isolated mitochondria.* Mitochondria were isolated from 7 day old light grown cotyledons as described in Chapter 2. Mitochondria were incubated at a concentration of 1 mg protein ml^{-1} in Wash buffer (see 2.3.1) containing 12.5 µg µl^{-1} pronase, at 25°C. At the indicated time a sample was removed, and sufficient ice cold 100 mM PMSF added to it to give a final concentration of 1 mM. The mitochondria were then assayed for fumarase (■), cytochrome oxidase (▼) and hexokinase (●). The activity of the enzymes before the addition of protease was 133, 101, and 141 nmol min^{-1} (mg protein)$^{-1}$ for fumarase, cytochrome oxidase, and hexokinase, respectively.

TABLE 4.1. *Effect of protease treatment on the flux control coefficient of the adenine nucleotide translocator in isolated cucumber cotyledon mitochondria.* Mitochondria were isolated and treated with protease as described in the legend to Figure 4.7 for 6 minutes or incubated in Wash buffer (see 2.3.1) at 25°C for the same period of time. The flux control coefficient of the adenine nucleotide translocator was determined by titration with carboxyatractyloside under the conditions described in the legend to Figure 4.2.

	Flux control coefficient	
Days post-imbibition	- Protease	+ Protease
Light grown		
3	0.26	0.28
7	0	0
Dark grown		
3	0	0
7	0.14	0.10

TABLE 4.2. *Flux control coefficients for state 3 succinate oxidation in mitochondria isolated from cucumber cotyledons.* Mitochondria were isolated from each stage and oxygen uptake measured in the presence of 10 mM succinate, 0.25 mM ATP and 1 µmol ADP. Flux control coefficients were determined from inhibitor titration curves as described in the text. Values are the mean (± range) of 2 independent experiments.

	3 DPI		7 DPI	
Step	Light	Dark	Light	Dark
Complex II	0	0	0.295 ± 0.075	0.145 ± 0.045
Complex III	0	0	0.405 ± 0.035	0.405 ± 0.015
Complex IV	0	0.390 ± 0.070	0.370 ± 0.030	0.285 ± 0.025
AdNT	0.285 ± 0.095	0	0	0.165 ± 0.005
Alt. Oxidase*	0	0.04	0.09	0.08
Dicarb. Transporter**	0.715	0.570	-0.160	-0.08

* Calculated from branch point relation.

** Calculated from summation theorem.

4.3.2 Distribution of flux control coefficients.

The flux control coefficients for succinate oxidation in mitochondria isolated from 3 and 7 day old light and dark grown cucumber cotyledons are shown in Table 4.2. There are variations in the distribution of control due to both cotyledon age and light environment. In 3 day old cotyledons a large amount of control is located at the dicarboxylate translocator, responsible for the uptake of succinate into the mitochondria. The majority of the remaining control is vested in the adenine nucleotide translocator in light grown cotyledons, and Complex IV (cytochrome oxidase) in dark grown material. At 7 days post-imbibition the control of succinate oxidation rests largely on the respiratory chain, with the dicarboxylate transporter having a very low, or possibly negative, flux control coefficient. At this stage significant amounts of control are located in Complexes II, III and IV in both light and dark grown cotyledons, with some additional control also located at the adenine nucleotide translocator in mitochondria from dark grown material. At all stages the flux control coefficient of the alternative oxidase is low.

4.4 Developmental changes in major controlling steps.

A possible explanation for the increase in succinate oxidation rates by isolated mitochondria from 3 and 7 day old cotyledons is the synthesis of one or more of the enzymes in the pathway. The most likely sites for such regulation are the steps where most of the control is located at 3 days post-imbibition. The preceding section identifies the dicarboxylate transporter and the adenine nucleotide translocator as the major controlling steps at this stage.

The activity of the dicarboxylate transporter was measured in isolated mitochondria using the ammonium salt swelling technique (Zoglowek *et al.*, 1988). This method has the advantage that the assay is quick and easy to perform, but does not yield quantitative information about the absolute rate of solute uptake, since the relationship between increase in mitochondrial volume and uptake is unclear (Day and Wiskich, 1984). Nevertheless, such measurements give some indication of the relative transport capacities of mitochondria from different stages. The variation in the succinate transport rate during development is shown in Figure 4.8. In both light and dark grown cotyledons there is an increase in the capacity for succinate uptake by isolated mitochondria between 3 and 7 days post-imbibition, suggesting that synthesis or activation of the protein catalysing this step may be important in the observed increase in succinate oxidation rates.

The level of the adenine nucleotide translocator in light grown cotyledons was estimated by immunoblotting (Figure 4.9). The abundance of this protein increases between 3 and 7 days post-imbibition, confirming that the increase in succinate oxidation is due, in part, to *de novo* protein synthesis. The level of adenine nucleotide translocator in dark

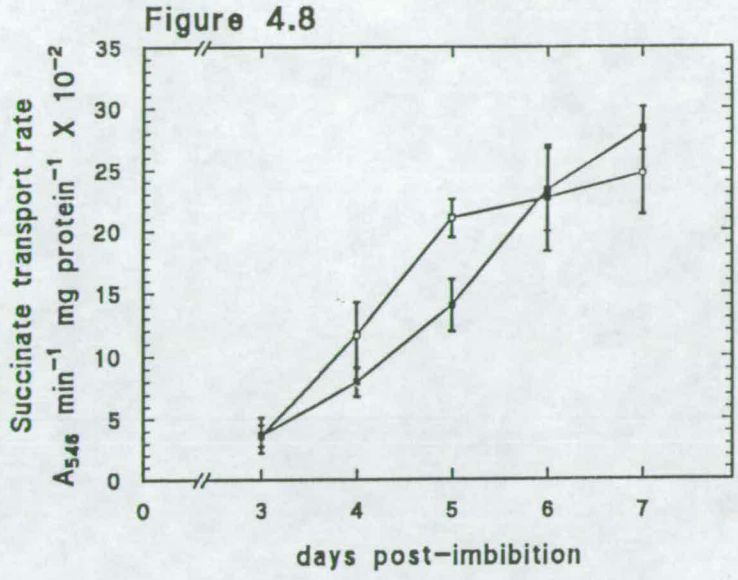

FIGURE 4.8. *Developmental variation in the activity of the dicarboxylate transporter.* Mitochondria were isolated at each stage and the rate of succinate uptake measured as the decrease in light scattering at 546 nm in 100 mM ammonium succinate. (□), light grown cotyledons; (■), dark grown cotyledons. Points are the mean (± SEM) of 3 independent experiments.

FIGURE 4.9. *Developmental variation in the level of the adenine nucleotide translocator.* Proteins were isolated from cotyledons at 3 to 7 days post-imbibition, fractionated by SDS-polyacrylamide gel electrophoresis, transferred to nitrocellulose and probed with an antibody specific for the adenine nucleotide translocator, as described in Chapter 2. Each track contains the protein isolated from 1/20 cotyledon. The position of molecular weight markers is indicated on the left.

grown cotyledons remained below the limit of detection by immunoblotting at all stages (data not shown).

4.5 Discussion.

4.5.1 Fine control of succinate oxidation.

The general conclusion from the work presented in this chapter is that the control of succinate oxidation under state 3 conditions is shared between a number of steps. This phenomenon was expected and predicted during the first description of metabolic control theory (Kacser and Burns, 1973; Heinrich and Rapoport, 1974). Similar results have been obtained with rat liver mitochondria. Inhibitor titration experiments analysed using the methods described in this chapter show that the control of state 3 succinate oxidation is shared between the adenine nucleotide translocator, dicarboxylate transporter and cytochrome oxidase (Groen *et al.*, 1982). Further evidence in support of this distribution of control is provided by measurements of the elasticities of the respiratory chain, phosphorylation system and proton leak fluxes to the mitochondrial membrane potential, analysed using the 'top-down' approach (Hafner *et al.*, 1990; Brown, Hafner, and Brand, 1990). Under state 3 conditions control is shared between the respiratory chain (including the dicarboxylate transporter) and the phosphorylating system (Hafner *et al.*, 1990). At intermediate rates of respiration the control coefficient of the phosphorylating system increases, whereas that of the respiratory chain decreases (Groen *et al.*, 1982; Hafner *et al.*, 1990). Under state 4 conditions control is almost exclusively located at the passive proton leak (Hafner *et al.*, 1990).

The control of state 3 succinate oxidation in turnip mitochondria, determined by the inhibitor titration approach, is shared between the respiratory chain complexes and the dicarboxylate transporter, with the adenine nucleotide translocator having negligible control (Padovan *et al.*, 1989). The control of succinate oxidation during lipid mobilisation and photosynthesis will be considered separately

a. *Control during lipid mobilisation.* The control coefficients measured at 3 days post-imbibition are typical of early lipid mobilisation (see 3.2.1). The dicarboxylate transporter has a very high control coefficient at this stage (Table 4.2), so that this is a major regulatory step in the mitochondrial part of the gluconeogenic pathway. No regulatory properties have been described for the dicarboxylate transporter. Its function is dependent on the operation of the phosphate translocator, since dicarboxylates are taken up in exchange for phosphate. Phosphate is itself cotransported into the mitochondria with protons, which flow in along the proton gradient generated by the respiratory chain (Heldt and Flugge, 1987; Figure 4.10). Thus the high control coefficient of the dicarboxylate transporter may in fact be partly due to control at the phosphate translocator. This,

combined with the high control coefficient of the adenine nucleotide translocator at 3 days post-imbibition, suggests that the rate of gluconeogenesis is controlled by the rate of succinate supply, cytosolic ATP/ADP ratio, and the cytosolic phosphate level. The following hypothesis for control is proposed. Under conditions of low rates of sucrose synthesis (for example, when sucrose removal to the growing regions of the seedling is saturated, causing sucrose build up) there is a drop in the cytosolic phosphate level (due to the accumulation of phosphorylated intermediates) and an increase in the ATP/ADP ratio (due to a reduction in flux through ATP consuming reactions). This leads to a drop in the rate of succinate oxidation. At the onset of lipid mobilisation there is an increase in the cytosolic succinate level, activating succinate oxidation. Support for this hypothesis is provided by comparison with sucrose synthesis in leaves. Under conditions when sucrose accumulates in the cytosol, the sucrose synthesis flux is reduced as a result of a drop in cytosolic phosphate levels (Stitt *et al.*, 1987a). In conclusion, mitochondrial reactions in gluconeogenesis may be under feedback control from cytosolic sucrose synthesis, and feedforward control from the glyoxylate cycle, acting as a 'balance point' between the ATP synthesising degradative reactions of lipid breakdown and the ATP consuming reactions of sucrose production.

The control of succinate oxidation in mitochondria from 7 day old dark grown cotyledons, where lipid mobilisation is still the major metabolic activity (see 3.2.1), is different from 3 day old cotyledons (Table 4.2). The adenine nucleotide translocator is still important, indicating that mitochondria are still responding directly to the ATP/ADP ratio, but there is significant control located at the respiratory chain. This suggests that mitochondrial succinate oxidation may remain under feedback control from sucrose synthesis, but is less sensitive to feed forward from the glyoxylate cycle, allowing sucrose synthesis to continue despite a low rate of lipid mobilisation.

b. *Control during photosynthesis.* Under photosynthetic conditions succinate oxidation is regulated by the respiratory chain (Table 4.2), and is therefore not under the direct control of the cytosolic ATP/ADP ratio. Complex III has a high control coefficient, and may be important in regulating the partitioning of electrons between the phosphorylating and non-phosphorylating pathways of electron transport. The significance of these observations for photosynthetic metabolism is unclear.

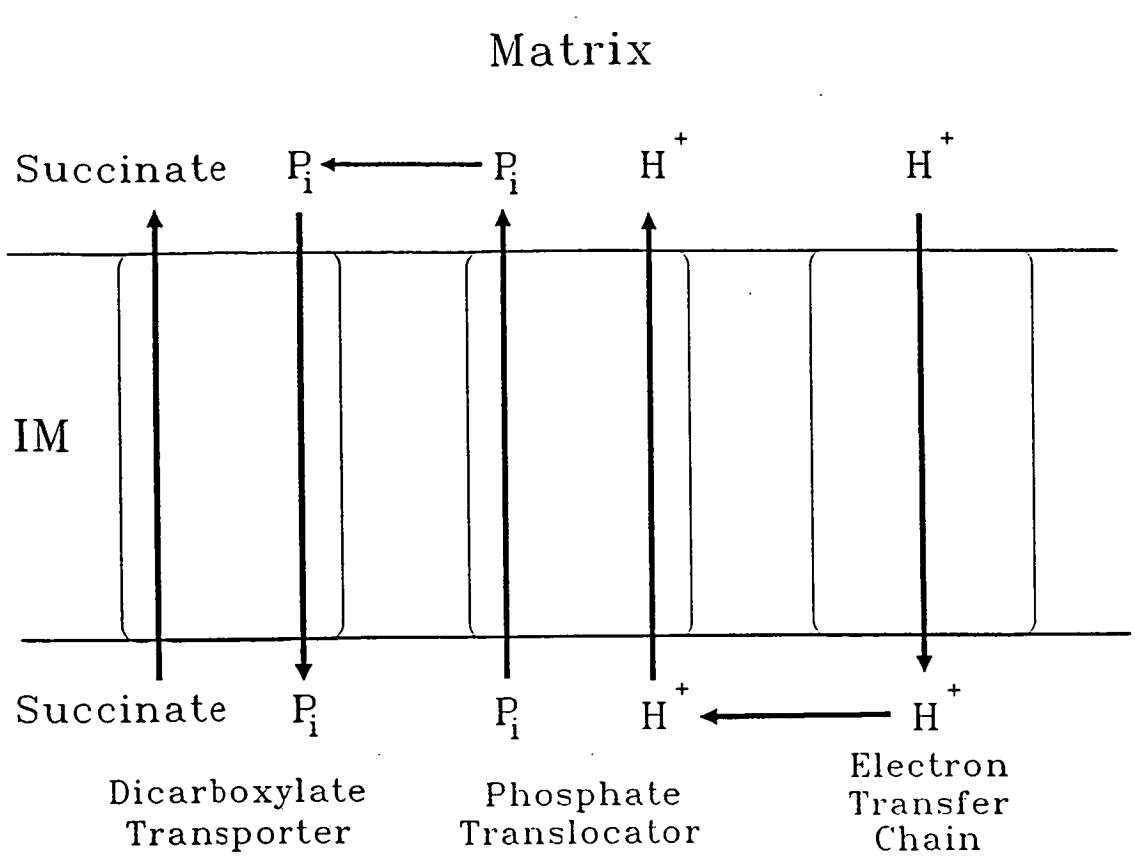

FIGURE 4.10: *The mechanism of dicarboxylate uptake into mitochondria.*

4.5.2 Coarse control of succinate oxidation.

The data presented in this chapter supports the following conclusion. The increase in succinate oxidation rates between 3 and 7 days post-imbibition is due to the *de novo* synthesis of the dicarboxylate transporter and the adenine nucleotide translocator (Figures 4.8 and 4.9). This is the first reported description of such coarse control of mitochondrial activity. The general significance of these observations will be discussed in Chapter 7. The regulation of the levels of these transport proteins differs: the dicarboxylate transporter is temporally regulated (Figure 4.8), whilst changes in the synthesis and/or degradation of the adenine nucleotide translocator is induced by light, or as a metabolic consequence of illumination (Figure 4.9).

The following additional facts may also be inferred. Since malate oxidation rates do not increase between 3 and 7 days post-imbibition in dark grown cotyledons (Figure 3.8b), this process is not regulated by the dicarboxylate transporter. Similarly, since 2-oxoglutarate oxidation rates do not change during development (Figure 3.8) this process is unlikely to be regulated by the dicarboxylate transporter or the adenine nucleotide translocator. The increase in pyruvate oxidation rate at day 6 in light grown cotyledons (Figure 3.8a) may be due to the increase in adenine nucleotide translocator levels, but this is unlikely as the adenine nucleotide translocator level begins to increase from day 4 onwards, before any increase in the rate of pyruvate oxidation is observed.

4.6 Conclusions.

1. There is evidence to suggest that mitochondria may play an important role in the integration of synthetic and degradative reactions during lipid mobilisation. This is further investigated in Chapter 6.

2. Mitochondrial function appears to be regulated by environmentally and temporally controlled *de novo* protein synthesis.

CHAPTER 5.
MITOCHONDRIAL PYRUVATE METABOLISM.

5.1 Introduction and Aims.

The experiments with isolated mitochondria described in Chapter 3 demonstrate that the rates of pyruvate oxidation in cucumber cotyledon mitochondria are very low, except during the photosynthetic phase (Figure 3.7). Pyruvate utilisation by mitochondria is of prime importance, since it is the only means by which carbon from C-3 compounds can enter the TCA cycle, allowing operation of mitochondrial decarboxylation reactions. Thus the control of pyruvate metabolism is likely to be of significance in the partitioning of carbon between biosynthesis and the release of carbon dioxide. In castor bean endosperm, a tissue whose only metabolic activity is the conversion of lipid to sucrose, there is evidence for the diversion of pyruvate away from the TCA cycle (Neal and Beevers, 1960; Millhouse *et al.*, 1983). The evidence presented in Chapter 3 suggests that a similar situation exists in cucumber cotyledons during the lipid mobilisation phase, but the restriction on pyruvate entry into the TCA cycle is lifted during photosynthesis.

This chapter describes investigations into the pathways of pyruvate production and utilisation both in the mitochondrial and cytosolic compartments, in order to better understand the regulation of pyruvate metabolism *in vivo*.

5.2 Regulation of Pyruvate Oxidation.

The pathway of oxidation of externally supplied pyruvate by isolated mitochondria is shown in Figure 5.1. Pyruvate oxidation rates in isolated mitochondria are much lower than those of, for example, malate and succinate (Table 3.5), reducing the possibility that steps in the respiratory chain or phosphorylation system are important in the limitation of pyruvate oxidation. Potential sites of regulation are more likely to be pyruvate uptake into the mitochondria or the activity of pyruvate dehydrogenase complex.

5.2.1 Pyruvate transport.

If pyruvate uptake limits the rate of oxidation then pyruvate generated within the mitochondria should be oxidised more rapidly than that supplied from outside. This hypothesis was tested as follows. Pyruvate was synthesised within the mitochondria through the action of NAD-malic enzyme, by supplying malate and carrying out the reaction at pH 6.8 (a pH at which NAD-malic enzyme is active, but malate dehydrogenase is inactive). Because pyruvate oxidation in isolated cucumber cotyledon mitochondria is completely dependent on the presence of the co-factor thiamine pyrophosphate (TPP) (data not shown), comparison of the pyruvate accumulation rates in the presence and absence of TPP gives a measure of the rate of pyruvate oxidation. This approach is valid because NAD-malic enzyme is irreversible, due to the rapid reoxidation of NADH by the respiratory chain. The results of this analysis are shown in Figure 5.2, together with the rates of oxidation of externally supplied pyruvate for comparison. As predicted, at most stages the

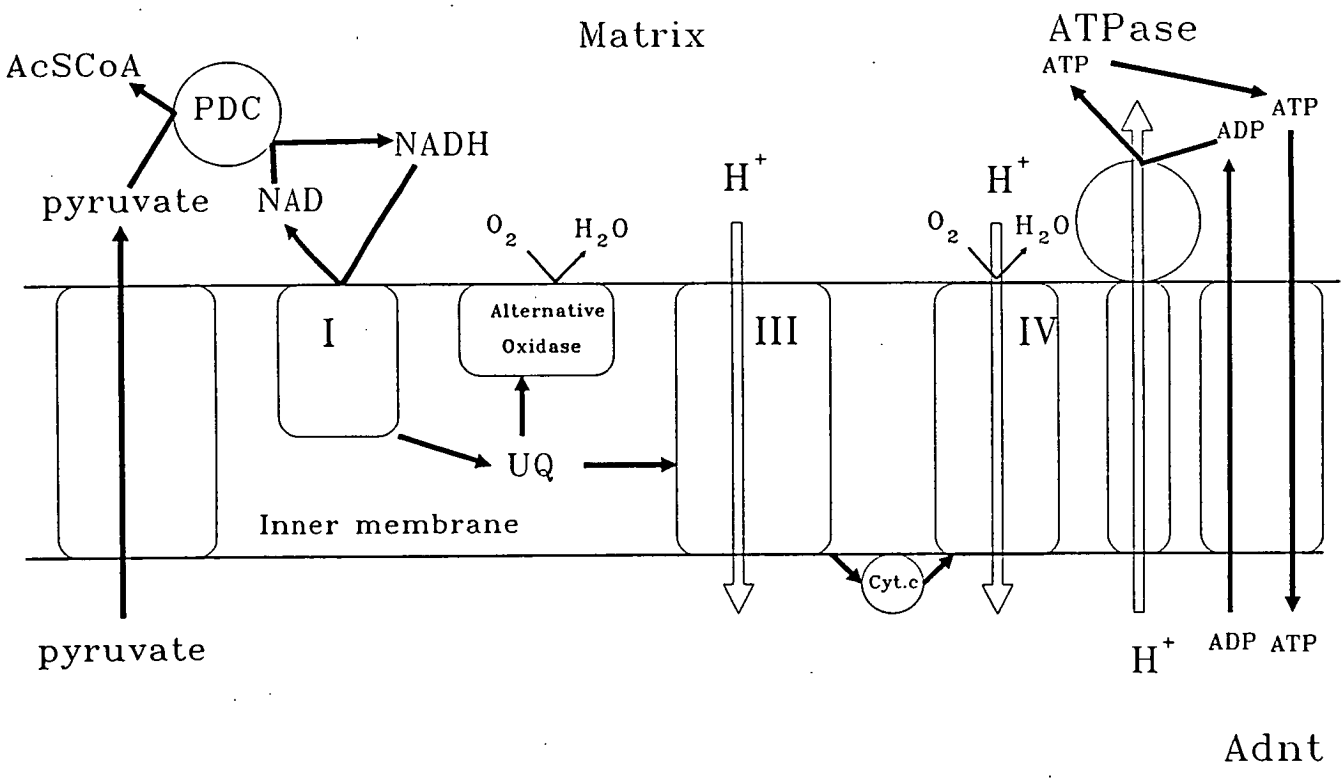

FIGURE 5.1: *The pathway of pyruvate oxidation by isolated mitochondria.*

rate of internal pyruvate oxidation is greater than that of externally supplied pyruvate, confirming the hypothesis that pyruvate transport may be limiting oxidation. The oxidation rate of externally supplied pyruvate exceeds that of internally synthesised pyruvate at 6 and 7 days post-imbibition in light grown cotyledons, at which point more rapid rates of external pyruvate oxidation are observed (Figure 3.7). In light grown cotyledons there is an increase in internal pyruvate oxidation rates between days 3 and 4, and then a reduction between days 4 and 7. In dark grown cotyledons there is no significant change in the rate of internal pyruvate oxidation.

The rate of pyruvate uptake into isolated mitochondria was measured using the ammonium salt swelling technique (Zoglowek *et al.*, 1988). The variation in the rate of pyruvate uptake during development is shown in Figure 5.3. The rate of pyruvate uptake is low at all stages, except in light grown cotyledons at 6 and 7 days post-imbibition. This confirms that pyruvate transport plays a role in limiting oxidation. An explanation for the low rates of internal pyruvate oxidation in mitochondria from 6 and 7 day old light grown cotyledons (Figure 5.2a) is that the pyruvate synthesised by NAD-malic enzyme is transported out of the mitochondria.

Both the peak in the rates of internal pyruvate oxidation and the increase in pyruvate transport are specific to light grown tissue. Since the former reaches a maximum at 4 days post-imbibition it may be associated with the processes of chloroplast development, whereas the latter is more likely to be involved in photosynthesis itself.

5.2.2 Pyruvate dehydrogenase complex (PDC).

The activity of PDC in isolated mitochondria was measured, and the variation in its activity during development is shown in Figure 5.4. The activity is sufficient to account for the observed rates of pyruvate oxidation (Figure 5.2). In light grown tissue there is a peak in PDC activity at 4 days post-imbibition, whereas in dark grown material there is no significant change. This increase correlates directly with the observed increase in internal pyruvate oxidation rate (Figure 5.2a), suggesting that an increase in PDC activity is, at least in part, responsible for the increase in oxidation rate. The change in PDC activity would also therefore appear to be correlated with chloroplast biogenesis.

FIGURE 5.2

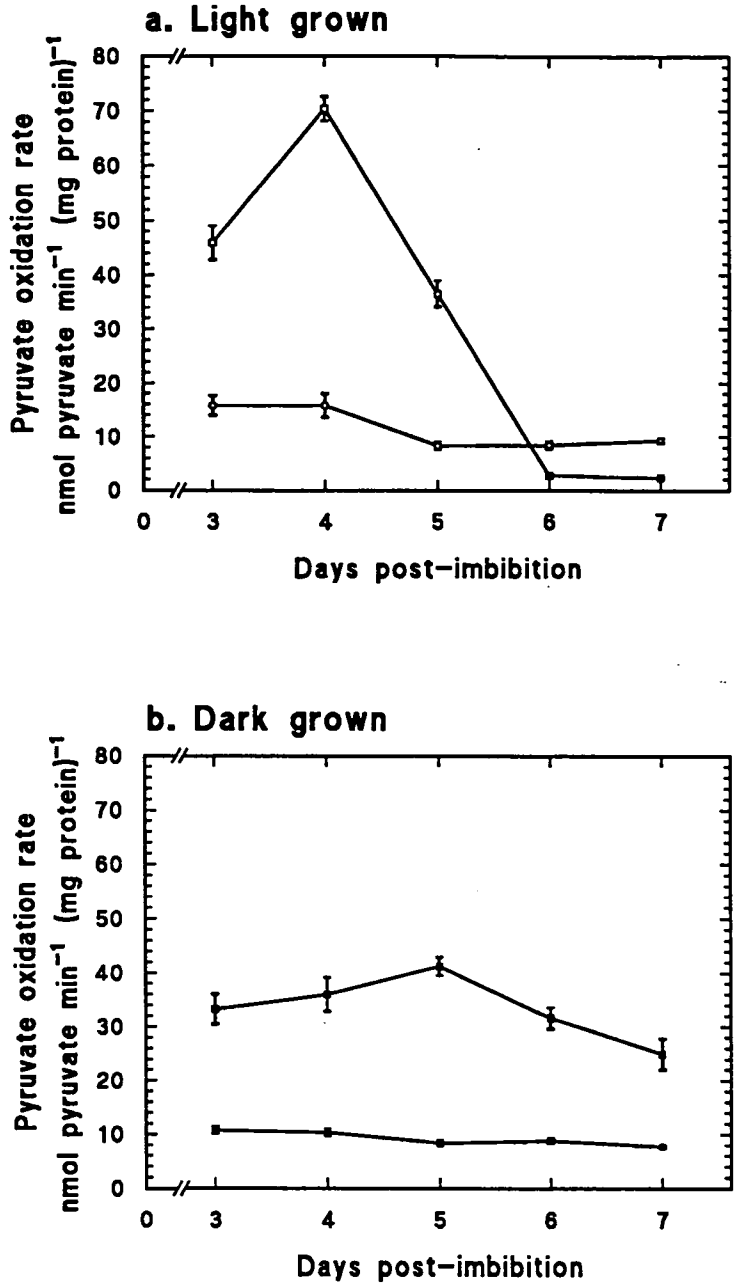

FIGURE 5.2. *Developmental variation in the rates of oxidation of internally and externally supplied pyruvate by isolated cucumber cotyledon mitochondria.* Mitochondria were isolated at each stage as described in Chapter 2. For external pyruvate oxidation (○,●) oxygen uptake rate was measured in the presence of 10 mM pyruvate, 0.1 mM thiamine pyrophosphate (TPP), 0.1 mM malate and 1 µmol ADP, at pH 6.8. Oxygen consumption rates were corrected for the component due to malate and converted to the pyruvate consumption rate by doubling. For internal pyruvate oxidation (□,■) the rate of pyruvate accumulation was measured directly in the presence of 10 mM malate and 1 µmol ADP at pH 6.8 with or without 0.1 mM TPP. The pyruvate oxidation rate was calculated as the difference between the pyruvate accumulation rate in the absence and presence of TPP. Points represent the mean (± SEM) of 3 independent experiments.

a. Light grown cotyledons.

b. Dark grown cotyledons.

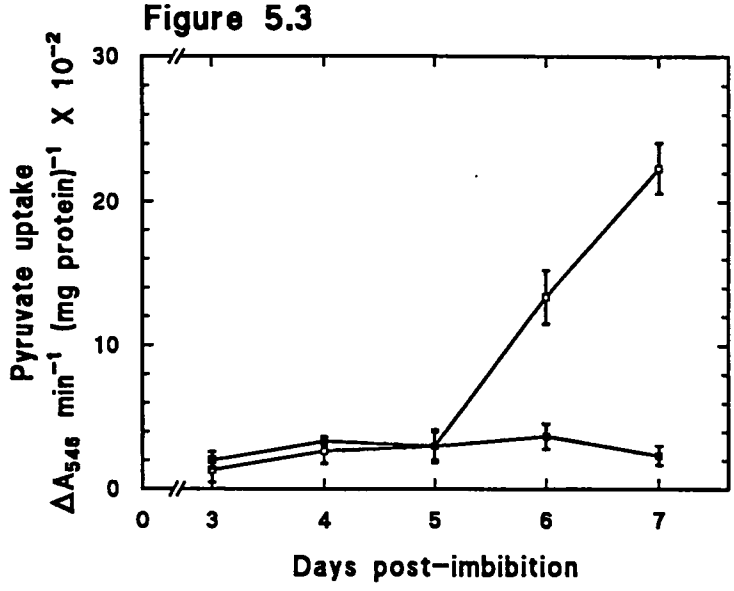

FIGURE 5.3. *Developmental variation in the activity of the pyruvate transporter.* Mitochondria were isolated at each stage and the rate of pyruvate uptake measuerd as the increase in light scatering at 546 nm in 100 mM ammonium pyruvate. (□), light grown cotyledons; (■), dark grown cotyledons. Points are the mean (± SEM) of 3 independent experiments.

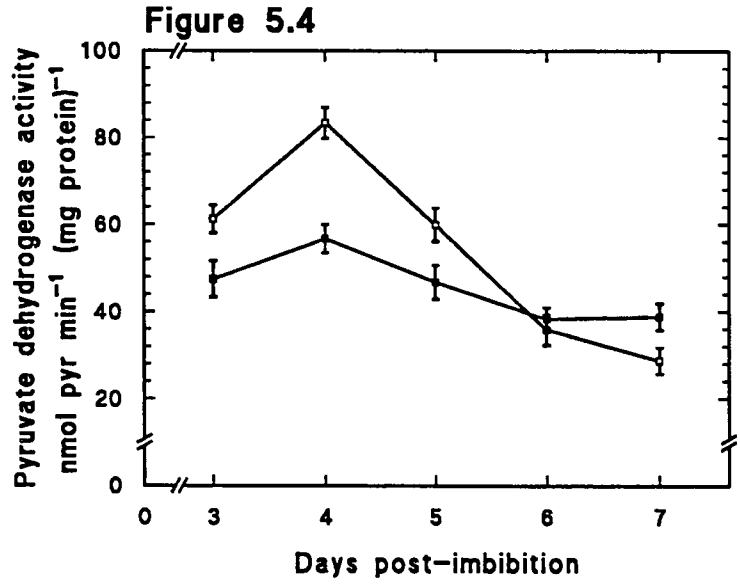

FIGURE 5.4 *Developmental variation in the activty of pyruvate dehydrogenase.* Mitochondria were isolated at each stage and assyed for pyruvate dehydrogenase as described in Chapter 2. (□), light grown cotyledons; (■), dark grown coptyledons. Points are the mean (± SEM) of 3 independent experiments.

5.3 Pyruvate Synthesis.

The results already presented in this chapter can be summarised as follows. Despite the low rates of oxidation of externally supplied pyruvate by cucumber cotyledon mitochondria, there is a large capacity for the oxidation of internally generated pyruvate, which appears to be associated with chloroplast biogenesis. During the photosynthetic phase, the mitochondria become competent to oxidise externally supplied pyruvate, due to an increase in the activity of the pyruvate transporter. The significance of these observations was tested by examining the pathways of pyruvate production both in the mitochondria and the cytosol.

5.3.1 Mitochondrial pyruvate synthesis.

The only enzyme within the mitochondria capable of synthesising pyruvate is NAD-malic enzyme. The variation in activity of this enzyme during development is shown in Figure 5.5. There are significant activities at all stages. In mitochondria from light grown cotyledons there is a peak in activity at 5 days post-imbibition, which is not found in mitochondria from dark grown tissue. The activity of NAD-malic enzyme follows a similar pattern of developmental variation as the capacity for internal pyruvate oxidation (Figure 5.2).

The level of NAD-malic enzyme in light grown cotyledons was measured by immunoblotting (Figure 5.6). The polypeptide is present at high levels at 3 and 4 days post-imbibition, and declines thereafter.

5.3.2 Cytosolic pyruvate synthesis.

The major cytosolic enzyme synthesising pyruvate is pyruvate kinase. The developmental variation in its activity is shown in Figure 5.7 and Table 5.1. There is a 3-fold increase in pyruvate kinase activity between 3 and 7 days post-imbibition in both light and dark grown cotyledons. Increases in pyruvate kinase activity are also observed in dark grown marrow cotyledons (Thomas and ap Rees, 1972b) There is capacity for high rates of cytosolic pyruvate production both when the mitochondrial capacity for pyruvate oxidation is high and low. After day 6 in light grown cotyledons pyruvate produced in the cytosol is likely to be mitochondrially oxidised, whereas in dark grown cotyledons pyruvate is available only to cytosolic reactions, primarily transamination. The metabolic significance of these observations is unclear.

The effect of the changing activity of pyruvate kinase on the equilibrium position of the reaction was estimated by measuring the levels of pyruvate and phospho(enol)pyruvate(PEP) *in vivo* at the beginning of the light period.

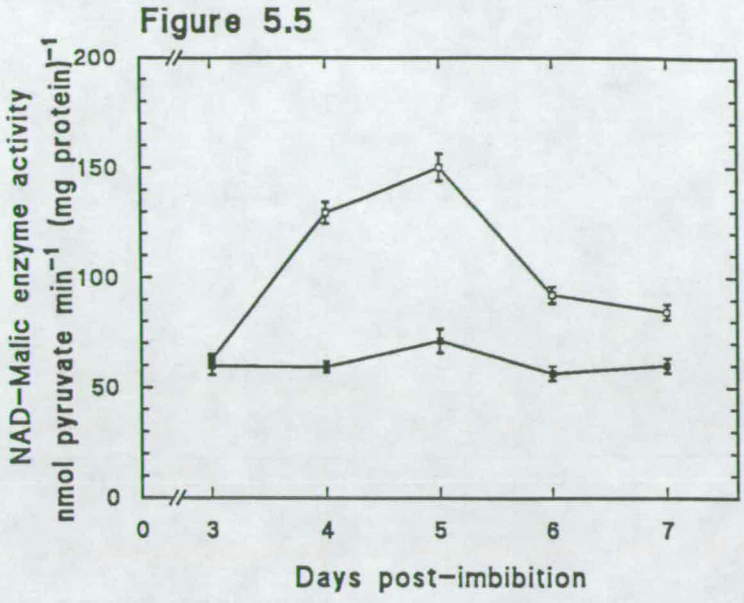

FIGURE 5.5. *Developmental variation in the activty of NAD-malic enzyme.* Mitochondria were isoalated at each stage and assyed for NAD-malic enzyme as described in Chapter 2. (□), light grown cotyledons; (■), dark grown coptyledons. Points are the mean (± SEM) of 3 independent experiments.

FIGURE 5.6. *Developmental variation in the level of NAD-malic enzyme.* Proteins were isolated from cotyledons at 3 to 7 days post-imbibition, fractionated by SDS-polyacrylamide gel electrophoresis, transferred to nitrocellulose and probed with an antibody specific for NAD-malic enzyme, as described in Chapter 2. Each track contains the protein isolated from 1/20 cotyledon. The position of molecular weight markers is indicated on the left.

Figure 5.7

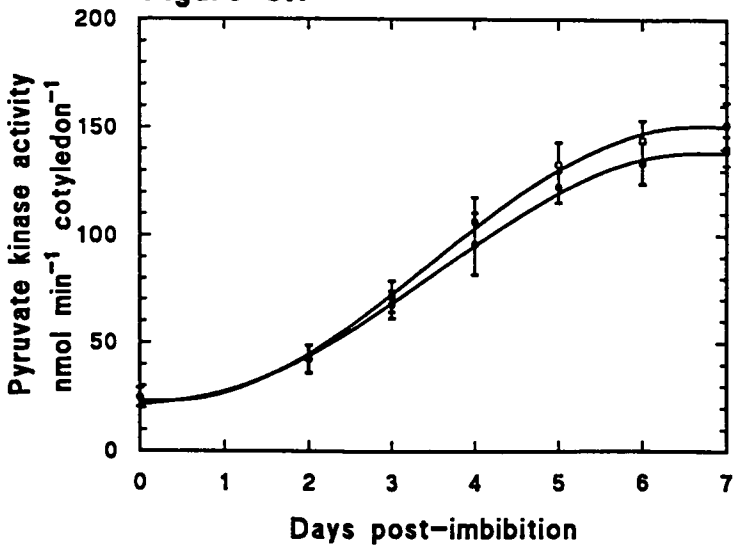

FIGURE 5.7. *Developmental variation in pyruvate kinase activity.* Cotyledon extracts were prepared at each stage and assayed for pyruvate kinase as described in Chapter 2. (○), light grown; (●), dark grown. Points are the mean (± SEM) of 3 independent extracts.

TABLE 5.1: *Variation in pyruvate kinase (PK) activity in extracts of cucumber cotyledons.* Cotyledon extracts were prepared at each stage and assayed for pyruvate kinase as described in Chapter 2. Recoveries were measured as described in Chapter 2. Values are the mean (± SEM) of 3 independent extracts.

Days post-imbibition	PK activity nmol min^{-1} cotyledon^{-1}	Recovery %
0	24.7 ± 4.3	97 ± 8
2	42.2 ± 6.3	101 ± 7
Light grown		
3	71.3 ± 7.3	103 ± 9
4	106 ± 11	105 ± 9
5	133 ± 10	94 ± 9
6	144 ± 9	97 ± 7
7	151 ± 10	95 ± 8
Dark grown		
3	67.5 ± 6.3	107 ± 8
4	95.9 ± 14.3	93 ± 5
5	122 ± 7	95 ± 6
6	133 ± 10	90 ± 8
7	139 ± 7	92 ± 8

The levels of these substrates and the ratio of pyruvate to PEP is shown in table 5.2. The measurements are in general agreement with those of Leegood and ap Rees (1978c) in marrow cotyledons. The ATP/ADP ratio calculated if pyruvate kinase is at equilibrium (assuming an apparent equilibrium constant of 2000; Leegood and ap Rees, 1978c) is also shown. At all stages this ratio is considerably higher than that measured in similar tissues (Leegood and ap Rees, 1978c), indicating that pyruvate kinase is well displaced from equilibrium throughout development. The steady state level of pyruvate reaches a maximum at around day 4, suggesting that at this point there are relatively high rates of pyruvate synthesis compared to the rate of utilisation. This may be a result of the rapid flux of carbon due to lipid mobilisation, or the diversion of carbon into the TCA cycle. The level of PEP increases during development.

TABLE 5.2. *Variation in the levels of pyruvate (pyr) and phospho(enol)pyruvate (PEP) in cucumber cotyledons.* Extracts were made from cotyledons at each stage and assayed for pyruvate and PEP as described in Chapter 2. Recoveries, measured as described in Chapter 2, were between 95 and 105 % for both substrates.

Days post-imbibition	Substrate level, nmol cotyledon^{-1}		Pyr/PEP Ratio	Calculated ATP/ADP Ratio
	Pyruvate	PEP		
1	1.2 ± 0.2	0.8 ± 0.1	1.1 ± 0.5	1820
2	4.2 ± 0.3	1.7 ± 0.3	2.7 ± 0.5	740
3	9.4 ± 0.9	4.3 ± 0.3	2.3 ± 0.4	870
4	10.6 ± 0.7	6.3 ± 0.3	1.7 ± 0.1	1180
5	6.3 ± 0.8	7.4 ± 0.4	0.9 ± 0.1	2220
6	4.2 ± 0.2	8.3 ± 0.5	0.5 ± 0.1	4000
7	2.4 ± 0.2	8.0 ± 0.4	0.3 ± 0.1	6670

5.4 Discussion.

5.4.1 Pyruvate metabolism during lipid mobilisation.

The results presented in this chapter, together with those of Chapter 3, provide evidence that cytosolically produced pyruvate is metabolised via the TCA cycle at very low rates in cucumber cotyledons. A similar situation has been described in castor bean endosperm (Neal and Beevers, 1960; Canvin and Beevers, 1961; Millhouse *et al.*, 1983). Significant rates of pyruvate oxidation by isolated castor bean endosperm mitochondria have been described by Brailsford *et al.* (1986), but the *in vivo* data of Neal and Beevers (1960) casts doubt on the physiological significance of these results. The pyruvate metabolism of cucumber cotyledons and castor bean endosperm contrasts with that of

soybean cotyledons, where rapid rates of pyruvate oxidation by isolated mitochondria are found (Bryce and Day, 1990; Bryce *et al.*, 1990). This difference may reflect the quantitatively less important role of lipid mobilisation in this species, as compared to the other two.

Studies with dark grown marrow cotyledons have shown that pyruvate is converted to acetyl-CoA *in vivo* (Thomas and ap Rees, 1972b). However, the acetyl-CoA produced is not respired to any great extent, but is used for the biosynthesis of lipid and other high molecular weight compounds (Thomas and ap Rees, 1972a). These results will be discussed further in section 5.4.3.

5.4.2 Pyruvate metabolism during chloroplast biogenesis.

The data of sections 5.2.2 and 5.3.1 indicates that during the chloroplast biogenesis phase there are peaks in activity of NAD-malic enzyme (ME) and pyruvate dehydrogenase (PDC). This is consistent with the operation of the full TCA cycle with succinate as input and a branch point at malate. Pyruvate dehydrogenase can be activated, even during succinate oxidation, by pyruvate production due to the activity of ME (Budde *et al.*, 1988). This would allow generation of TCA cycle intermediates and ATP for biosynthesis of chloroplast components. Greening soybean cotyledons also show high levels of ME (Bryce and Day, 1990), whereas the enzyme has a much lower activity in castor bean endosperm mitochondria (Millhouse *et al.*, 1983), again correlation of this phenomenon with photosynthetic development. It should be noted that, although the peak in activity of this potential pathway correlates with the chloroplast biogenesis phase, the capacity for full TCA cycle operation exists in both light and dark grown cotyledons at all times (Figures 5.4 and 5.5), but inactivation of PDC during succinate oxidation may prevent this (Budde *et al.*, 1988).

Full TCA cycle activity could also be achieved by the export of oxaloacetate or malate from the mitochondria, cytosolic conversion of oxaloacetate to pyruvate, and import of pyruvate into the mitochondria. The significance of these contrasting routes of pyruvate metabolism are discussed in the following section.

5.4.3 Integration of lipid mobilisation and biosynthesis.

The results described in this chapter indicate that pyruvate metabolism may be crucial in regulating the proportion of the carbon derived from lipid breakdown which enters respiratory metabolism. The following hypothesis is proposed to explain how this may be regulated. During high rates of lipid mobilisation and sucrose synthesis, in the absence of high demands for TCA cycle intermediates, the cytosolic pyruvate level would be low. This would result, because of the low activity of the pyruvate transporter, in very low mitochondrial pyruvate levels, insufficient to activate pyruvate dehydrogenase, inactivated

by high rates of succinate oxidation (Budde *et al.*, 1988). As the demand for TCA cycle intermediates is low, the free CoA pool would also be expected to be low, due to high pools of CoA intermediates, such as acetyl-CoA, and succinyl-CoA. This low level of mitochondrial CoA, combined with the high matrix pH due to rapid succinate oxidation, would result in low activities of NAD-malic enzyme (Macrae, 1971), preventing entry of carbon by this route.

Two sets of circumstances would allow entry of pyruvate into the TCA cycle:

a. If the demand for TCA cycle intermediates increased, then this would lead to an increase in the free CoA pool in the mitochondria, activating NAD-malic enzyme (Macrae, 1971). This would produce pyruvate within the mitochondria, activating pyruvate dehydrogenase (Budde *et al.*, 1988), and therefore allowing carbon to enter the decarboxylating arm of the TCA cycle.

b. If the rate of lipid breakdown and sucrose synthesis fell, then this would result in an decrease in the cytosolic ATP/ADP ratio. By the argument of comparative biochemistry, this is likely to activate pyruvate kinase, and there would be an increase in the level of pyruvate. The pyruvate transporter would become saturated and the resulting increase in mitochondrial pyruvate levels, combined with the now lower rate of succinate oxidation, would activate pyruvate dehydrogenase (Budde *et al.*, 1988), again allowing carbon entry into the TCA cycle.

In summary, carbon is diverted into the decarboxylating arm of the TCA cycle when the demand for biosynthetic intermediates is high, or when the rate of sucrose synthesis is low. It should be emphasised that the regulatory mechanisms discussed above are, as yet, unsupported.

This hypothesis explains the observations of Thomas and ap Rees (1972b) that pyruvate is metabolised to acetyl-CoA in dark grown marrow cotyledons. Their labelling experiments were carried out with cotyledons that were removed from the axis for 5 hours before analysis. Due to the removal of the major sucrose sink outside the cotyledons, this would be expected to reduce the rate of sucrose synthesis and divert pyruvate into the TCA cycle. This would not appear to be supported by the results of Leegood and ap Rees (1978b), who show no difference in pyruvate levels between cut and intact cotyledons. However, the substrate levels in the cut cotyledons were measured after only 2 1/2 hours. Thomas and ap Rees (1972b) demonstrated an increase in the carbon dioxide release from pyruvate between 1 and 5 hours after excision.

5.4.4 Pyruvate metabolism during photosynthesis.

This chapter contains the following evidence that cytosolically synthesised pyruvate enters the TCA cycle during the photsynthetic phase. The cytosolic enzyme responsible for pyruvate production, pyruvate kinase, has a high activity (Figure 5.7 and

Table 5.1) and the position of equilibrium is such that it catalyses irreversible pyruvate synthesis (Table 5.2). The rate of mitochondrial pyruvate oxidation is relatively high, owing to the increased activity of the pyruvate transporter (Figures 3.8a and 5.3). The functioning of the TCA cycle in photosynthetic tissue is consistent with the observations of Azcon-Bieto *et al.* (1989), that maximum activities of TCA cycle substrate oxidation by isolated soybean cotyledon mitochondria coincide with the stage of maximum chlorophyll content. TCA cycle operation may occur in the light period, dark period, or both. Since PDC from pea leaves is inactivated by photorespiration and light (Schuller and Randall, 1989; Budde and Randall, 1989), it is unlikely that pyruvate enters the TCA cycle in the light period. In the dark period, operation of the cycle may be required to generate ATP or intermediates. The importance and role of TCA cycle operation in photosynthetic tissues will be considered in detail in Chapter 7.

5.5 Conclusions.

1. During lipid mobilisation pyruvate entry into the TCA cycle is restricted by low activities of the pyruvate transporter.

2. There is evidence to suggest that full TCA cycle operation, based on pyruvate synthesis within the mitochondria, occurs during chloroplast biogenesis.

3. The capacity for the oxidation of cytosolic pyruvate is correlated with photosynthesis.

4. Pyruvate metabolism in cucumber cotyledons is under coarse control at the level of the pyruvate transporter, NAD-malic enzyme, pyruvate dehydrogenase, and pyruvate kinase.

CHAPTER 6.

THE ROLE OF MITOCHONDRIA IN THE CONTROL OF GLUCONEOGENESIS.

6.1 Introduction and Aims.

The results described in Chapter 4 suggest that mitochondria in cucumber cotyledons may act as a regulatory balance point between lipid breakdown and sucrose synthesis. It is also clear from the data of Chapter 5 that interactions between mitochondria and the cytosol are finely regulated. The aim of the work presented in this chapter is to investigate the interaction between mitochondria and cytosol in the context of lipid mobilisation. The means by which this is achieved is to attempt to describe in quantitative terms the regulatory role of key mitochondrial steps in the pathway of sucrose production from lipid, by reconstituting the pathway *in vitro*, using cytosolic extracts and isolated mitochondria. This utilises the 'auxiliary enzyme' approach of Torres *et al.*(1986). The enzymes phosphoglucomutase and phosphoglucose isomerase were supplied in excess, in order to provide an end-point for the pathway. The work described in this chapter is concerned with two *in vitro* systems: first, a reconstitution of the cytosolic steps between oxaloacetate and hexose; and secondly, a more complex system carrying out the conversion of succinate to hexose, involving both cytosolic and mitochondrial steps. Both systems are based on extracts from 4 day old light grown cotyledons, where the rate of lipid mobilisation is maximal (Figure 3.1).

6.2 Experimental Systems.

6.2.1 Oxaloacetate to hexose.

The system consists of a cytosolic extract of cucumber cotyledons (see 2.5.1(i)), a phosphocreatine/creatine kinase ATP regenerating system, and high activities of the enzymes phosphoglucomutase and phosphoglucose isomerase. The system is supplied with a saturating concentration of oxaloacetate (10 mM). The expected pathway is shown in Figure 6.1a. The pathway is assumed to branch at phospho(enol)pyruvate, due to the presence of pyruvate kinase. As a result the fluxes through each branch were measured independently, as NADH removal and pyruvate production. Pyruvate production can be used to measure the flux of the pyruvate kinase branch because pyruvate is not further metabolised in this system (data not shown), and pyruvate kinase is virtually irreversible (Kobr and Beevers, 1971; Leegood and ap Rees, 1978c).

Results of a representative experiment are shown in Figure 6.1b. There is a long transition time of approximately 2 minutes, before linear rates of NADH removal and pyruvate production are observed. The period of linear rates is deemed to be steady state since:

1. the oxaloacetate concentration is very high, so that it does not change significantly during the course of the experiment.

2. the pyruvate kinase step is irreversible.

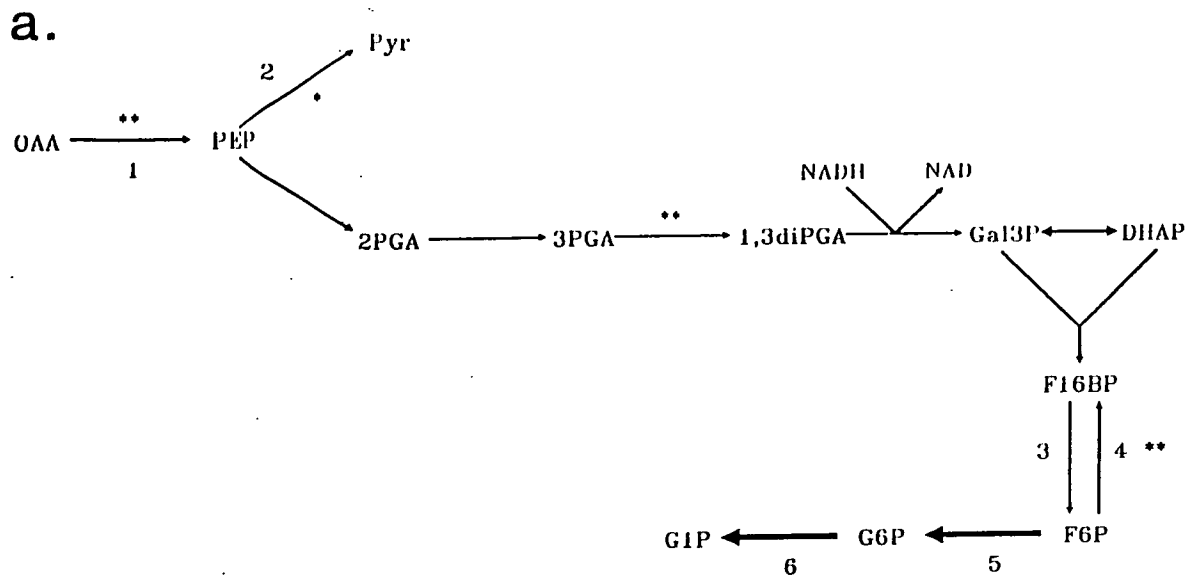

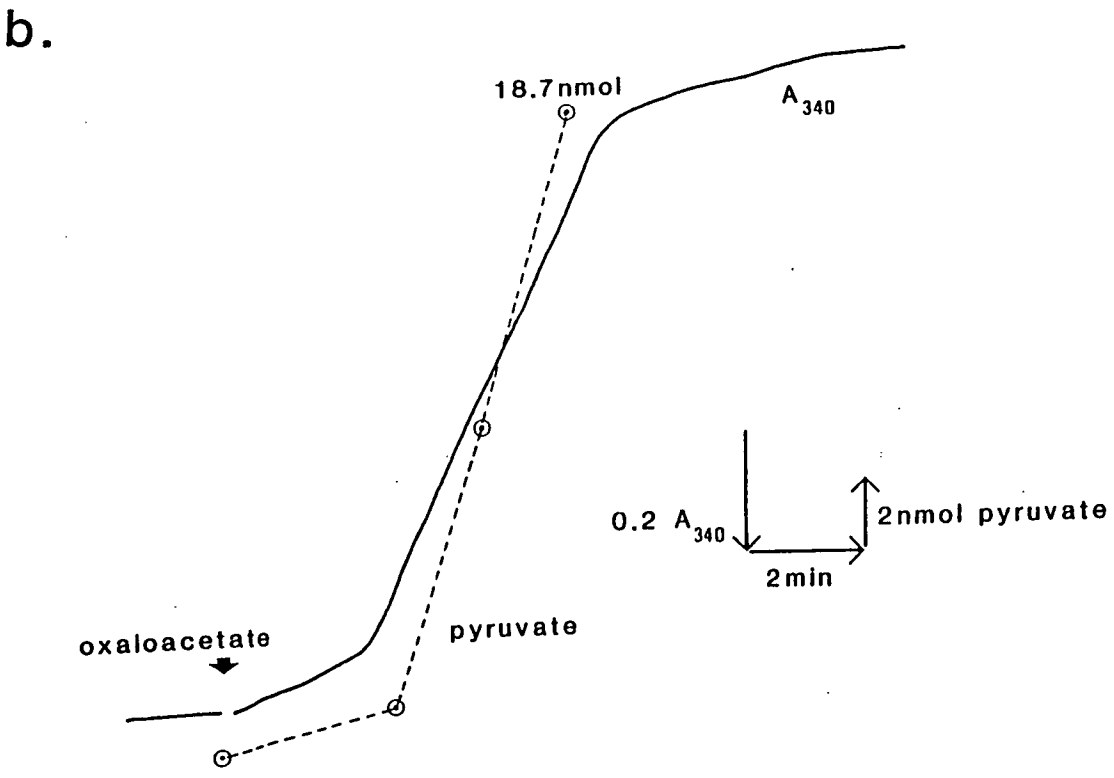

FIGURE 6.1: *The* in vitro *system for the conversion of oxaloacetate into hexose.*
a. The expected pathway. * = ATP producing reaction; ** = ATP consuming reaction; 1. phospho(enol)pyruvate carboxykinase; 2. pyruvate kinase; 3. fructose bisphophatase; 4. phosphofructokinase; 5. phosphoglucose isomerase; 6. phosphoglucomutase.
b. Representative traces. The reaction was carried out as described in the legend to Table 6.1. The addition was of 10 mM oxaloacetate.

Figure 6.2

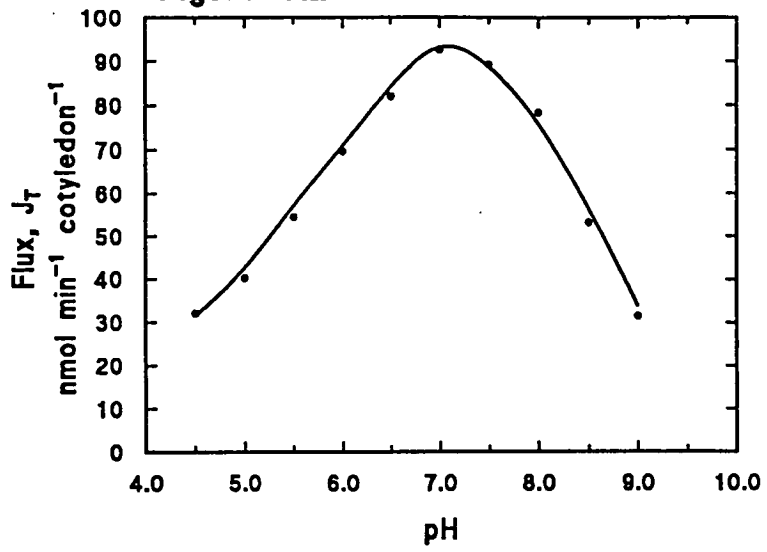

FIGURE 6.2 *pH optimum of the* in vitro *system for the conversion of oxaloacetate to hexose.* Reactions were set up as described in the legend to Table 6.1, except at differing pHs. MES-HCl buffer (50 mM) was used to produce pHs in the range 4.5-6.5; triethanolamine-HCl (50 mM) was used to produce pHs in the range 7.0-9.0. The flux to hexose was measured.

TABLE 6.1. *Characteristics of the* in vitro *system for the conversion of oxaloacetate into hexose.* A cytosolic extract was prepared from 4 day old light grown cotyledons as described in Chapter 2. Enzymes were assayed with saturating substrate concentrations. Fluxes were measured in mixtures containing extract corresponding to 0.4 cotyledons and 10 mM oxaloacetate, 1 mM ATP, 2.5 mM phosphocreatine, 0.3 mM NADH, and 10 units each of creatine kinase, phosphoglucomutase, and phosphoglucose isomerase. The flux to hexose (J_H) was measured as NADH disappearance by following the decrease in absorbance at 340 nm; the flux to pyruvate (J_P) was measured directly by estimating the pyruvate content of samples taken at intervals; the total flux (J_T) was calculated as the sum of J_H and J_P. Values are the mean ($\pm$ SEM) of 3 independent experiments.

Reaction	Flux, nmol min^{-1} $cotyledon^{-1}$
Enzyme activities	
Pyruvate kinase	130 $\pm$ 8
Fructose-1,6-bisphosphatase	372 $\pm$ 10
Phosphofructokinase	17.8 $\pm$ 1.5
Fluxes	
Total (J_T)	99 $\pm$ 4
To hexose (J_H)	84 $\pm$ 3
To pyruvate (J_P)	15 $\pm$ 1
Branch point	
J_P/J_T	0.150 $\pm$ 0.001

---

3. Phosphoglucose isomerase and phosphoglucomutase are present at very high levels, allowing the rapid removal of fructose-1-phosphate.

The flux through the pathway (J_T) was optimised for pH, as shown in Figure 6.2. Maximum rates were achieved at pH 7.0, so this pH was used in subsequent experiments.

The fluxes through the pathway and activities of some of the enzymes in the system are shown in Table 6.1. The flux through the unbranched part of the pathway (J_T) is greater than that predicted from the rate of lipid breakdown (see 3.5.2). An explanation for this is that there are major controlling steps in the pathway of lipid breakdown and sucrose synthesis outside the steps reconstituted. Possibilities include lipase, the enzymes of β-oxidation and the glyoxylate cycle, mitochondrial steps, sucrose phosphate synthase, and sucrose phosphatase. The rate of sucrose transport from the cell may also be important *in vivo*. Alternatively the difference between the *in vivo* and *in vitro* rates may reflect an underestimate in the rate of lipid breakdown *in vivo* due to simultaneous lipid synthesis. The flux through the pyruvate kinase branch (J_P) is low, accounting for only 15 % of J_T, presumably as result of inhibition of pyruvate kinase by the high ATP/ADP ratio.

6.2.2 Succinate to hexose.

The system consists of a cytosolic extract of cucumber cotyledons (see 2.5.1(i)) and isolated cotyledon mitochondria (in the correct *in vivo* proportion, based on fumarase activity), together with high activities of phosphoglucomutase and phosphoglucose isomerase. The system was supplied with saturating levels of succinate (10 mM).

The most likely route of carbon export from the mitochondria is as malate, which is then converted to oxaloacetate by cytosolic malate dehydrogenase. If this is allowed to occur, the measurement of flux is complicated as an NADH producing reaction is occurring in the cytosolic fraction. It would be more convenient experimentally if oxaloacetate were exported. However cucumber cotyledon mitochondria are similar to those of castor bean endosperm in that they do not readily transport oxaloacetate (data not shown; Millhouse *et al.*, 1983). In castor bean endosperm there is considerable evidence to suggest export of carbon from mitochondria by means of a glutamate/aspartate/2-oxoglutarate shuttle (Mettler and Beevers, 1980; Millhouse *et al.*, 1983), so this system was forced in the *in vitro* system by adding exogenous glutamate/2-oxoglutarate aminotransferase and glutamate. This also reduces the flux of carbon through NAD-malic enzyme, by ensuring rapid removal of oxaloacetate produced within the mitochondria.

A second reaction potentially confusing the measurement of J_H by NADH removal is the mitochondrial external NADH dehydrogenase (Table 3.4). This enzyme is calcium dependent so EGTA was included to inhibit it (Moller *et al.*, 1981; Moore and Akerman, 1982). The pool of NAD/NADH within the mitochondria was assumed to be small compared to the total and to be rapidly cycling, so that it has negligible effect on the flux

a.

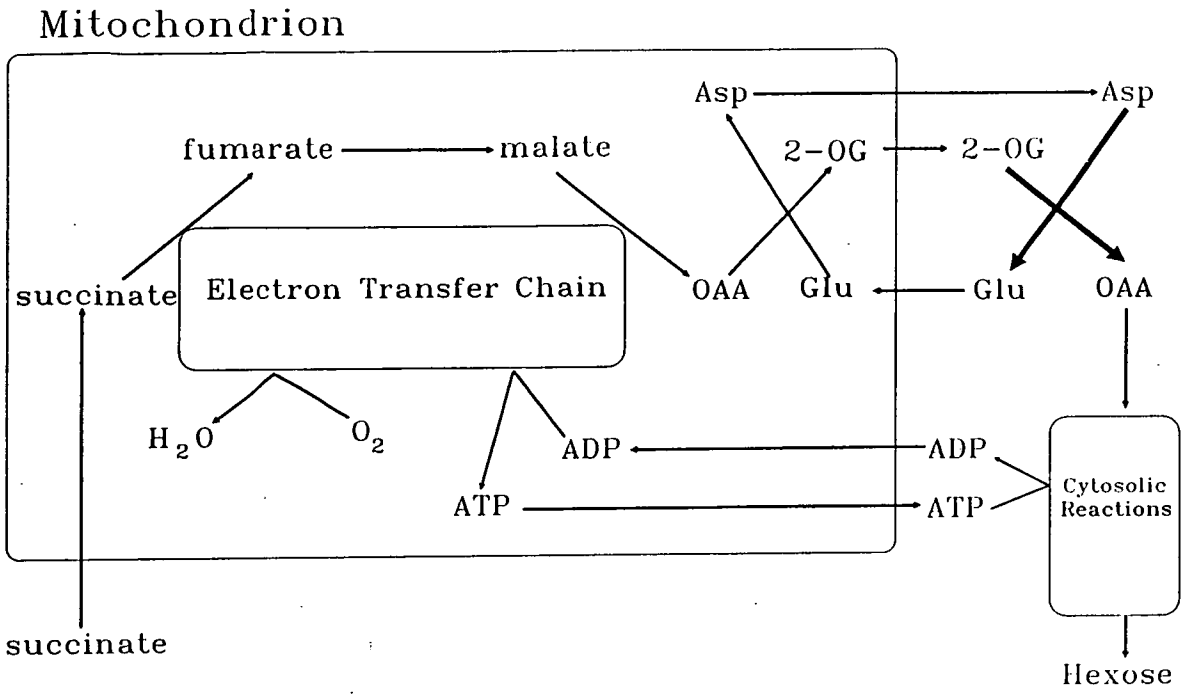

b.

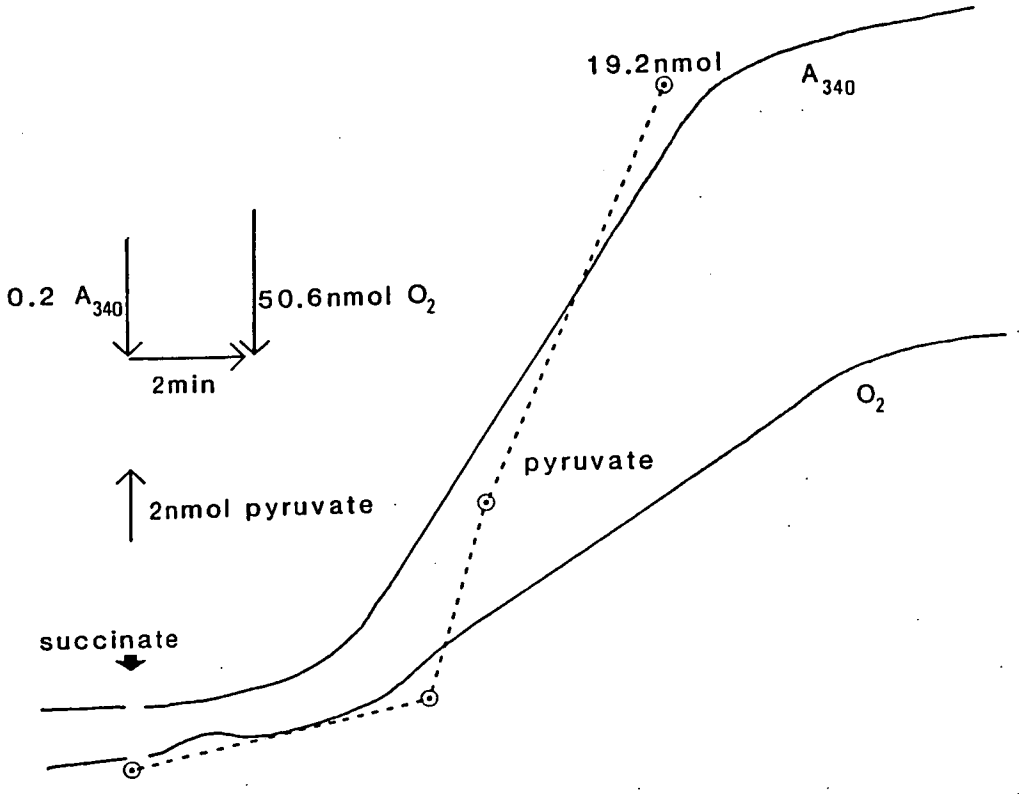

FIGURE 6.3: *The* in vitro *system for the conversion of succinate into hexose.*
a. The expected pathway.
b. Representative traces. The reaction was carried out as described in the legend to Table 6.2. The addition was of 10 mM succinate.

measurements. Similarly cytosolic malate dehydrogenase was assumed to be in equilibrium at the steady state.

Pyruvate production was again used to measure the flux to pyruvate, since the system does not metabolise pyruvate (data not shown). The pH optimum of 7.0 determined for the cytosolic system was also used for this system.

The pathway expected under these conditions is shown in Figure 6.3, together with the results of a representative experiment. There was a transition time of approximately 3 minutes before linear rates of NADH removal, pyruvate production and oxygen uptake were achieved. As in the simpler system this was taken as the steady state. The fluxes through the pathway and activities of some of the enzymes are shown in Table 6.2. Once again, the fluxes are higher than those measured *in vivo*, with similar possible explanations.

TABLE 6.2. *Characteristics of the* in vitro *system for the conversion of succinate into hexose.* A cytosolic extract and mitochondria were prepared from 4 day old light grown cotyledons as described in Chapter 2. Enzymes were assayed with saturating substrate concentrations. Fluxes were measured in mixtures containing extract and mitochondria corresponding to 0.4 cotyledons and 10 mM succinate, 0.5 mM ATP, 0.5 mM ADP, 10 mM phosphate, 10 mM glutamate, 1 mM EGTA, 0.3 mM NADH, and 10 units each of 2-oxoglutarate/aspartate aminotransferase, phosphoglucomutase, and phosphoglucose isomerase. The flux to hexose (J_H) was measured as NADH disappearance by following the decrease in absorbance at 340 nm; the flux to pyruvate (J_P) was measured directly by estimating the pyruvate content of samples taken at intervals; the total flux (J_T) was calculated as the sum of J_H and J_P; the oxygen uptake flux (J_O) was measured polarographically in an oxygen electrode. The state 3 oxygen uptake rate was measured in standard reaction medium (2.4.3) in the presence of 10 mM succinate, 10 mM glutamate and 100 nmol ADP. Values are the mean (± range) of 2 independent experiments.

Reaction	Rate, nmol min^{-1} $cotyledon^{-1}$
Enzyme activities	
Pyruvate kinase	115 ± 8
Fructose-1,6-bisphosphatase	325 ± 58
Phosphofructokinase	20.2 ± 1.5
Fluxes	
Total (J_T)	72 ± 3
To hexose (J_H)	62 ± 2
To pyruvate (J_P)	10 ± 1
Oxygen uptake (J_O)	38 ± 2
State 3 J_O	43 ± 4
Branch point	
J_P/J_T	0.13 ± 0.01

The oxygen uptake rate is approximately 90 % of the state 3 rate in the presence of succinate and glutamate. The following evidence demonstrates the importance of the mitochondrial reactions. Addition of high concentrations of the inhibitors malonate (Complex II) and rotenone (Complex I) completely inhibits the pathway (data not shown). Carboxyatractyloside (inhibitor of the adenine nucleotide translocator) reduces J_T to 20-30 % of its maximal rate (see later), but increases the relative flux through the pyruvate kinase branch (J_P/J_T = 0.36). This implies that under conditions of low ATP/ADP ratio pyruvate kinase can generate ATP for the conversion of oxaloacetate to hexose.

6.2.3 The effect of enzyme concentration on the systems.

The aim of the experiments described in this chapter is to infer the distribution of control *in vivo* from measurements made on the reconstituted *in vitro* systems. A major weakness in the experimental approach described is that, although the enzymes are all present in approximately the same proportions as *in vivo* (with the exception of the auxiliary enzymes), their absolute concentrations will be different, so that any concentration dependent effects will be lost. This problem will be particularly acute if enzymes with high flux control coefficients display marked non-linearity between enzyme activity and concentration. A method to determine the effects of such non-linearity on a metabolic system has been developed by Acerenza and Kacser (1990). They define the coordinate control operation (CCO) as the simultaneous change in all the enzyme concentrations in a system by the same, non-infinitesimal factor, α, and show that if both the steady state assumption and the proportionality between enzyme concentration and activity hold, the behaviour of system variables during the CCO can be predicted.

Variables divide into two classes: the so-called S-type variables, such as metabolite concentrations, which remain constant; and the so-called J-type variables, such as flux, which change by a factor α (Acerenza and Kacser, 1990). Thus, if J_α is the flux after the CCO and J_r the reference flux, then a plot of J_α/J_r against α (the direct coordinate control plot) is expected to give a straight line of gradient 1 if the assumptions hold (Acerenza and Kacser, 1990).

In order to test the effect of the CCO on the *in vitro* systems discussed in this chapter the fluxes were measured with varying amounts of extract and mitochondria present in the same assay volume. This is not a strict CCO, since metabolites and other factors present in the extract change in addition to the enzyme concentrations. Direct coordinate control plots are shown for both systems in Figure 6.4. In both cases the fluxes behave as expected, except for the flux to pyruvate which displays non-linearity. This suggests a concentration dependent effect of pyruvate kinase. As a result, flux control coefficients of pyruvate kinase were measured at a number of extract concentrations (see later).

FIGURE 6.4

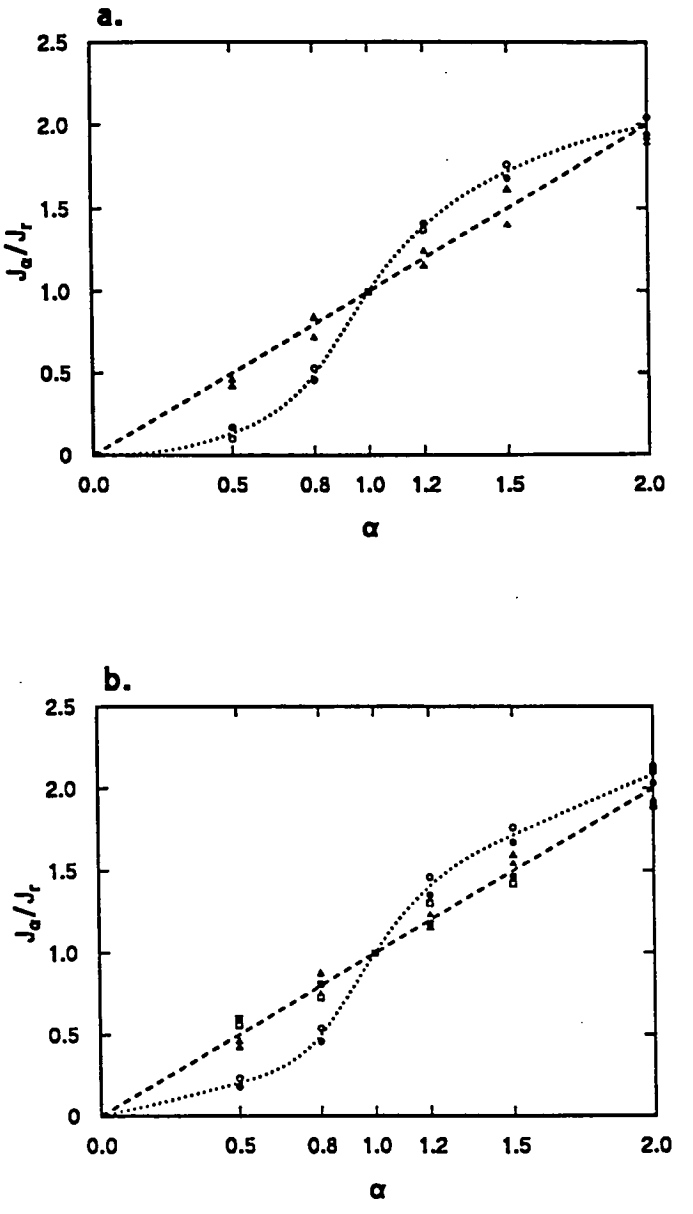

FIGURE 6.4 *Effect of the coordinate control operation on system fluxes.*

a. Reactions were set up as described in the legend to Table 6.1, and the fluxes measured in the presence of varying amounts of extract. The experiment was carried out with two independent extracts (open and closed symbols). The fluxes are expressed relative to the flux in the presence of extract from 0.4 cotyledons. The hexose (△,▲) and pyruvate fluxes (○,●) were measured. The fluxes in the presence of extract from 0.4 cotyledons were: △, 31.4 nmol NADH min^{-1}; ▲, 33.2 nmol NADH min^{-1}; ○, 5.7 nmol pyruvate min^{-1}; ●, 6.1 nmol pyruvate min^{-1}.

b. Reactions were set up as described in the legend to Table 6.2, and the fluxes measured in the presence of varying amounts of extract. The experiment was carried out with two independent extracts (open and closed symbols). The fluxes are expressed relative to the flux in the presence of extract from 0.4 cotyledons. The hexose (△,▲), oxygen uptake (□,■) and pyruvate fluxes (○,●) were measured. The fluxes in the presence of extract from 0.4 cotyledons were: △, 25.5 nmol NADH min^{-1}; ▲, 24.1 nmol NADH min^{-1}; □, 14.3 nmol O_2 min^{-1}; ■, 15.8 nmol O_2 min^{-1}; ○, 4.3 nmol pyruvate min^{-1}; ●, 3.4 nmol pyruvate min^{-1}.

6.3 Theory and Experimental Approach.

6.3.1 Enzyme titrations.

The flux control coefficients of pyruvate kinase and the enzymes responsible for the inter-conversion of fructose-1,6-bisphosphate and fructose-6-phosphate (fructose-1,6-bisphosphatase, FBPase; phosphofructokinase, PFK; and pyrophosphate fructose-6-phosphate 1-phosphotransferase, PFP) were measured using the enzyme titration approach of Torres *et al.*, (1986). These steps were chosen as they have previously been identified as potential points of regulation (Kobr and Beevers, 1971; Leegood and ap Rees, 1978c). Flux control coefficients were measured by determination of the effect on the system fluxes of exogenously added pyruvate kinase and PFK. As the enzymes added were of a different biological source from the *in vitro* extracts (commercial preparations from rabbit liver), kinetic differences were corrected for by using enzyme concentration, e, rather than activity, V, where,

$$e = V/K_m \tag{6.1}$$

K_m is the Michaelis-Menton coefficient (or its equivalent $K_{0.5}$) for the enzyme, under the conditions of the *in vitro* experiments (Torres *et al.*, 1986). In calculating the net activity of the FBPase/PFK/PFP system the activity of PFP was ignored as this enzyme is generally at equilibrium (ap Rees, 1985).

A hyperbolic relationship was assumed between the flux through the branch of the pathway in which the an enzyme is located and the concentration of that enzyme (Kacser and Burns, 1979):

$$J = \frac{Q_1 e_i}{Q_2 + e_i} \tag{6.2}$$

In this case flux control coefficients were determined by fitting the data to equation 6.2, and substituting the value of Q_1 obtained in equation 3 of Torres *et al.* (1986):

$$C^J = \frac{Q_1 - J}{Q_1} \tag{6.3}$$

For the other branches (that is, those which do not contain the enzyme under investigation) the relationship between flux and enzyme concentration is less clear. Consequently the gradient of a flux against enzyme concentration plot was determined by linear regression and the flux control coefficient calculated from its definition:

$$C^J = \frac{dJ}{de_i}\cdot\frac{e_i}{J} \tag{6.4}$$

6.3.2 Oxaloacetate to hexose system.

The flux control coefficients of pyruvate kinase and the FBPase/PFK/PFP cycle on the 3 system fluxes were calculated as described above. The flux control coefficients of the steps between oxaloacetate (OAA) and fructose-1,6-bisphosphate (FBP) were calculated from the summation theorem (Kacser and Burns, 1973):

$$C_{OAA \rightarrow FBP} = 1 - C_{PK} - C_{FBP} \qquad (6.5)$$

6.3.3 Succinate to hexose system.

Flux control coefficients for the mitochondrial steps (succinate to oxaloacetate) were obtained as follows. The distribution of the control of the oxygen uptake flux in isolated mitochondria , in the presence of succinate, glutamate, and 2-oxoglutarate/aspartate aminotransferase was determined using inhibitor titrations similar to those described in Chapter 4. These experiments were carried out at oxygen uptake rates of 90 % of state 3, the rate achieved in the *in vitro* system, maintained by a glucose/hexokinase ADP regenerating system. The flux control coefficients of the whole mitochondrial system on all the system fluxes, including the oxygen uptake flux, were measured by titrating in additional isolated mitochondria. The flux control coefficients of the mitochondrial steps were calculated using equation 6.6:

$$^{Ji}C_m = {}^{Ji}C_{mit} \cdot \frac{{}^{JO}C_m}{{}^{JO}C_{mit}} \qquad (6.6)$$

Where, $^{Ji}C_m$ is the flux control coefficient of mitochondrial step, m, on flux J_i, $^{Ji}C_{mit}$ is the flux control coefficient of mitochondria on flux J_i, $^{JO}C_{mit}$ is the flux control coefficient of mitochondria on the oxygen uptake flux in the complete system, and $^{JO}C_m$ is the flux control coefficient of step m on the oxygen uptake flux in the isolated mitochondria system. The flux control coefficients of the reactions between oxaloacetate and fructose-1,6-bisphosphate were calculated from the summation theorem (Kacser and Burns, 1973):

$$C_{OAA \rightarrow FBP} = 1 - \sum_{mit} C - C_{PK} - C_{PFK} \qquad (6.7)$$

6.4 Flux control coefficients.

6.4.1 Oxaloacetate to hexose system.

Representative titration experiments are shown in Figures 6.5 and 6.6. The flux control coefficients calculated from these and similar experiments are shown in Table 6.3. The following points are emphasised. The control of both the total flux (J_T) and the flux to hexose (J_H) is shared primarily between the FBPase/PFK/PFP regulator cycle and reactions between oxaloacetate and fructose-1,6-bisphosphate. Pyruvate kinase has only a

small effect on these fluxes, but is responsible for the majority of the control of the flux to pyruvate (J_P). Both the steps between oxaloacetate and fructose-1,6-bisphosphate, and the FBPase/PFK/PFP cycle have some control on J_P.

TABLE 6.3. *Flux control coefficients for the* in vitro *system converting oxaloacetate to hexose.* Reactions were set up as described in the legend to Table 6.1. Flux control coefficients were determined from enzyme titrations as described in the text. Values are the mean (± SEM or range), with the number of independent experiments shown in parentheses.

	Flux control coefficients.		
Flux	OAA→FBP	PK	FBPase/PFK/PFP
Total (J_T)	0.39*	0.04 ± 0.01(3)	0.57 ± 0.02(2)
Hexose (J_H)	0.54*	-0.06 ± 0.01(3)	0.52 ± 0.02(2)
Pyruvate (J_P)	0.30*	0.85 ± 0.01(3)	-0.15(1)

TABLE 6.4. *Effect of the coordinate control operation on the flux control coefficient of pyruvate kinase on the flux to pyruvate* (${}^{JP}C_{PK}$). Reactions were set up as described in the legend to Table 6.1 in the presence of varying amounts of cotyledon extract. The value α is the amount of extract normalised with respect to extract from 0.4 cotyledons. Values are the mean (± SEM or range), with the number of independent experiments shown in parentheses.

α	${}^{JP}C_{PK}$
0.5	0.80 ± 0.02(2)
1.0	0.85 ± 0.01(3)
1.5	0.83 ± 0.05(2)

The effect of the CCO on the flux control coefficient of pyruvate kinase on the flux to pyruvate is shown in Table 6.4. The control coefficient behaves as an S-type variable, indicating that the non-linearity revealed in Figure 6.4 does not appear to effect

* Calculated using the summation theorem.

FIGURE 6.5

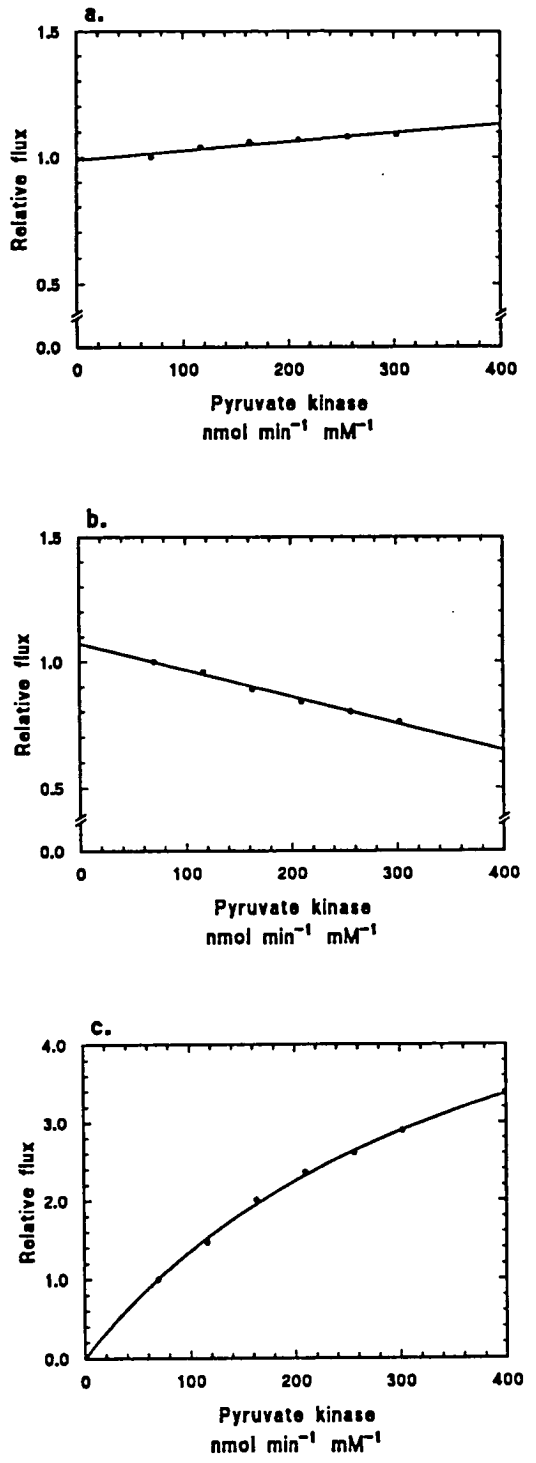

FIGURE 6.5. *Effect of varying pyruvate kinase activity on the fluxes in the* in vitro *system for the conversion of oxaloacetate to hexose.* Reactions were set up as described in the legend to Table 6.1 and fluxes measured after the addition of varying amounts of pyruvate kinase. The fluxes were normalised with respect to the flux without enzyme addition.

a. Total flux, basal level, 37.1 nmol oxaloacetate min^{-1}.
b. Hexose flux, basal level, 31.4 nmol NADH min^{-1}.
c. Pyruvate flux, basal level, 5.7 nmol pyruvate min^{-1}.

FIGURE 6.6

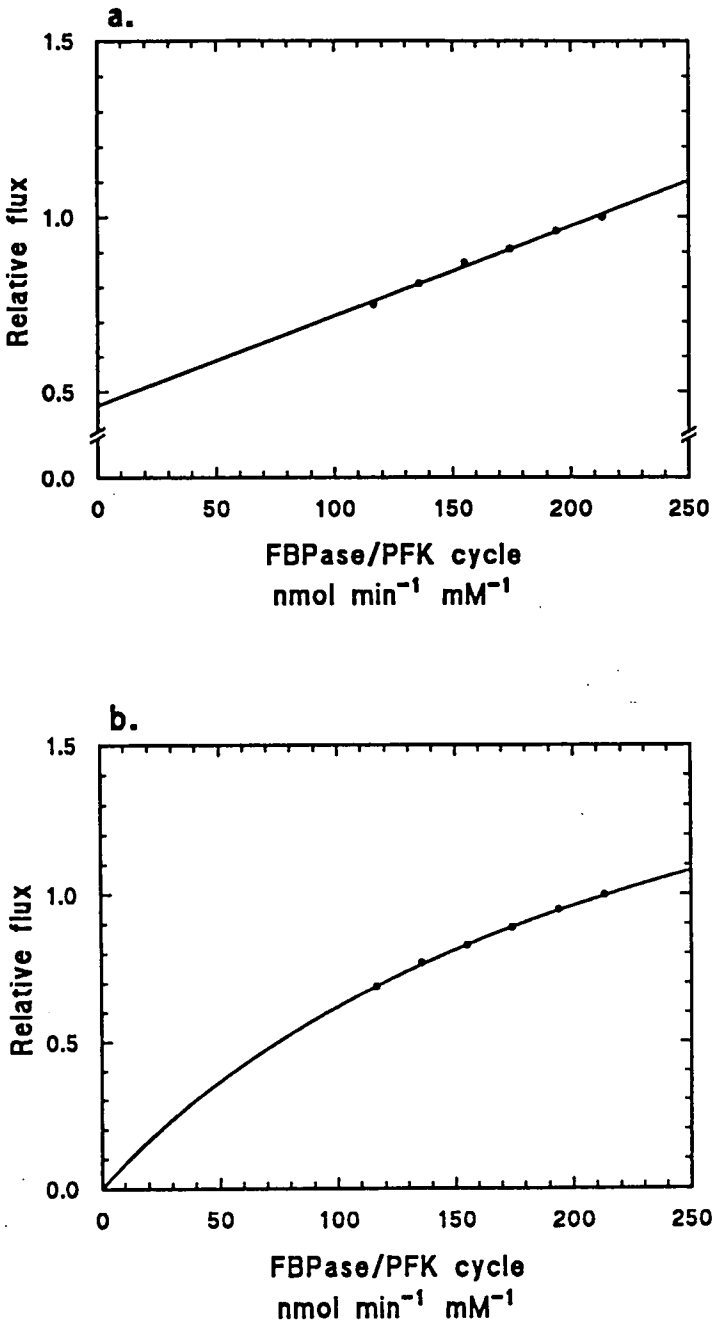

FIGURE 6.6. *Effect of varying phosphofructokinase activity on the fluxes in the* in vitro *system for the conversion of oxaloacetate to hexose.* Reactions were set up as described in the legend to Table 6.1 and fluxes measured after the addition of varying amounts of phosphofructokinase. The level of enzyme activity is expressed as the difference between activity of fructose-1,6-bisphosphatase and phosphofructokinase. The fluxes were normalised with respect to the flux without enzyme addition.

a. Total flux, basal level, 37.1 nmol oxaloacetate min^{-1}.

b. Hexose flux, basal level, 31.3 nmol NADH min^{-1}.

the flux control coefficient. It is therefore asserted that the flux control coefficient values presented reflect those *in vivo*.

6.4.2 Succinate to hexose system.

The flux control coefficients for mitochondrial steps on the pathway between succinate and oxaloacetate are shown in Table 6.5. Of the steps examined only the adenine nucleotide translocator has a significant control coefficient. By the summation theorem (Kacser and Burns, 1973) the remaining control of 0.68 $\pm$ 0.08 is located in the steps not examined. These include the dicarboxylate transporter, a number of other membrane transport processes, Complex I, and the TCA cycle enzymes fumarase and malate dehydrogenase (see Figure 6.3b).

Representative titration experiments with the complete system are shown in Figures 6.7, 6.8, 6.9, and 6.10. The flux control coefficients calculated from these and similar experiments are shown in Table 6.6. Control of the flux to hexose is shared primarily between mitochondrial steps (38 %), the steps between oxaloacetate and fructose-1,6-bisphosphate (19 %) and the FBPase/PFK/PFP cycle (47 %). The adenine nucleotide translocator makes a significant contribution to the control of this flux (C = 0.23). A similar distribution of control is also found for the total flux (J_T). Control of the oxygen uptake flux (J_O) is shared between mitochondrial steps (55 %) and the FBPase/PFK/PFP cycle (38 %). The effect of the FBPase/PFK/PFP cycle on J_O will be due to both its effect on the total flux, and therefore the rate of oxaloacetate removal, and the ATP/ADP ratio.

TABLE 6.5. *Flux control coefficients for succinate oxidation in isolated mitochondria under conditions similar to those of the* in vitro *system for the conversion of succinate to hexose.* Mitochondria were isolated from 4 day old light grown cotyledons. Oxygen uptake was measured in the presence of 10 mM succinate, 10 mM glutamate, 10 units aspartate/2-oxoglutarate aminotransferase, 5 mM glucose, 0.5 mM ATP, and sufficient hexokinase to obtain an oxygen uptake rate of 90 % the state 3 rate (in the presence of 1 µmol ADP). Flux control coefficients were determined by inhibitor titrations as described in Chapter 4. Values are the mean ($\pm$ range) of 2 independent experiments.

Step	Flux control coefficient
Complex II	0
Complex III	0
Complex IV	0
AdNT	0.32 $\pm$ 0.08

FIGURE 6.7

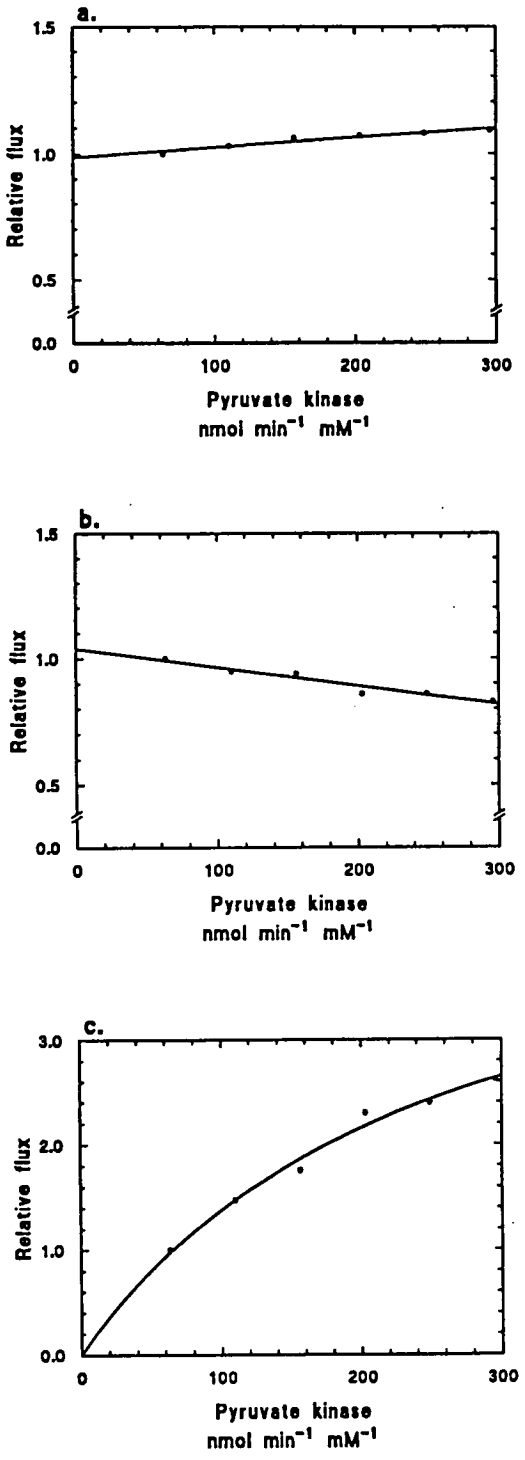

FIGURE 6.7. *Effect of varying pyruvate kinase activity on the fluxes in the* in vitro *system for the conversion of succinate to hexose.* Reactions were set up as described in the legend to Table 6.2 and fluxes measured after the addition of varying amounts of pyruvate kinase. The fluxes were normalised with respect to the flux without enzyme addition.

a. Total flux, basal level, 29.8 nmol oxaloacetate min^{-1}.
b. Hexose flux, basal level, 25.5 nmol NADH min^{-1}.
c. Pyruvate flux, basal level, 4.3 nmol pyruvate min^{-1}.

FIGURE 6.8

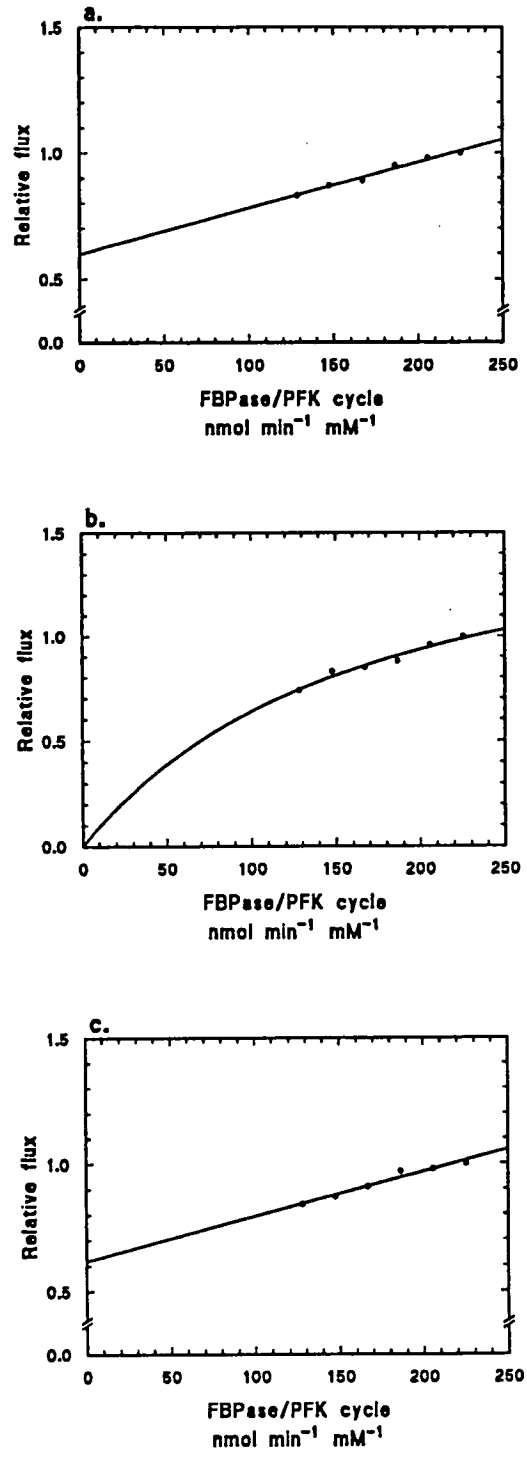

FIGURE 6.8. *Effect of varying phosphofructokinase activity on the fluxes in the* in vitro *system for the conversion of succinate to hexose.* Reactions were set up as described in the legend to Table 6.2 and fluxes measured after the addition of varying amounts of phosphofructokinase. The level of enzyme activity is expressed as the difference between activity of fructose-1,6-bisphosphatase and phosphofructokinase. The fluxes were normalised with respect to the flux without enzyme addition.

a. Total flux, basal level, 29.8 nmol oxaloacetate min^{-1}.
b. Hexose flux, basal level, 25.5 nmol NADH min^{-1}.
c. Oxygen uptake flux, basal level, 14.3 nmol O_2 min^{-1}.

FIGURE 6.9

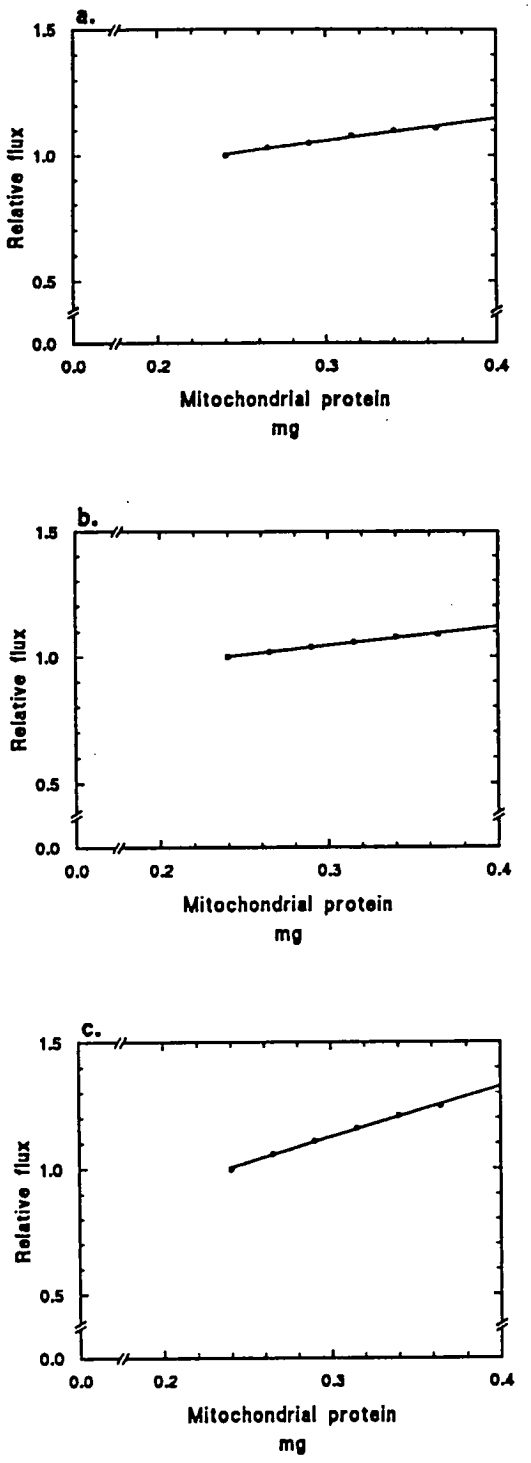

FIGURE 6.9. *Effect of varying mitochondrial protein content on the fluxes in the* in vitro *system for the conversion of succinate to hexose.* Reactions were set up as described in the legend to Table 6.2 and fluxes measured after the addition of varying amounts of mitochondrial protein. The fluxes were normalised with respect to the flux without enzyme addition.

a. Total flux, basal level, 29.8 nmol oxaloacetate min^{-1}.

b. Hexose flux, basal level, 25.5 nmol NADH min^{-1}.

c. Oxygen uptake flux, basal level, 14.3 nmol O_2 min^{-1}.

FIGURE 6.10

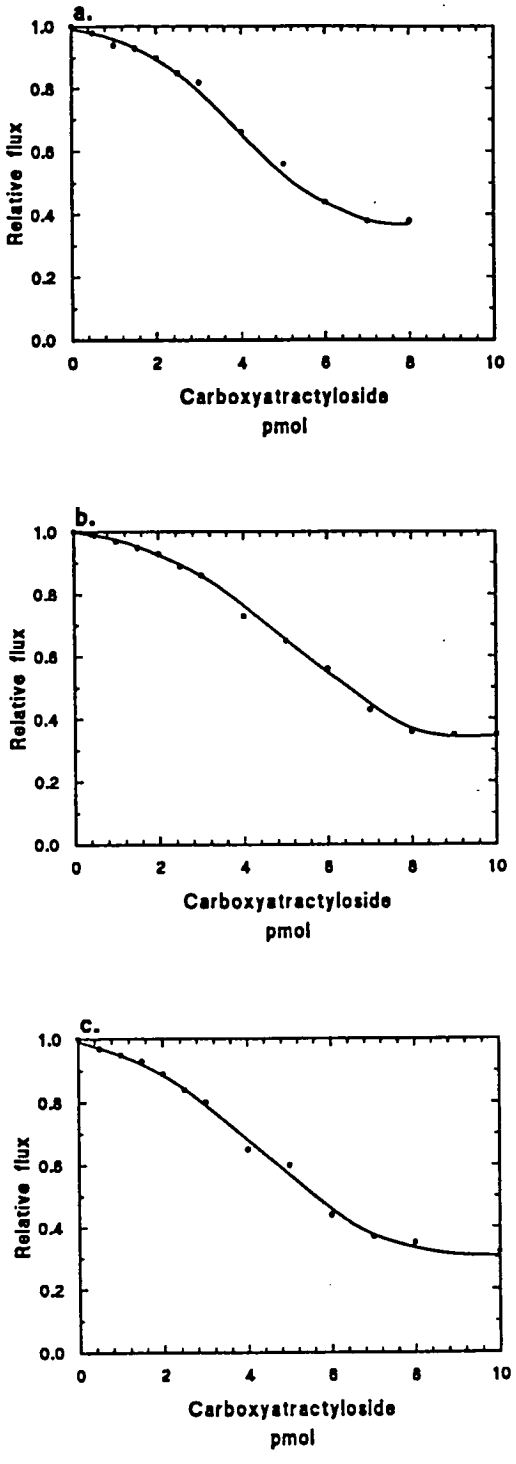

FIGURE 6.10. *Effect of carboxyatractyloside on the fluxes in the* in vitro *system for the conversion of succinate to hexose.*

a & b. Reactions were set up as described in the legend to Table 6.2 and fluxes measured after the addition of varying amounts of carboxyatractyloside. The fluxes were normalised with respect to the flux without inhibitor addition.

a. Total flux, basal level, 29.8 nmol oxaloacetate min^{-1}.

b. Hexose flux, basal level, 25.5 nmol NADH min^{-1}.

c. Oxygen uptake was measured in isolated mitochondria as described in the legend to Table 6.5, in the presence of increasing amounts of carboxyatractyloside. The flux were normalised with respect to the flux without inhibitor addition (163 nmol O_2 min^{-1} mg $protein^{-1}$).

TABLE 6.6. *Flux control coefficients for the* in vitro *system converting succinate to hexose.* Reactions were set up as described in the legend to Table 6.2. Flux control coefficients were determined from enzyme titrations as described in the text. Coefficients for mitochondrial steps were calculated from the data of Table 6.5 and the flux control coefficients for mitochondria on the system fluxes, which were 0.27 ± 0.05, 0.22 ± 0.05, 0, and 0.54 ± 0.06 for the total, hexose, pyruvate, and oxygen uptake fluxes, respectively. Values are the mean (± range) of 2 independent experiments.

	Flux control coefficients				
Flux	Mit. Steps	AdNT	OAA→FBP	PK	FBPase/PFK/PFP
Total (J_T)	0.18*	0.28 ± 0.06	0.06**	0.03 ± 0.01	0.45 ± 0.04
Hexose (J_H)	0.15*	0.23 ∓ 0.06	0.19**	-0.04 ∓ 0.01	0.47 ∓ 0.01
Pyruvate (J_P)	0*	0	0.20**	0.80 ∓ 0.01	0
Oxygen uptake (J_O)	0.37*	0.18	0.07**	0	0.38 ± 0.01

* Calculated from the data of Table 6.5, and the flux control coefficients of mitochondria on each flux.

** Calculated from the summation theorem.

6.5 Discussion.

6.5.1 Inherent problems with the use of *in vitro* reconstituted systems.

The results presented in this chapter are dependent for their interpretation on the assumption that the *in vitro* systems reflect the distribution of control *in vivo*. The following points should be kept in mind when interpreting this data.

a. Flux control coefficients have been shown to be dependent on the flux (Groen *et al.*, 1982, 1986; Hafner *et al.*, 1990). The flux in the *in vitro* systems represents a very high rate of sucrose synthesis.

b. In the system for the conversion of succinate to hexose, the oxaloacetate produced by the mitochondria was used directly in sucrose synthesis. However, in the accepted pathway *in vivo* sucrose is produced from malate exported from the glyoxysome, and the products of succinate oxidation return directly to the glyoxysome (Mettler and Beevers, 1980).

6.5.2 Control of the conversion of oxaloacetate to hexose.

Identification of the regulatory steps in sucrose synthesis from oxaloacetate is in agreement with the work of Leegood and ap Rees (1978b) on marrow cotyledons and Kobr and Beevers (1971) on castor bean endosperm. The regulatory mechanisms proposed in the light of this distribution of control have been discussed in detail in Chapter 1 (see 1.1.2). In summary, the flux is predicted to respond to the levels of ATP, ADP, AMP, fructose-6-phosphate and 3-phosphoglycerate. The low flux control coefficients measured for pyruvate kinase on the hexose synthesis flux indicates that high levels of this enzyme has little impact under conditions of high flux. This explains, in part, the somewhat surprising increase in pyruvate kinase activity during cotyledon development (Figure 5.7; Thomas and ap Rees, 1972b). The only regulatory property ascribed to pyruvate kinase is stimulation in activity by low ATP/ADP ratios (Turner and Turner, 1980), so this is presumably the means by which the flux to pyruvate is regulated.

6.5.3 Control of the conversion of succinate to hexose.

This is the first description of the control of sucrose synthesis from succinate by mitochondrial steps in any system. The major difference in the distribution of control between this and the cytosolic system is the redistribution of control away from the reactions between oxaloacetate and fructose-1,6-bisphosphate. Phospho(enol)pyruvate carboxykinase (PEPCK) has previously been identified as a potential regulatory step, but no regulatory properties have been identified *in vitro* (Leegood and ap Rees, 1978a, 1978b). The data presented here explains this, because PEPCK does not appear to be an important regulatory step ($C < 0.19$).

The mitochondrial steps regulating the hexose flux are the adenine nucleotide translocator and a number of steps which are substantially transport reactions. Dicarboxylate uptake is dependent on the operation of the phosphate translocator (Heldt and Flugge, 1987). This presents further evidence for the hypothesis presented in Chapter 4, that mitochondrial reactions, responding to the ATP/ADP ratio, level of inorganic phosphate, and succinate concentration, are involved in maintaining the balance between lipid breakdown and sucrose synthesis.

The adenine nucleotide translocator is also important in the control of gluconeogenesis from lactate in rat liver cells (Groen *et al.*, 1986), suggesting that this step may be involved in the integration of biosynthesis and degradation in diverse organisms.

6.6 Conclusions.

1. Further evidence is provided to suggest an important role for mitochondria in the integration of synthetic and degradative metabolism.

2. The major cytosolic control point for sucrose synthesis is confirmed as the FBPase/PFK/PFP regulator cycle.

3. Pyruvate kinase is identified as the major cytosolic controlling step for the diversion of carbon to respiration.

CHAPTER 7.
GENERAL DISCUSSION.

The data presented in this thesis has already been discussed in some detail in the individual chapters. Consequently, the aim of this chapter is to bring together the conclusions reached and attempt to identify the general significance of the results contained in this thesis.

7.1 Summary of Results.

The results described in chapters 3-6 of this thesis can be summarised as follows (refer to Figure 7.2):-

(i) The composition of cucumber cotyledon mitochondria is modified during early seedling development in terms of both the enzymes and membrane transport proteins present. These changes, which are at least in part brought about by variation in the rate of synthesis or turnover of mitochondrial proteins (mitochondrial biogenesis), can be correlated with the varying biochemistry and metabolic role of the tissue.

(ii) During the initial phase of lipid mobilisation the activity of mitochondrial enzymes and transporters is such that carbon released from lipid is directed away from the decarboxylation reactions of the TCA cycle. The respiratory flux in isolated mitochondria is primarily controlled by the dicarboxylate transport system (flux control coefficient *ca.* 0.70) and the adenine nucleotide translocator (flux control coefficient *ca.* 0.30). These steps also have significant control coefficients for the sucrose synthesis flux, at least in cell free extracts (flux control coefficients *ca.* 0.15 and 0.25, respectively).

(iii) During chloroplast biogenesis and the acquisition of photosynthetic competence, the activities of NAD-malic enzyme and pyruvate dehydrogenase increase, providing a mechanism for the entry of pyruvate, derived from malate, into the TCA cycle. This may be related to the provision, by mitochondrial reactions, of intermediates required for biosynthesis of chloroplast components.

(iv) During the photosynthetic phase, the capacity exists for the full operation of the TCA cycle. At this stage the control of succinate oxidation is primarily shared between the complexes of the respiratory chain (flux control coefficients for complexes II, III, and IV of *ca.* 0.30, 0.40, and 0.35, respectively).

7.2 Mitochondrial membrane transporters and the regulation of respiratory flux.

Metabolism of succinate and pyruvate by cucumber cotyledon mitochondria is largely controlled by membrane transporters, including the adenine nucleotide translocator, dicarboxylate transporter, phosphate translocator and pyruvate transporter. These steps have important roles in the coarse control of mitochondrial function, and a potential role in the integration of diverse branches of plant metabolism, in response to varying demands from within the cotyledons and elsewhere in the growing seedling.

Despite detailed work on the mechanism of metabolite transport into and out of mitochondria, little attention has been paid to the importance of these steps in the control

of specific pathways. In animal systems the dicarboxylate transporter and the adenine nucleotide translocator play a part in the regulation of succinate oxidation in isolated mitochondria (Groen *et al.*, 1982). The adenine nucleotide translocator has also been shown, under certain conditions, to have a significant flux control coefficient for gluconeogenesis in isolated rat liver cells (Groen *et al.*, 1986). In castor bean endosperm mitochondria the low activities of the oxaloacetate transporter may direct the pathway of NADH exchange between mitochondria and glyoxysomes (Millhouse *et al.*, 1983).

There is evidence to suggest that the adenine nucleotide translocator is of importance in the control of respiration in plant mitochondria. Regulation of respiration by the availability of ADP was first described in animal systems (Chance and Williams, 1956). In isolated pea leaf mitochondria, at low external ADP levels, the absolute concentration of ADP has more impact on the respiration rate than the ATP/ADP ratio, which only affects the flux at ratios greater than 20 (Dry and Wiskich, 1982). However, since, in the short term, the adenine nucleotide pool is conserved *in vivo*, low ADP levels are generally accompanied by high ATP levels. Measurement of cytosolic ATP/ADP ratios by rapid fractionation of protoplasts implies that respiration rate is modulated to maintain cytosolic ATP levels. During light-dark transitions there are only transient changes in the ATP/ADP ratio (Hampp *et al.*, 1982; Stitt *et al.*, 1982). Furthermore, inhibition of ATP generation by chloroplasts has no effect on the cytosolic ATP/ADP ratio (Stitt *et al.*, 1982), suggesting modulation of mitochondrial function to stabilise ATP/ADP ratios.

The use of ^{31}P-NMR to measure adenylate levels *in vivo* has shown that, in maize roots, the ATP/ADP ratio was greater than 25 (Roberts *et al.*, 1985), and therefore in the range where it could regulate respiration (Dry and Wiskich, 1982). The mechanism by which cytosolic ATP/ADP ratios could effect the respiratory flux by means of the adenine nucleotide translocator has been investigated in rat liver mitochondria. Despite a very low K_m for ADP (1-10 μM; Vignais, 1976), ADP uptake into mitochondria is competitively inhibited by high ATP levels (Vignais, 1976). Therefore the uptake of ADP is dependent on the ATP/ADP ratio. These properties, combined with a high flux control coefficient of the adenine nucleotide translocator on the respiratory flux, provide evidence that the ATP/ADP ratio may well, under certain conditions, have a key role in modulating mitochondrial respiration.

A major regulatory function has been ascribed to the phosphate translocator of the chloroplast membrane in the partitioning of fixed carbon between starch and sucrose during photosynthesis (Stitt *et al.*, 1987a). This transporter catalyses the exchange of phosphoglycerate, triose phosphate and inorganic phosphate across the chloroplast membrane, and is believed to play an important role in the communication between cytosol and chloroplast metabolism. Reduction in the rate of sucrose synthesis results in an increase

in the cytosolic level of phosphorylated intermediates (Gerhardt *et al.*, 1987; Stitt *et al.*, 1987b), which is likely to lead to a concomitant reduction in the cytosolic phosphate concentration. Technical difficulties in measuring cytosolic phosphate levels have prevented direct confirmation of this assertion (Stitt *et al.*, 1987a). Lack of availability of cytosolic phosphate would be expected to prevent its exchange for triose phosphate across the chloroplast envelope, directing carbon into starch production rather than sucrose synthesis.

The evidence contained in this thesis supports the proposal that mitochondrial membrane transporters have a similar function in controlling the partitioning of carbon, derived from lipid breakdown, between sucrose synthesis, biosynthesis of cellular components and respiration.

7.3 Role of plant mitochondria in biosynthesis of chloroplast components.

Major modulations in the enzyme complement of cucumber cotyledon mitochondria are associated with biosynthetic activity during the chloroplast biogenesis phase. It has been argued that these changes (increases in the activity of NAD-malic enzyme and pyruvate dehydrogenase) facilitate the production of TCA cycle intermediates required for biosynthesis. The evidence in support of the requirement for these intermediates will now be considered with specific reference to supply of acetyl-CoA.

Acetyl-CoA is the starting material for the biosynthesis of lipid and terpenoid derivatives, including haem, chlorophyll, and carotenoids (Stumpf, 1987). The initial steps of these pathways have been localised to the chloroplasts (Stumpf, 1987). However, since acetyl-CoA does not cross organelle membranes (Liedvogel, 1986), the route of carbon entry into these pathways has remained unclear. One possible route involves the activity of chloroplast pyruvate dehydrogenase (Camp and Randall, 1985). In this case the carbon is likely to be derived from triose or hexose phosphates via the action of the glycolytic pathway within the plastid (Liedvogel and Bauerle, 1986). An alternative route has been identified with the discovery of mitochondrially located acetyl-CoA hydrolase (Murphy and Stumpf, 1981; Liedvogel and Stumpf, 1982; Zeicher and Randall, 1990), which catalyses the release of acetate from acetyl-CoA. As acetate freely crosses biological membranes and chloroplasts contain the enzyme acetyl-CoA synthase in appreciable amounts (Kuhn *et al.*, 1981), this represents a means by which acetyl-CoA can be transferred from the mitochondria to the plastids. This latter pathway is illustrated in Figure 7.1. Acetate formation by acetyl-CoA hydrolase will only occur under conditions of rapid acetyl-CoA production and limited oxaloacetate synthesis, since the enzyme has a much higher K_m for acetyl-CoA than citrate synthase (Zeicher and Randall, 1990). Low rates of oxaloacetate production occur either when the mitochondrial NADH/NAD ratio is high (owing to the unfavourable equilibrium position of the malate dehydrogenase reaction) or when the rate of oxaloacetate removal is high. Under the former conditions excess malate can be converted

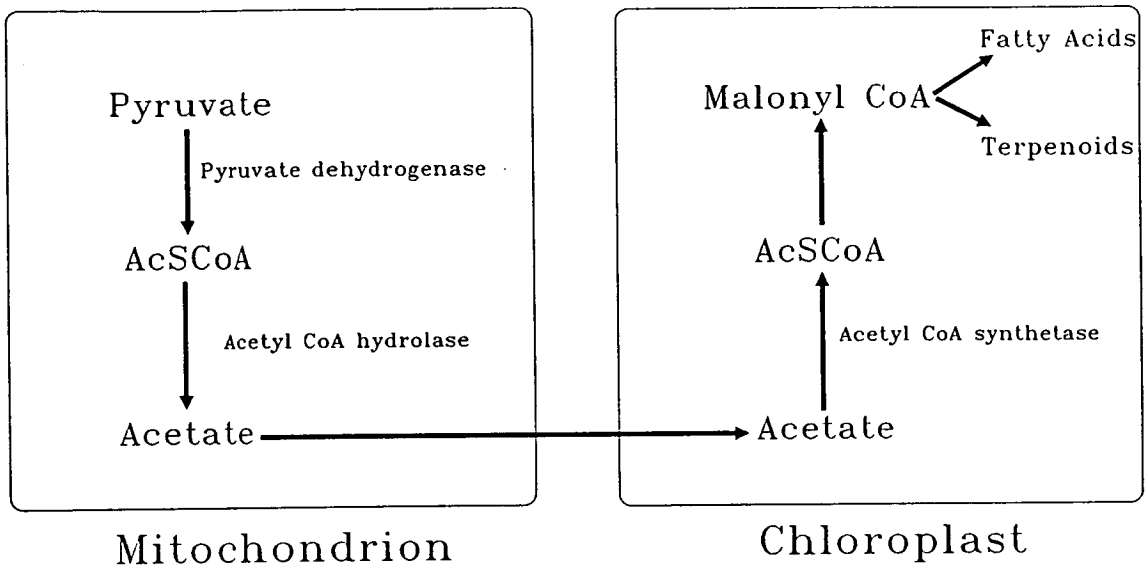

FIGURE 7.1: *Mitochondrial involvement in lipid biosynthesis.* A potential pathway by which acetyl CoA required for lipid and terpenoid biosynthesis within the chloroplast could be derived from mitochondrial pyruvate oxidation.

to pyruvate by NAD-malic enzyme, which is relatively insensitive to high NADH levels (Pascal *et al.*, 1990). One circumstance when the rate of oxaloacetate removal is high is during the operation of a malate/aspartate-2-oxoglutarate/glutamate shuttle during lipid mobilisation or photosynthesis (see below). A major problem with the scheme described above is a result of the properties of mitochondrial pyruvate dehydrogenase. This enzyme is inactivated by light (Budde and Randall, 1989), but lipid synthesis is generally considered to occur during photosynthesis (Stumpf, 1987). Moreover, even when in the active form, mitochondrial pyruvate dehydrogenase is inhibited by high NADH levels (Pascal *et al.*, 1990), required for the operation of acetyl-CoA hydrolase. Further work is required to fully establish the route of carbon entry into lipid and terpenoid biosynthesis, but there are indications that mitochondrially produced acetyl-CoA is a potential carbon source.

7.4 Mitochondrial function in illuminated photosynthetic tissues.

Mitochondria from cucumber cotyledons show their maximum rates of oxidation of a range of TCA cycle substrates during the photosynthetic phase of development. Similar results were also obtained by Azcon-Bieto *et al.* (1989) from experiments with soybean cotyledon mitochondria. These observations provide further support for the hypothesis that TCA cycle activity is necessary in photosynthetic tissues. There is also an appreciable body of evidence confirming both TCA cycle activity and oxidative phosphorylation in illuminated photosynthetic tissues, which will now be discussed.

Early work by Chapman and Graham (1974) demonstrated that, in mung bean seedlings, the rate of carbon dioxide release from TCA cycle intermediates, in the presence of DCMU to inhibit photosynthesis, was unaffected by light-dark transitions. The use of TCA cycle inhibitors, such as malonate, to measure flux through the cycle (as intermediate accumulation) also indicates similar fluxes in the light and dark (Chapman and Graham, 1974). This evidence is partially in conflict with the more recent data of Randall and co-workers. They have demonstrated that mitochondrial pyruvate dehydrogenase, a step essential for TCA cycle operation, is inactivated by high ATP levels (Budde *et al.*, 1988) and the products of photorespiration (Schuller and Randall, 1989). These properties result in a light dependent inactivation of pyruvate dehydrogenase *in vivo* (Budde and Randall, 1989).

Evidence indicating that oxidative phosphorylation does occur during illumination has been provided by studies measuring the ATP/ADP ratios in the mitochondria, chloroplasts, and cytosol of protoplasts from the leaves of barley and wheat, using rapid fractionation techniques. During light-dark transitions there are only small changes in the cytosolic ATP/ADP ratio (Hampp *et al.*, 1982; Stitt *et al.*, 1982). A difference exists between the mitochondrial (0.6) and cytosolic (9.2) ATP/ADP ratios in the dark, indicating mitochondrial energisation, which is reduced by light (Stitt *et al.*, 1982), suggesting that

oxidative phosphorylation is less active under the latter conditions. However, inhibition of photosynthesis has little impact on cytosolic ATP/ADP ratios, in contrast to inhibition of mitochondrial oxidative phosphorylation, which did (Stitt *et al.*, 1982). Mitochondria are thus able to maintain the cytosolic ATP/ADP level necessary to sustain ATP consuming reactions during any shortfall due to reduced photosynthetic rate. The specific inhibition of mitochondrial ATP synthesis, using low concentrations of oligomycin, causes a significant reduction in the rate of photosynthesis in intact protoplasts, although isolated chloroplasts are insensitive to such concentrations of inhibitor (Ebbighausen *et al.*, 1987; Kromer *et al.*, 1988). Moreover, low concentrations of oligomycin also cause a drop in the cytosolic ATP/ADP ratio and a dramatic increase in fructose-2,6-bisphosphate (Kromer *et al.*, 1989). Export of reducing equivalents from the chloroplast to support mitochondrial ATP synthesis is thought to occur by the action of an malate-oxaloacetate shuttle (Ebbighausen *et al.*, 1987). There is also evidence that reducing equivalents derived from oxidation of glycine produced by photorespiration are used within the mitochondria for ATP synthesis. Cytosolic ATP/ADP ratios in barley protoplasts, again measured by rapid fractionation, are higher under photorespiratory (low carbon dioxide) conditions than in the presence of high carbon dioxide levels (Gardestrom and Wigge, 1988). In addition, aminoacetonitrile, a specific inhibitor of glycine decarboxylase, had little effect on cytosolic ATP/ADP ratios under non-photorespiratory conditions, but significantly reduced them when carbon dioxide levels were low (Gardestrom and Wigge, 1988).

In the light of the evidence discussed above, the following reappraisal of mitochondrial function in illuminated photosynthetic tissues is offered. Mitochondrial oxidative phosphorylation is responsible for an appreciable proportion of cellular ATP synthesis during photosynthesis. The NADH which is the substrate for this ATP synthesis is almost certainly derived from glycine oxidation, and the partial operation of the TCA cycle, most notably the oxidation of malate to oxaloacetate. The following properties of cucumber cotyledon mitochondria during the photosynthetic phase support this. First, the light dependent increase in malate oxidation rates by isolated mitochondria; secondly, the light induction of the capacity for glycine oxidation; and thirdly, the high levels and activity of the adenine nucleotide translocator, required for the transport of ATP to the cytosol and concomitant uptake of ADP. It therefore seems likely that the synthesis of mitochondrial enzymes and membrane proteins observed during early seedling development is, at least in part, a necessary adjunct of photosynthetic development.

7.5 Importance of gene expression in the modulation of mitochondrial function.

The measurement of mitochondrial protein content and abundance of specific mitochondrial enzymes provides evidence that mitochondrial function and respiratory activity is modulated during development as a result of changes in protein synthesis and/or

degradation. It is the aim of this section to assess the importance of gene expression in this modulation.

There has only been a limited amount of work concerning the expression of genes encoding mitochondrial proteins in plants. In contrast, much detailed information is available concerning the expression of these genes in yeast. Metabolic and environmental signals have been shown to effect a number of the processes required for the production of functional mitochondrial enzymes including, transcription, mRNA splicing, translation, post-translational modification and protein import into mitochondria (Grivell, 1989). The products of nuclear genes are necessary for the expression of mitochondrially encoded genes, and represent a potential mechanism for the integration of the nuclear and mitochondrial genome expression (Fox, 1986; Grivell, 1989). *De novo* protein synthesis is essential for the transition between anaerobic and aerobic metabolism in yeast (Grivell, 1989). During embryogenesis in *Xenopus laevis* there are marked fluctuations in the steady state level of mitochondrial transcripts, which decrease in abundance after fertilisation and reappear during organogenesis (Meziane *et al.*, 1989).

The data available on expression of genes for mitochondrial proteins in plants is summarised as follows. First, there is an increase in the steady state level of mRNA transcripts encoding the α (mitochondrially encoded) and β (nuclear encoded) subunits of the mitochondrial ATPase early in tomato fruit development (Piechulla, 1988). Secondly, in maize embryos the steady state levels of transcripts encoding subunits of the ATPase and cytochrome oxidase increases between 6 and 12 hours after imbibition, followed by increased rates of synthesis of these proteins (Ehrenshaft and Brambl, 1990). Thirdly, leaf development and the associated structural and functional differentiation in wheat is accompanied by a fall in the mitochondrial genome copy number, and steady state levels of a number of mitochondrial transcripts (Topping and Leaver, 1990). However, at least in the case of ATPase, these changes do not result in changes in the steady state level of the protein (Topping and Leaver, 1990). The following criticisms are offered of these reports. In all 3 cases determination of transcript levels is based on Northern filter hybridisations, generally regarded as a nonquantitative technique. The immunoprecipitation and Northern blot data of Ehrenshaft and Brambl (1990) is of extremely poor quality, and it is difficult to appreciate how quantitative information can be described from these results. A general criticism which can be levelled at this, and indeed most, work concerning the mechanism of gene expression is that authors reach conclusions concerning identification of the steps controlling gene expression, despite their data providing little information on this phenomenon. In addition, no evidence is provided that the enzymes whose activities are modulated have flux control coefficients high enough to influence metabolism significantly.

In conclusion, whilst there is evidence that changing mitochondrial protein composition influences mitochondrial function, little is known concerning the mechanism by which differential gene expression or protein turnover is regulated.

7.6 Future Directions.

The results presented in this thesis, perhaps not surprisingly, suggest more questions than answers. The following represents a selection of the potential lines of further investigation into mitochondrial biogenesis and function, and its control during early seedling development in cucumber.

1. The results described in Chapter 4 represent an investigation into the control of succinate oxidation in isolated cotyledon mitochondria. This could be extended to an analysis of the control of mitochondrial respiration under conditions more similar to those found *in vivo*. This could be accomplished by applying the methods of Brown, Hafner and Brand (1990) to isolated cotyledon protoplasts. These workers studied the effects of inhibitors of mitochondrial respiration on the rate of oxygen uptake and the mitochondrial membrane potential in isolated rat liver cells. A similar system using isolated protoplasts could provide information on the control of respiration, and also be used to confirm the results of Chapter 6 by examining the effect of such inhibitors on the sucrose synthesis flux.

2. The *in vitro* system described in Chapter 6 could be used to investigate a number of questions:

(i) A more detailed picture of the distribution of control in this system could be achieved by using inhibitors, such as mercaptopicilinic acid (phospho(enol)pyruvate carboxykinase) and carboxyatractyloside to measure the complete set of elasticity coefficients.

(ii) The effect of the regulatory metabolite fructose-2,6-bisphosphate on the system could easily be investigated by determining the effect of adding exogenous fructose-2,6-bisphosphate on the system fluxes.

(iii) The hypothesis proposed in this thesis that the cytosolic ATP/ADP ratio is involved in the integration of mitochondrial and cytosolic steps could be tested by varying the ATP consumption load of the system using an ADP regenerating enzyme system. This could be achieved by adding, for example phosphocreatine to the system, and titrating in creatine kinase.

3. This developmental system presents a good opportunity to investigate the mechanisms of differential gene expression. The changes in mitochondrial protein composition may result from *de novo* protein synthesis, which is presumably due to variations in the rate of transcription or translation of both nuclear and mitochondrially encoded genes. Measurements of the abundance of mRNAs for the adenine nucleotide

translocator, NAD-malic enzyme, or glycine decarboxylase should reveal whether this is the case.

7.7 Conclusions.

The varying metabolic role of cucumber cotyledon mitochondria during early seedling development is summarised in Figure 7.2. The following points are emphasised. Mitochondria play a crucial role in cotyledon metabolism throughout the life of the tissue. At all stages of development the major metabolic function of the cotyledons is the production of sucrose for export to the growing regions of the seedling. During the photosynthetic phase there is a diurnal variation in cotyledon metabolism, but mitochondria appear to be important producers of ATP during both the light and dark periods. The details of cotyledon metabolism in the dark (that is, the conversion of starch to sucrose) are, as yet, unknown for any plant tissue.

The study discussed in this thesis represents a preliminary investigation into the respiratory metabolism of cucumber cotyledons during early seedling development. It provides a framework for further study into both the biochemistry and molecular biology of this complex, but experimentally convenient system.

Additionally, the application of metabolic control theory demonstrates the complexity of the control of integrated biochemical systems, but also, more importantly, provides a quantitative methodology for dealing with this complexity. Combined with this tool, the accurate and reproducible measurement of biochemical parameters can only lead to a greater understanding of how metabolism is regulated.

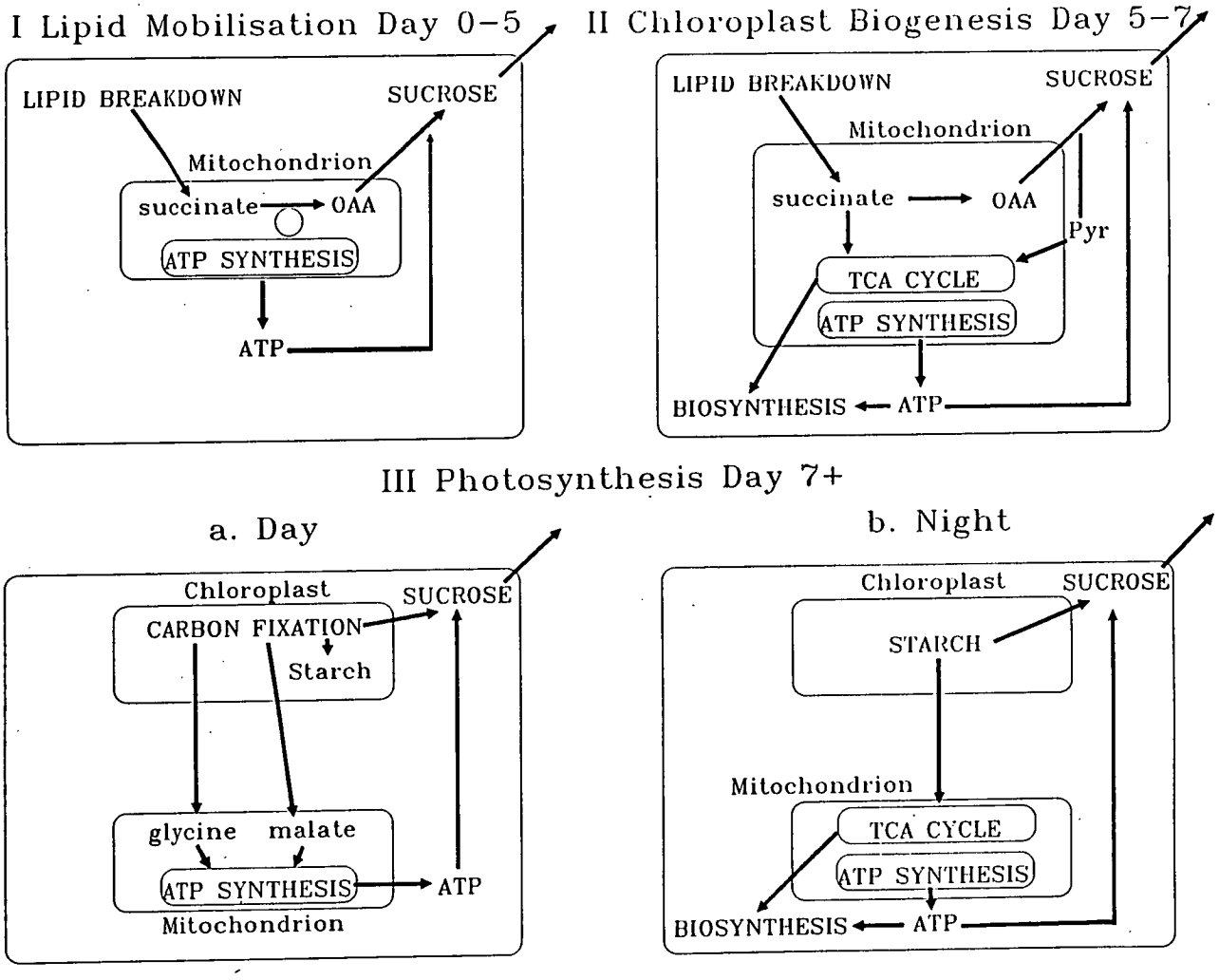

FIGURE 7.2: *Mitochondrial function in the cotyledons of cucumber during early seedling development.* A schematic diagram illustrating the metabolic role of cucumber cotyledon mitochondria during the lipid mobilisation, chloroplast biogenesis, and photosynthetic phases of early seedling development.

LITERATURE CITED

Acerenza, L and Kacser, H (1990).
Enzyme kinetics and metabolic control. A method to test and quantify the effect of enzymic properties on metabolic variables.
Biochem. J. 269, 697-707.

Allen, RD, Trelease, RN, and Thomas, TL (1988).
Regulation of isocitrate lyase gene expression in sunflower.
Plant Physiol. 86, 527-532.

ap Rees, T (1985).
The organisation of glycolysis and the oxidative pentose phosphate pathway in plants.
In "Higher Plant Cell Respiration" (R Douce and DA Day, Eds.) pp 391-417, Springer-Verlag, Berlin.

Arnon, DI (1949).
Copper enzymes in isolated chloroplasts. Polyphenoloxidase in *Beta vulgaris*.
Plant Physiol. 24, 1-15.

Azcon-Bieto, J, Salom, CL, Mackie ND, and Day, DA (1989).
The regulation of mitochondrial activity during greening and senescence of soybean cotyledons.
Plant Physiol. Biochem. 27, 827-836.

Azcon-Bieto, J and Osmond, CB (1983).
Relationship between photosynthesis and respiration. The effect of carbohydrate status on the rate of CO_2 production by respiration in darkened and illuminated wheat leaves.
Plant Physiol. 71, 574-581.

Azcon-Bieto, J, Lambers, H, and Day, DA (1983).
The effect of photosynthesis and carbohydrate status on respiratory rates and the involvement of the alternative path in leaf respiration.
Plant Physiol. 72, 598-603.

Bahr, JT and Bonner, WD (1973).
Cyanide-insensitive respiration. I The steady states of skunk cabbage spadix and bean hypocotyl mitochondria.
J. Biol. Chem. 248, 3441-3445.

Becker, WM, Leaver, CJ, Weir, EM, and Reizman, H (1978).
Regulation of glyoxysomal enzymes during germination of cucumber. I Developmental changes in cotyledonary protein, RNA, and enzyme activities during germination.
Plant Physiol. 62, 542-549.

Beer, S (1965).
The world, the flesh and the metal. The prerogatives of systems.
Nature 205, 223-231.

Beevers, H (1978).
The role of mitochondria in fatty seedling tissues.
In "Plant Mitochondria" (G Ducet and C Lance, Eds.), pp. 365-372, Elsevier, Amsterdam.

Beevers, H (1979).
Microbodies in higher plants.
Ann. Rev. Plant Physiol. 30, 159-197.

Beevers, H (1980).
The role of the glyoxylate cycle.
In "The Biochemistry of Plants" (PK Stumpf and EE Conn, Eds.), Vol. 4, pp. 117-130, Academic Press, New York.

Bendall, DS and Bonner, WD (1971).
Cyanide-insensitive respiration in plant mitochondria.
Plant Physiol. 47, 236-245.

Benedict, CR and Beevers, H (1961).
Formation of sucrose from malate in germinating castor beans. I Conversion of malate to phosphoenolpyruvate.
Plant Physiol. 36, 540-544.

Bergfeld, R, Hong, YN, Kuhne, T, and Schopfer, P (1978).
Formation of oleosomes (storage lipid bodies) during embryogenesis and their breakdown during seedling development in cotyledons of *Sinapsis alba* L..
Planta 143, 297-307.

Betsche, T and Gerhardt, B (1978).
Apparent catalase synthesis in sunflower cotyledons during the change in microbody function.
Plant Physiol. 62, 590-597.

Bewley, JD and Black, M (1985).
Seeds: physiology of development and germination. Plenum Press, New York.

Bingham, IJ and Farrar, JF (1987).
The alternative oxidase in barley roots of differing growth and respiration rates.
In "Plant Mitochondria: Structural, Functional and Physiological Aspects." (AL Moore and RB Beechy, Eds.), pp 365-368, Plenum Press, New York.

Blackman, FF (1905).
Optima and limiting factors.
Annal. Bot. 19, 281-295.

Blobel, G and Dobberstein, B (1975).
Transfer of proteins across membranes.
J. Cell Biol. 67, 835-851.

Bradford, M (1976).
A rapid and sensitive method for the quantification of microgram quantities of protein utilising the principle of protein-dye binding.
Anal. Biochem. 72, 248-252.

Brailsford, MA, Thompson, AG, Kaderbhai, N, and Beechey, RB (1986).
Pyruvate metabolism in castor-bean mitochondria.
Biochem. J. 239, 355-361.

Breidenbach, RW and Beevers, H (1967).
Association of the glyoxylate cycle enzymes in a novel subcellular particle from castor bean endosperm.
Biochem. Biophys. Res. Comm. 27, 462-469.

Breidenbach, RW, Castelfranco, P, and Peterson, C (1966).
Biogenesis of mitochondria in germinating peanut cotyledons.
Plant Physiol. 41, 803-809.

Breidenbach, RW, Castelfranco, P, and Criddle, RS (1967).
Biogenesis of mitochondria in germinating peanut cotyledons II. Changes in cytochromes and mitochondrial DNA.
Plant Physiol. 42, 1035-1041.

Breidenbach, RW, Kahn, A, and Beevers, H (1968).
Characterisation of glyoxysomes from castor bean endosperm.
Plant Physiol. 43, 705-713.

Brown, GC, Hafner, RP, and Brand, MD (1990).
A 'top-down' approach to the determination of control coefficients in metabolic control theory.
Eur. J. Biochem. 188, 321-325.

Brown, GC, Lakin-Thomas, PL, and Brand, MD (1990).
Control of respiration and oxidative phosphorylation in isolated rat liver cells.
Eur. J. Biochem. 192, 355-362.

Brunton, CJ and Palmer, JM (1973).
Pathways for the oxidation of malate and reduced pyridine nucleotide by wheat mitochondria.
Eur. J. Biochem. 39, 283-291.

Bryce, JH and Day, DA (1990).
Tricarboxylic acid cycle activity in mitochondria from soybean nodules and cotyledons.
J. Exp. Bot. 41, 961-967.

Bryce, JH, Azcon-Bieto, J, Wiskich, JT, and Day, DA (1990).
Adenylate control of respiration in plants: the contribution of rotenone-insensitive electron transport to ADP-limited oxygen consumption by soybean mitochondria.
Physiol. Plant. 78, 105-111.

Budde, RJA, Fang, TK, and Randall, DD (1988).
Regulation of the phosphorylation of mitochondrial pyruvate dehydrogenase complex *in situ*.
Plant Physiol. 88, 1031-1036.

Budde, RJA and Randall, DD (1989).
The mitochondrial pyruvate dehydrogenase complex from green pea seedlings is inactivated *in vivo* in a light-dependent manner.
Curr. Topics Plant Biochem. Physiol., 8, 284.

Burgess, N and Thomas DR (1986).
Carnitine acetyltransferase in pea cotyledon mitochondria.
Planta 167, 58-65.

Burke, JJ, Siedow, JN, and Moreland, DE (1982).
Succinate dehydrogenase: a partial purification from mung bean hypocotyls and soybean cotyledons.
Plant Physiol. 70, 1577-1581.

Camp, PJ and Randall, DD (1985).
Purification and characterisation of pea chloroplast pyruvate dehydrogenase complex: a source of acetyl-CoA and NADH for fatty acid biosynthesis.
Plant Physiol. 77, 571-577.

Canvin, DT and Beevers, H (1961).
Sucrose synthesis from acetate in the germinating castor bean: kinetics and pathway.
J. Biol. Chem. 236, 988-995.

Cerana, R, Colombo, R, and Lado, P (1974).
Promoting effects of oxygen on the synthesis of different enzymes in squash cotyledons in the early phase of germination.
Rendiconti-Academia Nazionale Dei Lincei 57, 701-709.

Chance, B, Holmes, W, Higgins, J, and Connelly, CM (1958).
Localization of interaction sites in multi-component transfer systems: theorems derived from analogues.
Nature 182, 1190-1193.

Chance, B and Williams, GR (1956).
The respiratory chain and oxidative phosphorylation.
Adv. Enzymol. 17, 65-134.

Chapman, EA and Graham, D (1974).
The effect of light on the tricarboxylic acid cycle in green leaves. I. Relative rates of the cycle in the dark and the light.
Plant Physiol. 53, 879-885.

Cheesebrough, TM and Moore, TS Jnr (1980).
Transverse distribution of phospholipid in organelle membranes from *Ricinus communis* L. var. Hale endosperm.
Plant Physiol. 65, 1076-1080.

Choinski, JS and Trelease, RN (1978).
Control of enzyme activities in cotton cotyledons during maturation and germination.
Plant Physiol. 62, 141-145.

Cooper, TG and Beevers, H (1969a).
Mitochondria and glyoxysomes from castor bean endosperm. Enzyme constituents and catalytic capacity.
J. Biol. Chem. 244, 3507-3513.

Cooper, TG and Beevers, H (1969b).
β-oxidation in glyoxysomes from castor bean endosperm.
J. Biol. Chem. 244, 3514-3520.

Cowley, RC and Palmer, JM (1980).
The interaction between exogenous NADH oxidase and succinate oxidase in Jerusalem artichoke (*Helianthus tuberosum*) mitochondria.
J. Exp. Bot. 31, 199-207.

Davies, HV and Chapman, JM (1979a).
The control of food mobilisation in seeds of *Cucumis sativus* L.. I The influence of the embryonic axis and testa on protein and lipid degradation.
Planta 146, 579-584.

Davies, HV and Chapman, JM (1979b).
The control of food mobilisation in seeds of *Cucumis sativus* L.. II The role of the embryonic axis.
Planta 146, 585-590.

Davies, HV and Slack, PT (1981).
The control of food mobilisation in seeds of dicotyledonous plants.
New Phytol. 88, 41-51.

Day, DA, Wiskich, JT, Bryce, JH, and Dry, IB (1987).
Regulation of ADP-limited respiration in isolated plant mitochondria.
In "Plant Mitochondria: Structural, Functional and Physiological Aspects" (AL Moore and RB Beechy, Eds.), Plenum Press, New York.

Day, DA, Moore, AL, Dry, IB, Wiskich, JT, and Azcon-Bieto, J (1988).
Regulation of non-phosphorylating electron transport pathways in soybean cotyledon mitochondria and its implication for fat metabolism.
Plant Physiol. 86, 1199-1204.

Day, DA, Salom, CL, Azcon-Bieto, J, Dry, IB, and Wiskich, JT (1988).
Glutamate oxidation by soybean cotyledon and leaf mitochondria.
Plant Cell Physiol., 29, 1193-1200.

Day DA and Wiskich, JT (1984).
Transport processes of isolated plant mitochondria.
Physiol. Veg. 22, 241-261.

Dizengremel, P and Tuquet C (1984).
Changes in respiration and mitochondrial activities in cotyledons from imbibition to senescence.
Physiol. Veg. 22, 687-700.

Donaldson, RP and Beevers, H (1977).
Lipid composition of organelles from germinating castor bean endosperm.
Plant Physiol. 59, 259-263.

Douce, R (1985).
Mitochondria in Higher Plants. Structure, Function and Biogenesis. Academic Press, New York.

Douce, R, Christenson, EL and Bonner, WD (1972).
Preparation of intact plant mitochondria.
Biochim. Biophys. Acta 275, 148-160.

Douce, R, Mannella, CA, and Bonner, WD (1973).
The external NADH dehydrogenases of intact plant mitochondria.
Biochim. Biophys. Acta 292, 105-116.

Douce, R, Moore, AL, and Neuberger, M (1977).
Isolation and oxidative properties of intact mitochondria isolated from spinach leaves.
Plant Physiol. 60, 625-628.

Dry, IB, Day, DA, and Wiskich, JT (1983).
Preferential oxidation of glycine by the respiratory chain of pea leaf mitochondria.
FEBS Lett. 158, 154-158.

Dry, IB, Nash, D, and Wiskich, JT (1983).
The mitochondrial localization of hexokinase in pea leaves.
Planta 158, 152-156.

Dry, IB, Moore AL, Day, DA, and Wiskich, JT (1985).
Regulation of alternative pathway activity in plant mitochondria: nonlinear relationship between electron flux and the redox poise of the quinone pool.
Arch. Biochem. Biophys. 273, 148-157.

Dry, IB, Bryce, JH, and Wiskich, JT (1987).
Regulation of mitochondrial respiration.
In "The Biochemistry of Plants" (PK Stumpf and EE Conn, Eds.), Vol. 11, pp. 213-252, Academic Press, New York.

Dry, IB and Wiskich, JT (1982).
Role of the external adenosine triphosphate/ adenosine diphosphate ratio in the control of plant mitochondrial respiration.
Arch. Biochem. Biophys. 217, 72-79.

Dry, IB and Wiskich, JT (1985).
Characteristics of glycine and malate oxidation by pea leaf mitochondria: evidence of differential access to NAD and respiratory chains.
Aust. J. Plant Physiol. 12, 329-339.

Ebbighausen, H, Hatch, MD, Lilley, RMcC, Kromer, S, Stitt, M, and Heldt, HW (1987).
On the function of malate-oxaloacetate shuttles in a plant cell.
In "Plant Mitochondria: Structural, Functional and Physiological Aspects." (AL Moore and RB Beechey, Eds.), pp 171-180, Plenum Press, New York.

Ehrenshaft, M and Brambl, R (1990).
Respiration and mitochondrial biogenesis in germinating embryos of maize.
Plant Physiol. 93, 295-304.

Fang, TK, Donaldson, RP, and Vigil, EL (1987).
Electron transport in purified glyoxysomal membranes from castor bean endosperm.
Planta 172, 1-13.

Fell, DA and Sauro, HM (1985).
Metabolic control and its analysis. Additional relationship between elasticities and control coefficients.
Eur. J. Biochem. 148, 555-561.

Fox, TD (1986).
Nuclear gene products required for translation of specific mitochondrially encoded mRNAs in yeast.
Trends in Genetics 2, 97-100.

Fujiki, Y, Rachubinski, RA, and Lazarow, PB (1984).
Synthesis of a major integral membrane polypeptide of rat liver peroxisomes on free polysomes.
Proc. Natl. Acad. Sci. USA 81, 7127-7131.

Gardestrom, P and Wigge, B (1988).
Influence of photorespiration on ATP/ADP ratios in the chloroplasts, mitochondria, and cytosol, studied by rapid fractionation of barley (*Hordeum vulgare*) protoplasts.
Plant Physiol. 88, 69-76.

Gerhardt, B (1983).
Localisation of β-oxidation enzymes in peroxisomes isolated from non-fatty plant tissues.
Planta 159, 238-246.

Gerhardt, B and Beevers, H (1970).
Developmental studies on glyoxysomes from castor bean endosperm.
J. Cell Biol. 40, 94-102.

Gerhardt, R, Stitt, M, and Heldt, HW (1987).
Subcellular metabolite levels in spinach leaves. Regulation of sucrose synthesis during diurnal alterations in photosynthetic partitioning.
Plant Physiol. 83, 399-407.

Giersch, C (1988).
Control analysis of biochemical pathways: A novel procedure for calculating control coefficients, and an additional theorem for branched pathways.
J. Theor. Biol. 134, 451-462.

Gonzalez, E and Beevers, H (1976).
Role of the endoplasmic reticulum in glyoxysome formation in castor bean endosperm.
Plant Physiol. 57, 406-409.

Graham, IA (1989).
Structure and function of the cucumber malate synthase gene and expression during plant development.
PhD Thesis, University of Edinburgh.

Graham, IA, Smith, LM, Brown, JWS, Leaver, CJ, and Smith, SM (1989).
The malate synthase gene of cucumber.
Plant Mol. Biol. 13, 673-684.

Graham, IA, Smith, LM, Leaver, CJ and Smith, SM (1990).
Developmental regulation of expression of the malate synthase gene in transgenic plants.
Plant Mol. Biol. 15, 539-549.

Grivell, LA (1989).
Nucleo-mitochondrial interactions in yeast mitochondrial biogenesis.
Eur. J. Biochem. 182, 477-493.

Groen, AK, Wanders, RJA, Westerhoff, HV, van der Meer, R, and Tager, JM (1982).
Quantification of the contribution of various steps to the control of mitochondrial respiration.
J. Biol. Chem. 257, 2754-2757.

Groen, AK, van Roermund, CWT, Vervoorn, RC, and Tager, JM (1986).
Control of gluconeogenesis in rat liver cells. Flux control coefficients of the enzymes in the gluconeogenic pathway in the absence and presence of glucagon.
Biochem. J. 237, 379-389.

Gruber, PJ, Trelease, RN, Becker, WM, and Newcomb, EH (1970).
A correlative ultrastructural and enzymatic study of cotyledonary microbodies following germination of fat-storing seeds.
Planta 93, 262-288.

Gut, H and Matile, P (1988).
Apparent induction of key enzymes of the glyoxylic acid cycle in senescent barley leaves.
Planta 176, 548-550.

Hafner, RP, Brown, GC, and Brand, MD (1990).
Analysis of the control of respiration rate, phosphorylation rate, proton leak rate and protonmotive force in isolated mitochondria using the 'top-down' approach of metabolic control theory.
Eur. J. Biochem. 188, 313-319.

Halmer, P and Bewley, JD (1979).
Mannase production by the lettuce endosperm. Control by the embryo.
Planta, 144, 333-340.

Hampp, R, Goller, M, and Ziegler, H (1982).
Adenylate levels, energy charge, and phosphorylation potential during dark-light and light-dark transitions in chloroplasts, mitochondria, and cytosol of mesophyll protoplasts from *Avena sativa* L..
Plant Physiol. 69, 448-455.

Heinrich, R and Rapoport, TA (1974).
A linear steady state treatment of enzymatic chains. General properties, control and effector strength.
Eur. J. Biochem. 42, 89-95.

Heldt, HW and Flugge, UI (1987).
Subcellular transport of metabolites in plant cells.
In "The Biochemistry of Plants" (PK Stumpf and EE Conn, Eds.), Vol. 12, pp. 49-85, Academic Press, New York.

Hill, RL and Bradshaw, RA (1969).
Fumarase.
Methods Enzymol. 13, 91-99.

Hiser, C and McIntosh, L (1990).
Alternative oxidase of potato is an integral membrane protein synthesised *de novo* during aging of tuber slices.
Plant Physiol. 93, 312-318.

Hofmeyr, J-HS, Kacser, H and van der Merwe, KJ (1986).
Metabolic control analysis of moiety-conserved cycles.
Eur. J. Biochem. 155, 631-641.

Hondred, D, Wadle, D-M, Titus, DE and Becker, WM (1987).
Light-stimulated accumulation of the peroxisomal enzymes hydroxypyruvate reductase and serine:glyoxylate aminotransferase
Plant Mol. Biol. 9, 259-275.

Huang, AHC (1987).
Lipases.
In "The Biochemistry of Plants" (PK Stumpf and EE Conn, Eds.), Vol. 9, pp. 91-119, Academic Press, New York.

Huang, AHC, Trelease, RN, and Moore, TS Jnr (1983).
Plant Peroxisomes, Academic Press, New York.

Jacobsen, JV and Beach, LR (1985).
Control of transcription of α-amylase and rRNA genes in barley aleurone by gibberellic and abscisic acid.
Nature (London) 316, 275-277.

Kacser, H (1987).
Control of metabolism.
In "The Biochemistry of Plants" (PK Stumpf and EE Conn, Eds.), Vol. 11, pp. 39-67, Academic Press, New York.

Kacser, H and Burns, JA (1973).
The control of flux.
Symp. Soc. Exp. Biol. 27, 65-104.

Kagawa, T and Beevers, H (1975).
The development of microbodies (glyoxysomes and leaf peroxisomes) in cotyledons of germinating seedlings.
Plant Physiol. 55, 258-264.

Kagawa, T and Gonzalez, E (1981).
Organelle specific isozymes of citrate synthase in the endosperm of developing *Ricinus* seedlings.
Plant Physiol. 68, 845-850.

Kagawa, T, Lord, JM, and Beevers, H (1975).
Lecithin synthesis during microbody biogenesis in water-melon seedlings.
Arch. Biochem. Biophys. 167, 45-53.

Kindl, H (1982a).
Glyoxysome biogenesis via cytosolic pools.
Ann. N. Y. Acad. Sci. 386, 314-326.

Kindl, H (1982b).
The biosynthesis of microbodies (peroxisomes, glyoxysomes).
Int. Rev. Cytol. 80, 193-229.

Kindl, H (1987).
β-oxidation of fatty acids by specific organelles.
In "The Biochemistry of Plants" (PK Stumpf and EE Conn, Eds.), Vol 9, pp. 31-52, Academic Press, New York.

Kobr, MJ and Beevers, H (1971).
Gluconeogenesis in castor bean endosperm. I Changes in glycolytic intermediates.
Plant Physiol. 47 48-52.

Koller, W and Kindl, H (1978).
Studies supporting the concept of glyoxyperoxisomes as intermediary organelles in transformation of glyoxysomes into peroxisomes.
Naturforsch. C: Biosci. 33C, 962-968.

Kolloffel, C and Sluys, JV (1970).
Mitochondrial activity in pea cotyledons during germination.
Acta Bot. Neerl. 19, 503-508.

Kombrink, E and Kruger, NJ (1984).
Inhibition by metabolic intermediates of pyrophosphate fructose-6-phosphate 1-phosphotransferase from germinating castor bean endosperm.
Z. Pflanzenphysiol. 114, 443-453.

Kombrink, E, Kruger, NJ, and Beevers, H (1984).
Kinetic properties of pyrophosphate fructose-6-phosphate 1-phosphotransferase from germinating castor bean endosperm.
Plant Physiol. 74, 395-401.

Kornberg, HL and Beevers, H (1957).
The glyoxylate cycle as a stage in the conversion of fat to carbohydrate in castor beans.
Biochim. Biophys. Acta, 26, 531-537.

Kornberg, HL and Krebs, HA (1957).
Synthesis of cell constituents from C_2-units by a modified tricarboxylic acid cycle.
Nature (London) 179, 988-991.

Krebs, HA (1957).
Control of metabolic processes.
Endeavour 16, 125-132.

Kromer, S, Stitt, M, and Heldt, HW (1988).
Mitochondrial oxidative phosphorylation participating in photosynthetic metabolism of a leaf cell.
FEBS Lett. 226, 352-356.

Kromer, S, Stitt, M, and Heldt, HW (1989).
The role of mitochondrial ATP production during photosynthesis.
Vortrage fur Pflanzenzuchtg 15, 24-6.

Kruckeberg, AL, Neuhaus, HE, Feil, R, Gottlieb, LD, and Stitt, M (1989).
Decreased-activity mutants of phosphoglucose isomerase in the cytosol and chloroplasts of *Clarkia xantiana*. I Impact on mass-action ratios and fluxes to starch and sucrose.
Biochem. J. 261, 457-467.

Kruger, NJ and Beevers, H (1984).
Effect of fructose-2,6-bisphosphate on the kinetic properties of fructose-1,6-bisphosphatase from germinating castor bean endosperm.
Plant Physiol. 76, 49-54.

Kruger, NJ and Beevers, H (1985).
Synthesis and degradation of fructose-2,6-bisphosphate in endosperm of castor bean seedlings.
Plant Physiol. 77, 358-364.

Kruger, NJ, Kombrink, E, and Beevers, H (1983).
Pyrophosphate fructose-6-phosphate 1-phosphotransferase in germinating castor bean seedlings.
FEBS Lett. 153, 409-412.

Kruse, C and Kindl, H (1982).
Integral proteins of the glyoxysomal membranes.
Ann. N. Y. Acad. Sci. 386, 499-502.

Kuhn, DN, Knauf, M, and Stumpf, PK (1981).
Subcellular localisation of acetyl-coenzyme A synthetase in leaf protoplasts of *Spinacea oleracea*.
Arch. Biochem. Biophys. 209, 441-450.

Laemmli, UK (1970).
Cleavage of structural proteins during the assembly of the head of bacteriophage T4.
Nature (London) 227, 680-685.

Lambers, H and Steingrover, E (1978).
Growth respiration of a flood-tolerant and a flood-intolerant *Senecio* species: Correlation between calculated and experimental values.
Plant Physiol. 43, 219-224.

Lambowitz, AM, Smith, EW, and Slayman, CW (1972).
Oxidative phosphorylation in *Neurospora* mitochondria. Studies on wild-type, *poky* and chloramphenicol induced wild-type.
J. Biol. Chem. 247, 4859-4865.

Lance, C, Chauveau, M, and Dizengremel, P (1985).
The cyanide resistant pathway of plant mitochondria.
In "Higher Plant Cell Respiration" (R Douce and DA Day, Eds.), pp 202-247, Springer-Verlag, Berlin.

Leegood, RC and ap Rees, T (1978a).
Phosphoenolpyruvate carboxykinase and gluconeogenesis in cotyledons of *Cucurbita pepo*.
Biochim. Biophys. Acta 524, 207-218.

Leegood, RC and ap Rees, T (1978b).
Dark fixation of CO_2 during gluconeogenesis by the cotyledons of *Cucurbita pepo* L..
Planta 140, 275-282.

Leegood, RC and ap Rees, T (1978c).
Identification of the regulatory steps in gluconeogenesis in cotyledons of *Cucurbita pepo*.
Biochim. Biophys. Acta 542, 1-11.

Liedvogel, B (1986).
Acetyl co-enzyme A and isopentyl-pyrophosphate as lipid precursors in plant cells biosynthesis and compartmentation.
J. Plant Physiol. 124, 211-222.

Liedvogel, B and Bauerle, R (1986).
Fatty acid synthesis in chloroplasts from mustard (*Sinapsis alba* L.) cotyledons: formation of acetyl-CoA by intraplastid glycolytic enzymes and a pyruvate dehydrogenase complex.
Planta 169, 481-489.

Liedvogel, B and Stumpf, PK (1982).
Origin of acetate in a spinach leaf cell.
Plant Physiol. 69, 897-903.

Lord, JM and Beevers, H (1972).
The problem of reduced nicotinamide adenine dinucleotide oxidation in glyoxysomes.
Plant Physiol. 49, 249-251.

Lunn, JE and ap Rees, T (1990).
Apparent equilibrium constant and mass-action ratio for sucrose-phosphate synthase in seeds of *Pisum sativum*.
Biochem. J. 267, 739-743.

Macey, MJK (1983).
β-oxidation and associated enzyme activities in microbodies from germinating peas.
Plant Sci. Lett. 30, 53-60.

Macey, MJK and Stumpf, PK (1983).
β-oxidation enzymes in microbodies from tubers of *Helianthus tuberosum*.
Plant Sci. Lett. 28, 207-212.

Macrae, AR (1971).
Isolation and properties of a 'malic' enzyme from cauliflower bud mitochondria.
Biochem. J. 122, 495-501.

Martin, C, Beeching, JR, and Northcote, DH (1984).
Changes in levels of transcripts in endosperm of castor beans treated with exogenous gibberellic acid.
Planta 162, 68-76.

Masterson, C, Wood, C, and Thomas, DR (1990).
β-oxidation enzymes in the mitochondria of *Arum* and oilseed rape.
Planta 182, 129-135.

Matsuoka, M and Asahi, T (1983).
Mechanism of the increase in cytochrome *c* oxidase activity in pea cotyledons during seed hydration.
Eur. J. Biochem. 134, 223-229.

Mazat, J-P, Jean-Bart, E, Rigoulet, M, and Guerin, B (1986).
Control of oxidative phosphorylation in yeast mitochondria. Role of the phosphate carrier.
Biochim. Biophys. Acta 849, 7-15.

Melendez-Hevia, E, Torres, NV, Sicilia, J and Kacser, H (1990).
Control analysis of transition times in metabolic systems.
Biochem. J. 265, 195-202.

Merril, CR, Goldman, D, Sedman, SA, and Ebert, MH (1981).
Ultrasensitive stain for proteins in polyacrylamide gels shows regional variation in cerebrospinal fluid proteins.
Science 211, 1437-1438.

Mettler, IJ and Beevers, H (1980).
Oxidation of NADH in glyoxysomes by a malate-aspartate shuttle.
Plant Physiol. 66, 555-560.

Meziane, AE, Callen, J-C, and Mounolou, J-C (1989).
Mitochondrial gene expression during *Xenopus laevis* development: a molecular study.
EMBO J. 8, 1649-1655.

Millhouse, J, Wiskich, JT, and Beevers, H (1983).
Metabolite oxidation and transport in mitochondria of endosperm from germinating castor bean.
Aust. J. Plant Physiol. 10, 167-177.

Milthorpe, FL and Moorby, J (1979).
An introduction to crop physiology.
Cambridge University Press, Cambridge.

Mitchell, P (1966).
Chemiosmotic coupling in oxidative and photosynthetic phosphorylation.
Biol. Rev., 41, 445-502.

Moller, IM and Palmer, JM (1982).
Direct evidence for the presence of a rotenone-resistant NADH dehydrogenase on the inner surface of the inner membrane of plant mitochondria.
Physiol. Plant. 54, 267-274.

Moller, IM, Johnston, SP, and Palmer, JM (1981).
A specific role for Ca^{2+} in the oxidation of exogenous NADH by Jerusalem artichoke (*Helianthus tuberosum*) mitochondria.
Biochem J. 194, 487-495.

Moore, AL and Akerman, KEO (1982).
Ca^{2+} stimulation of the external NADH dehydrogenase in Jerusalem artichoke (*Helianthus tuberosum*) mitochondria.
Biochem. Biophys. Res. Comm. 109, 513-517.

Mori, H and Nishimura, M (1989).
Glyoxysomal malate synthase is specifically degraded in microbodies during greening of pumpkin cotyledons.
FEBS Lett. 244, 163-166.

Murphy, DJ and Stumpf, PK (1981).
The origin of chloroplastic acetyl-CoA.
Arch. Biochem. Biophys. 212, 730-739.

Muto, S and Beevers, H (1974).
Lipase activities in castor bean endosperm.
Plant Physiol. 54, 23-28.

Neal, GE and Beevers, H (1960).
Pyruvate utilisation by castor-bean endosperm and other tissues.
Biochem. J. 74, 409-416.

Neuburger, M (1985).
Preparation of plant mitochondria, criteria for assessment of mitochondrial integrity and purity, survival *in vitro*.
In "Higher Plant Cell Respiration" (R Douce and DA Day, Eds.) pp 7-24, Springer-Verlag, Berlin.

Neuberger, M, Bourguignon, J, and Douce, R (1986).
Isolation of a large complex from the matrix of pea leaf mitochondria involved in the rapid transformation of glycine into serine.
FEBS Lett. 207, 18-22.

Neuhaus, HE and Stitt, M (1990).
Control analysis of photosynthate partitioning. Impact of reduced activity of ADP-glucose pyrophosphorylase or plastid phosphoglucomutase on the fluxes to starch and sucrose in *Arabidopsis thaliana* (L.) Heynh.
Planta 182, 445-454.

Neuhaus, HE, Kruckeberg, AL, Feil, R, and Stitt, M (1989).
Reduced-activity mutants of phosphoglucose isomerase in the cytosol and chloroplast of *Clarkia xantiana*. II Study of the mechanisms which regulate photosynthate partitioning.
Planta 178, 110-122.

Neuhaus, HE, Quick, WP, Siegl, G, and Stitt, M (1990).
Control of photosynthate partitioning in spinach leaves. Analysis of interaction between feedforward and feedback regulation of sucrose synthesis.
Planta 181, 583-592.

Smith, AL, Neuhaus, HE, and Stitt, M (1990).
The impact of decreased activity of starch-branching enzynme on photosynthetic starch synthesis in leaves of wrinkled-seeded peas.
Planta 181, 310-315.

Newsholme, EA and Start, C (1973).
Regulation in Metabolism, Wiley, New York.

Nishimura, M and Beevers, H (1979).
Subcellular location of gluconeogenetic enzymes in germinating castor bean endosperm.
Plant Physiol. 64, 31-37.

Northcote, DH (1986).
Hormonal and developmental control of gene expression in castor beans.
Biochem. Soc, Trans. 15, 11-12.

Opik, H and Simon, EW (1963).
Water content and respiration rate of bean cotyledons.
J. Exp. Bot. 14, 299-310.

Ory, RL, Yatsu, LY, and Kircher, HW (1968).
Association of lipase activity with the spherosomes of *Ricinus communis*.
Arch. Biochem. Biophys. 264, 255-264.

Padovan, AC, Dry, IB, and Wiskich, JT (1989).
An analysis of the control of phosphorylation-coupled respiration in isolated plant mitochondria.
Plant Physiol. 90, 928-933.

Palmer, JM and Ward, JA (1985).
The oxidation of NADH by plant mitochondria.
In "Higher Plant Cell Respiration" (R Douce and DA Day, Eds.) pp 173-201, Springer-Verlag, Berlin.

Pascal, N, Dumas, R, and Douce, R (1990).
Comparison of the kinetic behaviour towards pyridine nucleotides of NAD-linked dehydrogenases from plant mitochondria.
Plant Physiol. 94, 189-193.

Piechulla, B (1988).
Differential expression of nuclear- and organelle-encoded genes during tomato fruit development.
Planta 174, 505-512.

Plaut, WE (1969).
Isocitrate dehydrogenase (DPN-specific) from bovine heart.
Methods Enzymol. 13, 34-42.

Radin, NS (1969).
Preparation of lipid extracts.
Methods Enzymol. 14, 245-254.

Reder, C (1988).
Metabolic control theory: a structural approach.
J. Theor. Biol. 135, 175-201.

Riccio, P, Aquila, H, and Klingenberg, M (1975).
Purification of the carboxyatractyloside binding protein from mitochondria.
FEBS Lett. 56, 133-138.

Roberts, JKM, Lane, AN, Clark, RA, and Nieman, RH (1985).
Relationships between the rate of synthesis of ATP and the concentrations of the reactants and products of ATP hydrolysis in maize root tips, determined by ^{31}P nuclear magnetic resonance.
Arch. Biochem. Biophys. 240, 712-722.

Rodriguez, D, Dommes, J, and Northcote, DH (1987).
Effect of abscisic acid and gibberellic acids on malate synthase transcripts in germinating castor bean seeds.
Plant Mol. Biol. 9, 227-235.

Sauro, HM, Small, JR and Fell, DA (1987).
Metabolic control and its analysis. Extensions to the theory and matrix method.
Eur. J. Biochem. 165, 215-221.

Schopfer, P, Bajracharya, D, Bergfeld, R, and Falk, H (1976).
Phytochrome-mediated transformation of glyoxysomes into peroxisomes in the cotyledons of mustard seedlings.
Planta 133, 73-80.

Schuller, KA and Randall, DD (1989).
Regulation of pea mitochondrial pyruvate dehydrogenase complex. Does photorespiratory ammonium influence mitochondrial carbon metabolism.
Plant Physiol. 89, 1207-1212.

Slack, PT, Black, M, and Chapman, JM (1977).
The control of lipid mobilisation in *Cucumis* cotyledons.
J. Exp. Bot. 28, 569-577.

Small, JR and Fell DA (1990a).
Covalent modification and metabolic control analysis. Modification to the theorems and their application to metabolic systems containing covalently modifiable enzymes.
Eur. J. Biochem. 191, 405-411.

Small, JR and Fell, DA (1990b).
Metabolic control analysis. Sensitivity of control coefficients to elasticities.
Eur. J. Biochem. 191, 413-420.

Smith, SM and Leaver, CJ (1986).
Glyoxysomal malate synthase of cucumber: molecular cloning of a cDNA and regulation of enzyme synthesis during germination.
Plant Physiol. 81, 762-767.

Smyth, DA, Wu, M-X, and Black, CC (1984).
Phosphofructokinase and fructose-2,6- bisphosphatase activities in developing corn seedlings (*Zea mays* L.).
Plant Sci. Lett. 33, 61-70.

Stitt, M (1989).
Control analysis of photosynthetic sucrose synthesis: assignment of elasticity coefficients and flux-control coefficients to the cytosolic fructose-1,6-bisphosphatase and sucrose phosphate synthase.
Phil. Trans. R. Soc. Lond. B 323, 327-338.

Stitt, M, Lilley, RMcC, and Heldt, HW (1982).
Adenine nucleotide levels in the cytosol, chloroplasts, and mitochondria of wheat leaf protoplasts.
Plant Physiol. 70, 971-977.

Stitt, M, Huber, S, and Kerr, P (1987a).
Control of photosynthetic sucrose formation.
In "The Biochemistry of Plants" (PK Stumpf and EE Conn, Eds.), Vol. 10, pp 328-409, Academic Press, New York.

Stitt, M, Gerhardt, R, Wilke, I, and Heldt, HW (1987b).
The contribution of fructose-2,6-bisphosphate to the regulation of sucrose synthesis during photosynthesis.
Physiol. Plant. 69, 377-386.

Stumpf, PK (1987).
The biosynthesis of fatty acids.
In "The Biochemistry of Plants" (PK Stumpf and EE Conn, Eds.), Vol. 9, pp 121-136.

Thomas, DR and Wood, C (1986).
The two β-oxidation sites in pea cotyledons. Carnitine palmitoyltransferase: location and function in pea mitochondria.
Planta 168, 261-266.

Thomas, SM and ap Rees, T (1972a).
Gluconeogenesis during the germination of *Cucurbita pepo*.
Phytochemistry 11, 2177-2185.

Thomas, SM and ap Rees, T (1972b).
Glycolysis during gluconeogenesis in cotyledons of *Cucurbita pepo*.
Phytochemistry 11, 2187-2194.

Titus, DE and Becker, WM (1985).
Investigation of the glyoxysome-peroxisome transition in germinating cucumber cotyledons using double-label immunoelectron microscopy.
J. Cell Biol. 101, 1288-1299.

Tolbert, NE (1971).
Isolation of leaf peroxisomes.
Methods Enzymol. 23, 665-682.

Topping, JT and Leaver, CJ (1990).
Mitochondrial gene expression during wheat leaf developement.
Planta 182, 399-407.

Torres, NV, Mateo, F, Melendez-Hevia, and Kacser, H (1986).
Kinetics of metabolic pathways. A system *in vitro* to study the control of flux.
Biochem. J. 234, 169-174.

Torres, NV, Souto, R and Melendez-Hevia, E (1989).
Study of the flux and transition time control coefficient profiles in a metabolic system *in vitro* and the effect of an external stimulator.
Biochem. J. 260, 763-769.

Towbin, H, Staehelin, T, and Gordon, J (1979).
Electrophoretic transfer of proteins from polyacrylamide gels to nitrocellulose sheets: procedure and some applications.
Proc. Natl. Acad. Sci. USA 76, 4350-4354.

Trelease, RN (1984).
Glyoxysome biogenesis.
Ann. Rev. Plant Physiol. 35, 321-347.

Trelease, RN, Becker, WM, Gruber, PJ, and Newcomb, EH (1971).
Microbodies (glyoxysomes and peroxisomes) in cucumber cotyledons. Correlative biochemical and ultrastructural study in light- and dark-grown seedlings.
Plant Physiol. 48, 461-475.

Tuquet, C and Dizengremel P (1984).
Changes in respiratory process in soybean cotyledons during development and senescence.
Z. Pflanzenphysiol. 114, 355-359.

Turner, JF and Turner, DH (1980).
The regulation of glycolysis and the pentose phosphate pathway.
In "The Biochemistry of Plants" (PK Stumpf and EE Conn, Eds.), Vol. 2, pp. 279-316, Academic Press, New York.

Vignais, PV (1976).
Molecular and physiological aspects of adenine nucleotide transport in mitochondria.
Biochim. Biophys. Acta 456, 1-38.

Walden, R and Leaver, CJ (1981).
Synthesis of chloroplast proteins during germination and early seedling development of cucumber.
Plant Physiol. 67, 1090-1096.

Walker, DA (1987).
The use of the oxygen electrode and fluorescence probes in simple measurements of photosynthesis, Oxygraphics Ltd., Sheffield.

Walsh, K and Koshland, DE (1985).
Characterisation of rate-controlling steps *in vivo* by use of an adjustable expression vector.
Proc. Natl. Acad. Sci USA 82, 3577-3581.

Webster, BD and Leopold, AC (1977).
The ultrastructure of dry and imbibed soybean cotyledons.
Amer. J. Bot. 64, 1286-1293.

Westerhoff, HV and Kell, DB (1987).
Matrix method for determining steps most rate-limiting to metabolic fluxes in biotechnological processes.
Biotech. and Bioeng. 30, 101-107.

Wiener, N (1948).
Cybernetics. Control and communication in the animal and the machine, Wiley, New York.

Winter, K, Foster, JG, Edwards, GE, and Holtum, JAM (1982).
Intracellular localisation of enzymes of carbon metabolism in *Mesembryanthemum crystallinum* exhibiting C3 photsynthetic characteristics or performing Crassulacean acid metabolism.
Plant Physiol. 69, 300-307.

Wiskich, JT, Bryce, JH, Day, DA, and Dry, IB (1990).
Evidence for metabolic domains within the matrix compartment of pea leaf mitochondria.
Plant Physiol. 93, 611-616.

Wiskich, JT and Dry, IB (1985).
The tricarboxylic acid cycle in plant mitochondria: its operation and regulation.
In "Higher Plant Cell Respiration" (R Douce and DA Day, Eds.) pp 218-313, Springer-Verlag, Berlin.

Wong, KF and Davies, DD (1973).
Regulation of phospho(enol)pyruvate carboxylase in *Zea mays* by metabolites.
Biochem. J. 131, 451-458.

Wood, C, Noh Hj Jalil, M, McLaren, I, Yong, BCS, Ariffin, A, McNeil, PH, Burgess, N, and Thomas, DR (1984).
Carnitine long-chain acyltransferase and oxidation of palmitate, palmitoyl-CoA and palmitoylcarnitine by pea mitochondria preparations.
Planta 161, 255-260.

Wood, C, Burgess, N, and Thomas, DR (1986).
The dual location of β-oxidation enzymes in germinating pea cotyledons.
Planta 167, 54-57.

Youle, RJ and Huang, AHC (1976).
Development and properties of fructose-1,6-bisphosphatase in the endosperm of castor bean seedlings.
Biochem. J. 154, 647-652.

Zeiher, CA and Randall, DD (1990).
Identification and characterisation of mitochondrial acetyl-CoA hydrolase from *Pisum sativum* L. seedlings.
Plant Physiol. 94, 20-27.

Zoglowek, C, Kromer, S, and Heldt, HW (1988).
Oxaloacetate and malate transport by plant mitochondria.
Plant Physiol. 87, 109-115.